2010

Characterization of Histone H2A Functional Domains Important for Regulation of the DNA Damage Response

Elizabeta Gjoneska

CHARACTERIZATION OF HISTONE H2A FUNCTIONAL DOMAINS IMPORTANT FOR REGULATION OF THE DNA DAMAGE RESPONSE

A Thesis Presented to the Faculty of

The Rockefeller University

in Partial Fulfillment of the Requirements for

the degree of Doctor of Philosophy

by

Elizabeta Gjoneska

June 2010

CHARACTERIZATION OF HISTONE H2A DOMAINS IMPORTANT FOR REGULATION OF THE DNA DAMAGE RESPONSE

Elizabeta Gjoneska, Ph.D.

The Rockefeller University 2010

DNA double strand breaks represent deleterious lesions which can either be caused by environmental or endogenous sources of DNA damage. Efficient DNA damage response which ensures repair of these lesions is therefore critical for maintenance of genomic stability. The repair happens in the context of chromatin, a three-dimensional nucleoprotein complex consisting of DNA, histones and associated proteins. As such, mechanisms that modulate chromatin structure, many of which involve the histone component of chromatin, have been shown to play a role in regulation of the DNA damage response. In my thesis work I characterize two conserved histone H2A functional domains that are required for normal response to DNA damage.

In the first part of my thesis, my collaborators and I demonstrate that *Tetrahymena* major histone H2A.S contains an H2A.X variant-specific SQ motif within its C-terminal tail, providing the first description of this region in ciliated protozoa. The function of the SQ motif is mediated by post-translational phosphorylation of the conserved serine which is essential for normal progression through *Tetrahymena* life cycle, and in particular, meiosis. This study provides the first evidence for the existence of meiotic DSBs in *Tetrahymena* and defines the time interval of meiotic recombination in this organism.

In the second part of my thesis, I describe a functional domain which encodes a unique and previously unrecognized role for the histone H2A N-terminal tail in the DNA damage response in *S. cerevisiae*. A DNA damage survival property exists within the conserved SRS motif spanning residues 17-19 of a single turn α-helical region in the H2A tail, known as the 'knuckle'. I demonstrate that the SRS motif is required for efficient checkpoint recovery following successful repair, a function independent of post-translational modifications.

Another contribution of histone H2A in *S. cerevisiae*, specific to the MMS-induced DNA damage response, is provided by the three amino-terminal lysines which appear to be functionally redundant. My collaborators and I demonstrate that *in vivo* two of the lysines, H2A K4 and H2A K7, are acetylated individually as well as together, and identify the third lysine, H2A K13, as a novel acetylation site in *S. cerevisiae*.

ACKNOWLEDGEMENTS

TABLE OF CONTENTS

LIST OF FIGURES

LIST OF TABLES

LIST OF ABBREVIATIONS

aa	amino acid
Ab	antibody
Arp4	Actin related protein 4
ATM	ataxia telangiactesia mutated
ATP	adenosinetriphosphate
ATR	ATM related
AU	acid urea
Bbd	barr body deficient
BER	base excision repair
bp	base pairs
BP1	binding protein 1
BRCT	BRCA1 C terminus
C	celsius
cDNA	coding DNA
CENP-A	centromere protein A
CHIP	chromatin immunoprecipitation
CK2	casein kinase 2
DAPI	4′,6′-diamidino-2-phenylindole
DNA	deoxyribonucleic acid
DNA-PK	DNA dependent protein kinase
dNTP	deoxy nucleotide triphosphate
DSB	double strand break
EDTA	ethylenediaminetetraacetic acid
FACS	fluorescence activated cell sorting
5-FOA	5-fluoro-ortic acid
GAL	galactose
H2A.S	histone H2A slow
H2A.F	histone H2A fast
HA	hemaglutinin

HAT	histone acetyltransferase
HAR	histone H2A repression domain
HDAC	histone deacetylase
HEPES	2-[4-(2-hydroxyethyl)-1-piperazinyl]-ethanesulfonic acid
HMTase	histone methyltransferase
HO	homothallic
HPLC	high-performance liquid chromatography
HR	homologous recombination
HRP	horse-radish peroxidase
hrs	hours
HTP-C	histone phosphatase complex
HU	hydroxyurea
IF	immunofuorescence
Kb	kilo bases
kDA	kilo Dalton
LB	Luria-Bertani (broth)
μm	micro meters
min	minutes
mM	mili molar
LEU	leucine
MAb	monoclonal antibody
MALDI-TOF	matrix-assisted laser desorption ionization time-of-flight
MBT	malignant brain tumor
MDC1	mediator of DNA damage checkpoint protein 1
MMS	methyl methane sulfonate
MS	mass spectrometry
N	normal
NCP	nucleosome core particle
NER	nucleotide excision repair
NHEJ	non homologous end joining
NURF	nucleosome remodeling factor
OD_{600}	optical density at 600 nm
PAGE	polyacrylamide gel electrophoresis

PCR	polymerase chain reaction
PHD	plant homeodomain
PI	propidium iodide
PIKK	phosphoinositol 3-kinase-like kinase
PMSF	phenylmethanesulfonyl fluoride
PP2A	protein phosphatase 2A
PVDF	polyvinylidene fluoride
qPCR	quantitative polymerase chain reaction
RNA	ribonucleic acid
RNase	ribonuclease
RNR	ribonucleotide reductase
RPA	replication protein A
RP-HPLC	reversed-phase high-performance liquid chromatography
rpm	rotations per minute
RT-PCR	reverse transcriptase PCR
SC	synthetic complete
SDS	sodium dodecyl sulfate
SP	sphoeroplasting
SPP	super proteose peptone
SSA	single strand annealing
ssDNA	single strand DNA
TCA	trichloro acetic acid
TRP	triptophan
U	units
URA	uracil
UV	ultra violet
UV-DDB	UV damage DNA binding protein
WT	wild-type, original sequence without mutation
XPA	xeroderma pigmentosum A
XPC	xeroderma pigmentosum C
YPD	yeast peptone dextrose

CHAPTER 1

GENERAL INTRODUCTION

A fundamental question of biology is how eukaryotic cells maintain genomic integrity despite being subjected to many environmental and intrinsic sources of DNA damage. The question becomes even more outstanding given the compaction of the extensive eukaryotic genome into a three-dimensional nucleoprotein complex known as chromatin which represents a physiological substrate for the DNA-templated transactions, such as replication, transcription, recombination and repair. The packaging of DNA into chromatin therefore creates a number of significant barriers for detection of DNA lesions and their efficient repair. In response, cells have developed various mechanisms that modulate chromatin structure and ensure a timely and accurate repair.

In the following sections I will provide a general overview of chromatin organization and the mechanisms that govern its functions. In particular, I will summarize the current knowledge about the roles of relevant histone variants, histone modifications, and ATP remodeling complexes in regulation of chromatin dynamics during DNA damage. In that context, I will describe two distinct processes that elicit DNA damage response, meiotic recombination and DNA damage inflicted by exogenous agents, and point out outstanding questions which my research attempts to address. Finally, I will introduce *Tetrahymena thermophila*, the ciliate model organism used for part of this work, and provide a general overview of its biology.

The nucleosome

The fundamental building block of chromatin is the nucleosome core particle (NCP) which consists of 147 bp of DNA wrapped around an octamer containing two copies of each of the four core histone proteins H2A, H2B, H3 and H4. Various X-ray crystal structures of NCPs from different organisms (Davey et al., 2002; Luger et al., 1997; White et al., 2001), or reconstituted with recombinant histones (Luger et al., 1999), including histone variants (Suto et al., 2000) have been solved under high resolution. Based on the detailed information available from the three-dimensional structures and a wealth of biophysical analyses, the four core histones within the nucleosome core particle interact in pairs via a 'handshake motif.' Two histone H3-H4 dimers associate together further to form a hetero-tetramer which interacts with the middle and both ends of the nucleosomal DNA (Luger et al., 1997). The H3-H4 hetero-tetramer is flanked on each side by histone H2A-H2B dimers which are more weekly associated with the DNA (Oohara and Wada, 1987) and therefore more easily displaced from nucleosomes (Aragay et al., 1988; Kimura, 2005; Kimura and Cook, 2001; Kireeva et al., 2002; Vicent et al., 2004).

Protruding from the histone core are the largely unstructured N- and C-terminal tails which are only partially resolved in the structure of the nucleosome core particle (Luger et al., 1997). These tails exit the nucleosome most frequently through the DNA minor groove and make contacts primarily to the surface of the histone octamer of neighboring particles. Of particular interest to my research is a structural motif within the histone H2A N-terminus designated as the 'knuckle' (Figure 1.2) (Luger and Richmond, 1998). It is a single turn α-helix that precedes the histone H2A α1 helix and maps to the nucleosome surface in close proximity to the DNA. Interestingly, immediately adjacent to the location of this H2A region, the tail of H2B passes through a minor groove channel and

therefore it is plausable that the 'knuckle' might act to tether the H2A-H2B dimer to the nucleosome.

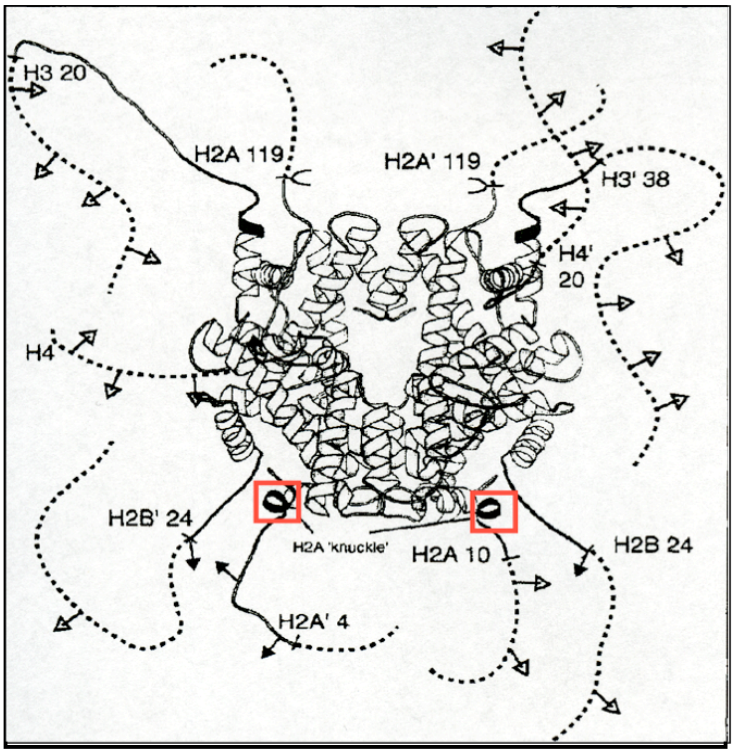

Figure 1.1: Histone H2A 'knuckle' localization within the NCP structure
The histone octamer from the nucleosome core structure viewed along the DNA superhelical axis direction. The first and last amino acid position of each histone tail observed in the crystal structure is labeled. The regions of the tails and histone-fold extension which are in contact with the DNA are shown by dark solid lines. The amino acids which could not be interpreted are shown in arbitrary positions (striped lines). Acetylation sites within the observed structure are indicated by filled arrows and the others by empty arrows. Ubiquitylation sites are marked as U's. The H2A 'knuckle' is indicated and boxed in red (adapted from Luger and Richmond, 1998).

Histones

Histones were first described in 1884 by Kossel when he isolated acid-soluble proteins from bird erythrocyte nuclei (reviewed by Van Holde, 1989). The core of the nucleosome particle consists of four types of histones, H2A, H2B, H3 and H4, also known as 'core' or canonical histones (Luger et al., 1997). They are small, basic proteins with molecular weights ranging from 11 to 16 kDa, exhibiting remarkable degree of sequence conservation throughout evolution. A fifth histone, linker histone H1, interacts with the nucleosome core in a presence of a linker DNA and plays an essential role in the formation of compact higher-order chromatin structure (Thomas, 1999).

Structurally, all core histones are composed of a distinct motif known as the 'histone fold' or a globular domain, and a highly dynamic flexible histone tail extension (Arents et al., 1991). The 'histone fold' domain is important for histone-histone interaction and nucleosome core formation. It constitutes ~70% of the histone mass and is characterized by three α-helices and two intervening loops. The remaining histone mass belongs to the tail extensions protruding from the nucleosome. These tail regions are enriched with charged residues which are thought to be important for DNA-histone interactions within the nucleosome, as well as histone-histone and DNA-histone interactions between the nucleosomes. Indeed, *in vitro* evidence suggests that the N-tails are important for nucleosome positioning along the DNA (Yang et al., 2007) and can mediate internucleosomal contacts required for the formation of higher-order chromatin structures (Gordon et al., 2005; Zheng and Hayes, 2003).

Importantly, the histone tail domains are primary sites of post-translational modifications and it is now well appreciated that they are key determinants of chromatin fiber dynamics (Strahl and Allis, 2000).

The higher-order structure

The fundamental level of DNA organization achieved by the nucleosome cannot fully explain the packaging of DNA observed in the nucleus (see 1, Figure 1.2). In fact, several successive levels of hierarchical organization are necessary to accomplish sufficient DNA compaction. The arrangement of individual nucleosomes onto the DNA produces a nucleosome array known as 11-nm fiber or 'beads on a string,' both designations derived from electron micrographs (see 2, Figure 1.2). This nucleosome array compacts the DNA ~six fold. Subsequent association of the linker histone H1 brings about the next level of organization in which the 11-nm 'beads on a string' nucleosome array is folded into an irregular rod-like structures ~30 nm in diameter in which the DNA is condensed another six fold (see 3, Figure 1.2). Two competing models have been proposed regarding the way in which the 30-nm fiber is organized. A 'solenoid' (one-start helix) model whereby 6-8 nucleosomes are coiled around a central axis, or an alternative, more open, 'zig-zag' (two-start helix) model which forms a condensed ribbon of linker DNA that connects two parallel rows of nucleosomes. Considerable evidence, some based on a X-ray crystal structure of a four nucleosome model system, supports the existence of an asymmetric zig-zag model as a basic principle of chromatin folding (Khorasanizadeh, 2004; Schalch et al., 2005).

The 30-nm fibers are subsequently further folded into higher-order structures by superhelical twisting of solenoid loops whose bases are attached to a non-histone protein scaffold (see 4, Figure 1.2). These higher-order structures partition the eukaryotic genome into distinct functional domains that impact on cellular processes, such as gene expression and chromosome stability. In particular, a combination of locally extended euchromatin associated with transcriptionally active regions and extensively condensed heterochromatin, or

Figure 1.2: DNA compaction into higher-order chromatin structure

Eukaryotic DNA is folded and packed in an efficient manner. Several successive levels of the hierarchical organization of DNA packing in a chromosome are schematically shown top to bottom. The basic level of DNA packaging into the chromatin structure is the mononucleosome, an octamer of histones (2 copies each of H2A, H2B, H3 and H4) with 147 base pairs of DNA wrapped nearly twice around. A short stretch of linker DNA connects the nucleosomes to one another to form a polynucleosome 10-nm 'bead-on-a-string' form of chromatin (see 2 in figure). A fifth histone, H1, binds to the DNA as it exits the nucleosome to bring about the next level of organization in which the string of nucleosomes is folded into a irregular rod-like structure to form a fiber about 30 nm in diameter (see 3 in figure). These fibers are then further folded into higher-order structures by superhelical twisting of solenoid loops the bases of which are attached to a non-histone protein scaffold (see 4 and 5 in figure) (adapted from Pearson Education, Inc,. publishing as Benjamin Cummings, 2006).

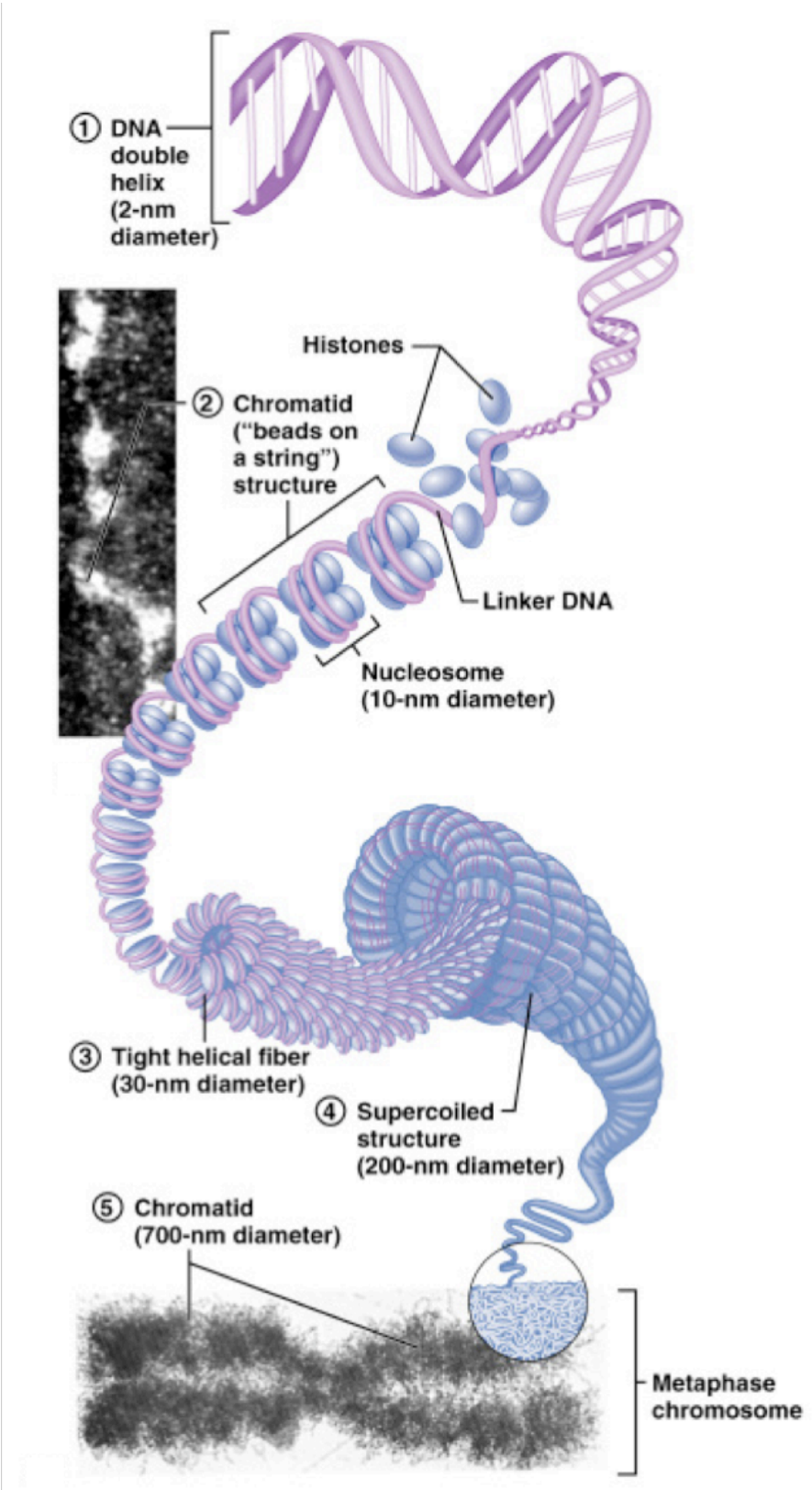
① DNA double helix (2-nm diameter)
Histones
② Chromatid ("beads on a string") structure
Linker DNA
Nucleosome (10-nm diameter)
③ Tight helical fiber (30-nm diameter)
④ Supercoiled structure (200-nm diameter)
⑤ Chromatid (700-nm diameter)
Metaphase chromosome

Figure 1.2

'silent' chromatin, which consists predominantly of transcriptionally inactive genes, can be observed within a single nucleus. Finally, the most condensed DNA structure is observed during metaphase of mitosis and meiosis which brings about a massive 10,000-fold overall compaction to allow for faithful genome segregation (see 5, Figure 1.2).

DNA damage

The genome integrity is continuously challenged by numerous exogenous and endogenous DNA damaging factors which induce a variety of lesions with a diverse and adverse consequences. Proper genome function therefore depends on the faithful maintenance of its integrity which is ensured by an intricate network of DNA damage response mechanisms.

There are at least four major damage repair pathways operational in eukaryotic cells depending on the type of DNA damage lesion: nucleotide excision repair (NER), base excision repair (BER), homologous recombination (HR) and non-homologous end joining (NHEJ) (reviewed by Hakem, 2008; Peterson and Cote, 2004). Lesions repaired by NER and BER affect only one of the DNA strands. Small types of base chemical alterations, such as alkylation or oxidation, are targeted by the BER pathway which is initiated by a large number of lesion-specific glycosylases that clip off damaged bases to create an abasic site. The NER pathway on the other hand, deals with large or bulky chemical adducts that destabilize the DNA double helix and potentially obstruct transcription and replication. This includes major UV-induced photoproducts, such as cyclobutane pyrimidine dimers and 6-4 photoproducts, which cause helix-distorting single-strand lesions detected by the xeroderma pigmentosum group C (XPC) complex and the UV damage DNA binding protein (UV-DDB) (Gillet and Scharer, 2006). Once bound, these complexes initiate NER by assembling repair factors such as

helicases as well as single strand DNA-binding proteins including XPA and RPA which stabilize the helicase-unwound DNA. The unwound DNA containing the injury is excised, the resulting single-strand gap is filled by the DNA replication machinery and sealed by DNA ligase, resulting in an error-free DNA repair (de Laat et al., 1999; Evans et al., 1997; Moser et al., 2007).

DNA double strand breaks (DSBs) affect both strands of the DNA and can lead to loss of genetic information and therefore are considered to be the most severe type of DNA damage. In addition to DSBs produced as normal intermediates of physiological recombination events such as meiosis and immunoglobulin gene rearrangements, DSBs can be induced by two of the commonly used DNA damaging agents in the laboratory, methyl methane sulfonate (MMS) and hydroxyurea (HU). The primary MMS-induced lesions are actually abasic sites, products of base excision repair removal of alkylated bases, however during replication these single-strand break-intermediates are converted into DSBs. HU on the other hand, directly affects the DNA synthesis process through inhibition of ribonucleotide reductase thereby causing nucleotide depletion and DSB formation at stalled replication forks.

In eukaryotic cells chromosomal DSBs are repaired by two conserved pathways: (1) homologous recombination (HR), which allows for error-free repair by using the genetic information from the undamaged sister chromatid or homologous chromosome as a template, and (2) the error prone non-homologous end joining (NHEJ) pathway, the predominant mode of DSB repair in mammals, which does not require any DNA sequence homology and involves direct ligation of broken DNA ends (Figure 1.3) (Pardo et al., 2009; van Attikum and Gasser, 2005). Members of the MRN (Mre11-Rad50-Nbs1) or MRX (Mre11-Rad50-XRS2) complex, in mammalian cells and yeast respectively, have an early role in the detection of DSBs during both HR and NHEJ. These complexes bind

eukaryotic cells have evolved various mechanisms that regulate the packaging of DNA into higher-order chromatin structures and allow genome accessibility to proteins involved in DNA transactions, including DNA damage repair. These include: (1) incorporation of histone variants into nucleosomes, (2) covalent histone post-translational modifications, and (3) ATP-dependent chromatin remodeling. Each of these will be discussed separately with a focus on DNA repair.

Histone variants

Chromatin structure and function *in vivo* is influenced by specialized histone variants. These variant or 'replacement' histones as they are commonly referred to, were identified based on differences in their primary amino acid sequence relative to the major, canonical histone species (Kamakaka and Biggins, 2005). They can also be distinguished from the canonical histones by their distinct expression and localization patterns. Unlike canonical histones, histone variants are expressed from a set of single genes which are not subject to stringent regulation. Instead, they are expressed throughout the cell cycle and assembled into chromatin independently of DNA replication. Their incorporation into chromatin has been shown to be important for gene regulation, meiotic events and DNA repair.

With exception of histone H4 which is invariant, variants have been identified for all of the remaining histones. A few variants of H2B and H1 are known to date, which have been shown to play an important role in chromatin compaction, particularly during spermatogenesis (Brown, 2003; Parseghian and Hamkalo, 2001; Poccia and Green, 1992). Histone H3 also has two major variants: CENP-A (centromere protein A), an evolutionarily conserved variant that is specific for centromeric chromatin and essential for centromere function

and process the broken DNA ends converting them into 3' single strand (ss) DNA overhangs. Generation of ssDNA overhang is a necessary binding platform for the RPA complex which helps load DNA repair proteins such as Rad52 and Rad51. These proteins ensure that a homologous DNA sequence is found that would result in a successful strand invasion into a homologous chromosome. After strand invasion, DNA polymerase extends the invading strand using the homologous chromosome as a template thereby effectively restoring the strand that was displaced during the invasion. Alternatively, single-strand annealing (SSA) is a form of homologous recombination that involves annealing of ssDNA tails at complementary sequences on both sides of the DSB and removal of the intervening DNA (Prado et al., 2003). In each case, the repair event is completed by DNA ligation that seals the break. During NHEJ the broken DNA ends are detected and bound by the Ku70/Ku80 heterodimer which holds the ends together to facilitate their direct re-ligation by DNA ligase 4. MRN (or MRX) complex resection of the DNA ends prior to the ligation generally results in an error prone repair of the break.

Finally, organisms have developed checkpoint mechanisms that delay cell-cycle progression in response to DNA damage or replication stress, in order to ensure that a break has been repaired. These checkpoint mechanisms rely on the activity of sensor proteins, adaptor kinases and effector kinases (Harrison and Haber, 2006). Sensor proteins detect the presence of DNA damage and relay the signal to effector kinases which regulate the activity of downstream targets responsible for expression of repair and cell-cycle progression proteins.

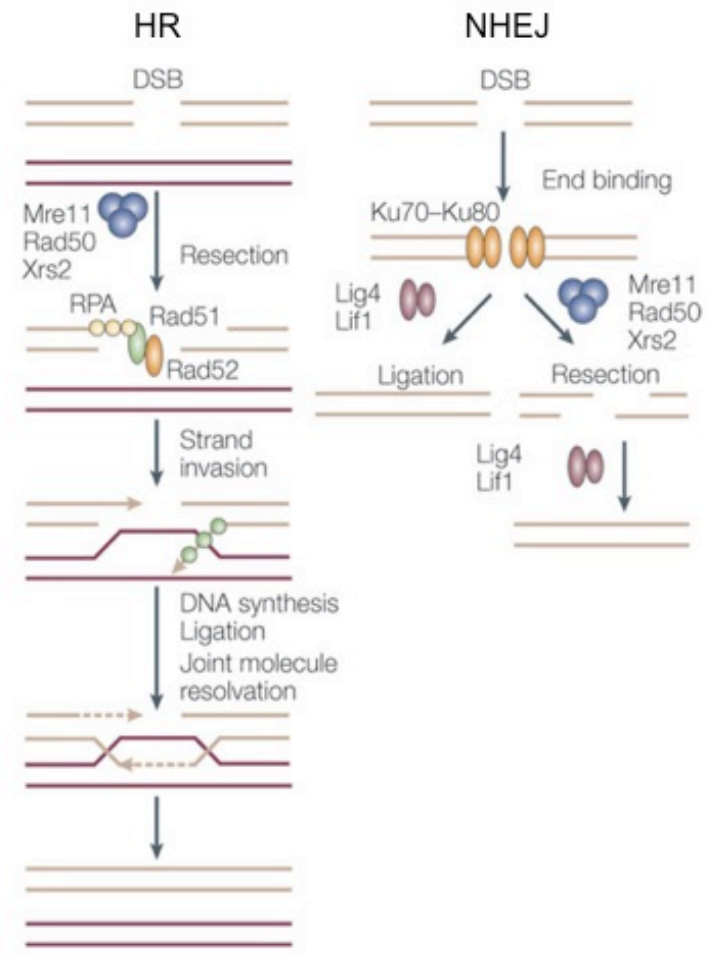

Figure 1.3: Pathways for DNA double strand break repair

A DNA double strand break can be repaired by homologous recombination (HR) or non-homologous end joining (NHEJ) pathway. Shown are the mechanisms and the key protein factors involved in each pathway in *S. cerevisiae* (adapted from van Attikum and Gasser, 2005).

Chromatin structure dynamics

Although chromatin has long been viewed as a stable entity, an inert structural scaffold that protects and organizes the genetic information encoded in the DNA, as such it would represent a physical barrier to the accessibility of the relevant biological machineries to the DNA substrate. It is now recognized that chromatin is much more dynamic than was previously understood. Indeed,

(Black and Bassett, 2008; Howman et al., 2000; Palmer et al., 1987), and H3.3, which is deposited preferentially at transcriptionally active regions (Ahmad and Henikoff, 2002; Sarma and Reinberg, 2005). Histone H2A has a largest family of variants documented to date. There are five H2A proteins with considerably different sequences from the major H2A. H2A.X and H2A.Z identified in the 1980s, localize throughout the genome, whereas macroH2A.1 and macroH2A.2 discovered in the 1990s, and H2A.Bbd (Barr body deficient) in 2001, localize to the inactive X or the autosomes, respectively (Chadwick and Willard, 2001, 2003; Costanzi and Pehrson, 1998). Here I will focus on the H2A.X variant, as it has been shown to play an important role in the cell's response to DNA damage.

H2A.X

H2A.X was first identified in human cells as an electrophoretic type of the core histone H2A (West and Bonner, 1980). Upon its sequencing in the late 80s (Mannironi et al., 1989), H2A.X became defined by the presence of a conserved SQ motif, usually localized within the last 4 residues in the C-terminus, followed by a penultimate acidic residue (E/D) and a terminal hydrophobic residue (Y/F/I/L). Another unique feature of H2A.X is its specific phosphorylation of the conserved serine within the C-terminal motif in response to DNA double-strand breaks produced by ionizing radiation (Rogakou et al., 1998) or in the course of programmed DNA rearrangements (Chen et al., 2000; Rogakou et al., 2000), including meiotic homologous recombination (Mahadevaiah et al., 2001). Interestingly, unlike other histone variants which have distinct chromatin localization patterns, H2A.X does not appear to be specifically targeted to DSBs as it accounts for different percent of the total H2A complement in various organisms (Rogakou et al., 1998). Thus H2A.X is likely to be randomly distributed throughout the genome. The phosphorylation of the conserved C-

terminal serine however, is limited to the regions flanking DSBs in what has become known as nuclear foci (Rogakou et al., 1999), where it serves as an assembly platform for the components of the DNA DSB response machinery, including proteins involved in checkpoint signaling, DNA repair and chromatin remodeling (Downs et al., 2004; Fernandez-Capetillo et al., 2002; Kobayashi et al., 2002; Lukas et al., 2004; Nakamura et al., 2004; Rappold et al., 2001; Strom et al., 2004; Ward et al., 2003).

Although it is not a primary recognition site for DNA damage response factors as it is dispensable for their initial recruitment to the DSB sites (Celeste et al., 2003), the phosphorylation of H2A.X at its C-terminal serine (S129 in *S. cerevisiae* and S139 in mammalian cells) also referred to as γH2A.X, is important for factor retention and accumulation. Additionally, γH2A.X promotes chromatin reorganization around the lesion site (Fernandez-Capetillo et al., 2003; Kruhlak et al., 2006a; Kruhlak et al., 2006b). Both of these functions which are likely related, serve to facilitate the synapsis of broken chromosome ends and are required for efficient DNA repair. Indeed, disruption of the γH2A.X phosphorylation site in *S. cerevisiae*, causes mild sensitivity to DSB-inducing agents (Downs et al., 2000). Moreover, heterozygous and homozygous null alleles of mammalian H2A.X in the absence of the p53 'gatekeeper' protein, known to safeguard against genomic instability, lead to increased cancer susceptibility phenotypes associated with impaired recruitment of DNA repair factors to DSBs, repair defects and chromosomal abnormalities (Bassing et al., 2002; Celeste et al., 2003; Celeste et al., 2002). As a result, H2A.X has been dubbed the 'histone guardian' of the genome (Fernandez-Capetillo et al., 2004b).

Although γH2A.X phosphorylation deficient mutants in *S. cerevisiae* have a relatively mild damage sensitivity phenotype, it has been reported that γH2A.X contributes to repair by both DSB repair pathways, NHEJ and HR (Downs et al.,

2000). Indeed, Downs and colleagues reported that sensitivity of strains carrying mutations that affect either NHEJ (*ku70, ku80*) or HR (*rad52*) is exacerbated by mutations in the γH2A.X phosphorylation site in *S. cerevisiae*. Nevertheless, and intriguing hypothesis has been put forth suggesting a specific role for H2A.X in the HR repair pathway (Malik and Henikoff, 2003). Namely, Malik and Henikoff argue that the number of H2A.X genes and their expression levels in different organisms seem to correlate directly with the extent the particular organism utilizes the homologous recombination mechanism. For example, although absent in nematodes that use little homologous recombination, H2A.X is the 'major' histone H2A in budding yeast which accordingly has high levels of homologous recombination. Similarly, in humans and flies the copy number of the gene that encodes H2A.X is low, which correlates with the low levels of homologous recombination. Interestingly, the ciliate *Tetrahymena thermophila* also appears to have an active homologous recombination mechanism (Yu et al., 1988), however a *Tetrahymena* H2A.X homologue had not been identified prior to my studies described in Chapter 1 of this thesis.

Post-translational modifications of histones

The first evidence that histones are post-translationally modified dates back to 1964 when Vincent Allfrey and colleagues' discovered that histones were subject to post-translational acetylation and methylation (Allfrey et al., 1964). It was the same study that first put forth the notion that histone modifications might be important regulatory elements of biological functions, based on the correlative relationship between histone acetylation levels and the rate of RNA synthesis. Ever since the pioneering studies of Allfrey and coworkers ~45 years ago, more than 70 different histone modification sites have been described, classified into 10 different modification types. They include, but are not limited to,

phosphorylation of serine and threonine residues, acetylation and ubiquitylation of lysines, mono- di- or tri- methylation of lysines and mono- or di- (symmetric or asymmetric) methylation of arginines (Kouzarides, 2007) (Figure 1.4). The functional implications of these histone modifications have been explored since the initial finding by Allfrey and colleagues. However, significant advances were only made within the past decade owing to the discovery of enzymes that regulate these modifications. In 1996, simultaneous discoveries by two independent groups, demonstrated that two known transcriptional regulators, namely Gcn5 and Rpd3, function as histone modifying enzymes with opposing activities responsible for regulation of histone acetylation steady-state levels (Brownell et al., 1996; Taunton et al., 1996). Thus, the first histone acetyltransferase (HAT) and deacetylase (HDAC) were identified, providing a direct connection between histone modifications and biological function. Since then, considerable progress has been made in dissecting the enzyme systems that govern the steady-state balance of histone modifications revealing several enzyme classes that establish ('write') histone modifications together with their enzyme counterparts that remove ('erase') the modification. For example, the histone kinase family of enzymes (Burma et al., 2001; Cheung et al., 2005) phosphorylate specific serines and threonines, and these phosphorylation marks are removed by phosphatases (PPTases) (Chowdhury et al., 2005; Keogh et al., 2006). In addition two general classes of histone methyltransferases (HMTases) have been described depending on whether their substrates are histone lysines (Lachner et al., 2003; Qian and Zhou, 2006) or arginines (Lee and Stallcup, 2009). Although until recently histone methylation was considered chemically stable, several classes of histone demethylating enzymes that catalyze the removal of specific histone methylation marks have been described in the last few years (Lan et al., 2008; Shi et al., 2004; Tsukada et al., 2006).

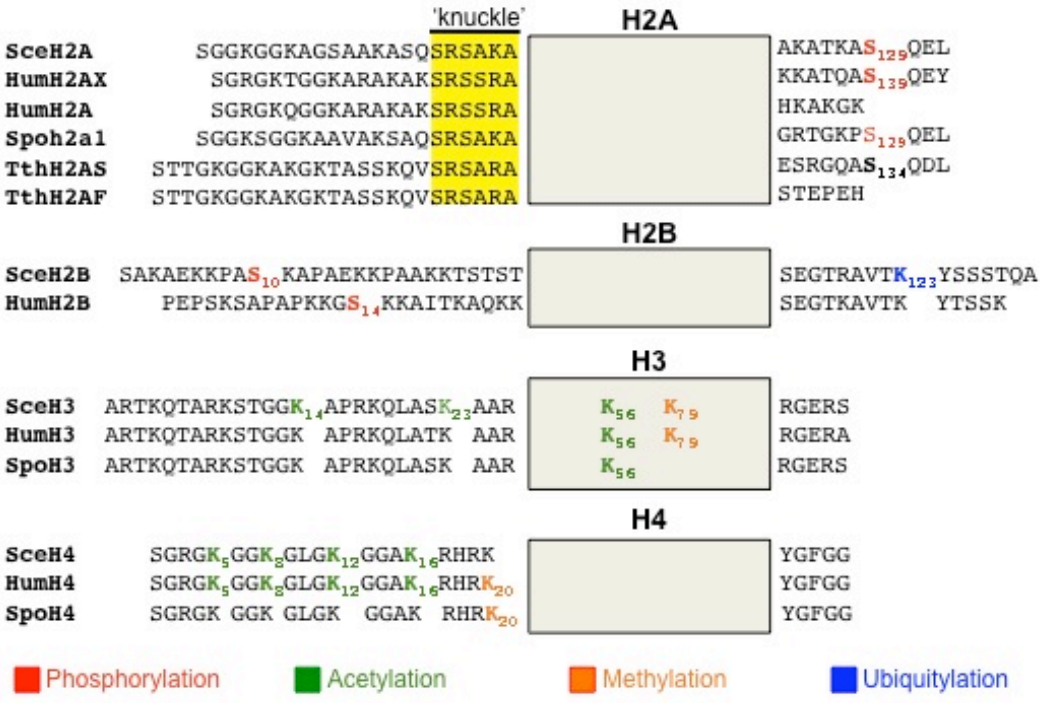

Figure 1.4: Histone post-translational modifications

The four histone proteins H2A, H2B, H3 and H4, and their variants are subject to post-translational modifications. Tail sequences from core histones and their variants from various organisms are shown. Hum = human; Sce = *S. cerevisiae;* Spo = *S.* pombe; Tth = *Tetrahymena thermophila.* The accession numbers are as follows: HumH2A, NP_254280; HumH2A.X, NP_002096; SpoH2A, NP_594421; SceH2A, NP_010511; TthH2A.S, AAC37291; TthH2A.F, AAC37292. Sequences are aligned with ClustalW identity algorithm based on the homology in the histone fold region (boxed area, sequence not shown). A suspected phosphorylation site in the *Tetrahumena* H2A.S SQ motif is bolded. The location of the H2A 'knuckle' region is noted and the residues are highlighted. For clarity, only the post-translational modifications with documented involvement in the DNA damage response are shown. Modified amino acids with subscript numbers corresponding to their position are colored according to the modification. Phosphorylation (red), methylation (orange), ubiquitylation (blue) and acetylation (green) are depicted. With exception of K56 and K79 which map to the histone-fold domain the remaining modification sites are localized within the N- and C-terminal tails.

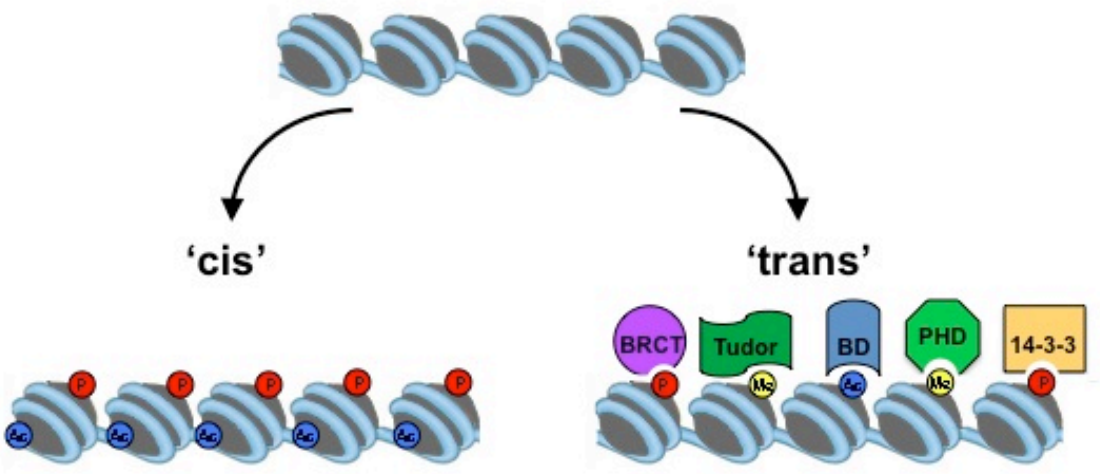

Figure 1.5: Molecular mechanisms of histone modifications

The dynamic functional readout of histone modifications is mediated by two general mechanisms. Covalent histone modifications can directly influence the state of chromatin compaction by charge-dependent alterations of internucleosomal interactions and histone-DNA contacts ('cis' mechanism). Examples of 'cis' mechanism include acetylation 'charged patches' associated with transcriptional activation, and phosphorylation patches that can potentially lead to chromatin condensation. Alternatively, histone modifications are interpreted by specific recognition modules within nuclear proteins known as 'effectors' which engage them in a context-dependent fashion to bring about distinct downstream events (trans' mechanism). Examples of histone modification-binding modules include tudor domains and PHD domains that bind methyl-lysines, BRCT and 14-3-3 domains that bind phosphorylated serines/threonines, and bromodomains that bind acetylated lysines. Ac: acetylation, Me: methylation, P: phosphorylation, BD: bromodomain, BRCT: breast cancer susceptibility protein C-terminal domain, PHD: plant homeodomain.

While histone modifications and their respective enzyme systems have been extensively studied in the context of transcriptional regulation, evidence accumulated within the past decade indicates that they also play a direct role during DNA repair by (i) marking the lesion, (ii) recruiting components of the repair machineries and (iii) facilitating their action. Two distinct, but certainly not mutually exclusive mechanisms, have been proposed to mediate the dynamic functional readout of histone modifications, both of which are relevant to the histone functions in DNA repair (Figure 1.5). These include a '*cis*' mechanism whereby covalent histone modifications directly influence the state of chromatin compaction by charge-dependent alterations of internucleosomal interactions and histone-DNA contacts. Alternatively, the 'trans' mechanism proposes that histone modifications are interpreted by specific recognition modules within nuclear proteins known as 'effectors' which engage them in a context-dependent fashion to bring about distinct downstream events. The significance of the two mechanisms in regulating chromatin dynamics in the context of the DNA damage response is discussed below.

Phosphorylation

Among the different histone modifications, phosphorylation appears to play a primary role in the DNA damage response. All canonical histones, including H1 and some of the histone variants undergo phosphorylation on serine and threonine residues *in vivo*. In fact, phosphorylation of the histone variant H2A.X at the C-terminal serine to produce a modified protein designated as γH2A.X in response to DNA damage is probably one of the better studied post-translational modifications to date (Rogakou et al., 1998). It is carried out by members of the phosphoinositol 3-kinase-like kinase (PIKK) family specifically ATM (Tel1 in *S. cerevisiae*), ATR (Mec1), and DNA-PK, which are recruited to

lesions through their association with DSB sensor and adaptor proteins (Burma et al., 2001; Stiff et al., 2004; Ward and Chen, 2001). Once the break is repaired either by NHEJ or HR, the phosphorylation mark is removed and this has been shown to be important for turning off the DNA damage response (Keogh et al., 2006).

Multiple mechanisms for eliminating γH2A.X after repair have been described, including removal by histone exchange followed by dephosphorylation. The enzymes that catalyze dephosphorylation of γH2A.X, namely PP2A in humans and the Pph3 subunit of the H2A phosphatase complex (HTP-C) in *S. cerevisiae,* have a high specific activity for their γH2A.X substrates *in vitro* and regulate γH2A.X status *in vivo* (Chowdhury et al., 2005; Keogh et al., 2006). However, *S. cerevisiae* Pph3 functions downstream of DNA repair, as it appears to target γH2A.X after its displacement from DNA (Keogh et al., 2006). Consistent with this observation, lack of functional *pph3* does not affect repair efficiency. Instead, Pph3 functions in checkpoint maintenance as *pph3* deficient cells are defective in checkpoint recovery, suggesting that active dephosphorylation of γH2A.X is an important step in signaling successful DNA repair (Keogh et al., 2006). It is also possible that rather than being a signaling event, dephosphorylation is simply necessary to restore native chromatin structure after repair, however the exact mechanism by which γH2A.X dephosphorylation contributes to checkpoint recovery is still unclear. The studies of *S. cerevisiae* histone H2A described in Chapters 2 and 3 of this thesis are likely to shed some light on this process.

In addition to γH2A.X, S122, another residue within the C-terminal tail of *S. cerevisiae* histone H2A, has also been linked to the DNA damage response. Indeed, mutation of this residue displays DNA damage sensitivity, and it functions independently from γH2A.X in mediating survival after damage

(Harvey et al., 2005). While S122 phosphorylation has been observed, the kinase has not been identified, and it is not yet understood whether phosphorylation is important for the DNA damage role of S122 (Wyatt et al., 2003).

Beside histone H2A.X, histones H2B and H4 are also subject to damage mediated phosphorylation events. The amino terminal tail of H2B is phosphorylated at S10 by the Ste20 protein kinase in response to the hydrogen peroxide-induced cell death pathway (Ahn et al., 2005a) and meiosis (Ahn et al., 2005b). In mammalian cells the Ste20 kinase (Mst1) phosphorylates H2B S14 instead, and this has also been implicated in apoptosis (Cheung et al., 2003). Additionally, Fernandez-Capetillo and colleagues reported that mammalian H2B S14 phosphorylation is also induced upon exposure to ionizing radiation or laser treatment, and it accumulates at DSBs following γH2A.X (Fernandez-Capetillo et al., 2004a). Interestingly, the accumulation of H2B S14 phosphorylaton at radiation-induced foci is dependent on γH2A.X, although loss of γH2A.X does not affect H2B S14 phosphorylaton itself. It is possible that S14 phosphorylation marks a subset of DSBs that are irreparable. Alternatively, it might simply facilitate the chromatin condensation process. Consistent with this function is the report that H2B N-terminal tail peptides have a property of self-aggregating when phosphorylated at S14 (Cheung et al., 2003).

The most recent DNA damage related phosphorylation event was found to occur on the N-terminal tail serine 1 of histone H4. Serine 1 phosphorylation is performed by the complex casein kinase II (CK2) in a DNA damage dependent manner (Cheung et al., 2005). Accordingly, CK2 subunits are also important for mediating survival after DNA damage as CK2-deficient cells are sensitive to damaging agents (Cheung et al., 2005).

Acetylation

Acetylation is an abundant histone modification mainly associated with transcriptional activation. Lysines within the N-terminal tail of histones H3 and H4 are the main targets for this modification which neutralizes the basic charge of the lysine, thereby potentially altering nucleosomal interactions. Two decades ago it was shown that in response to UV irradiation histones become hyperacetylated facilitating more efficient repair, suggesting that acetylation induced changes in chromatin structure increase DNA accessibility to DNA repair machinery, and not just transcriptional factors (Ramanathan and Smerdon, 1986, 1989).

The earliest detectable acetylation event at DSBs is acetylation of conserved lysines within the N-terminal tails of histone H3 and H4. Several histone acetyltransferases (HATs), including Nua4, Hat1 and Gcn5 have been shown to be responsible for these DNA-damage dependent modifications (Bird et al., 2002; Birger et al., 2005; Qin and Parthun, 2002; Tamburini and Tyler, 2005). Defects in H3 and H4 acetylaton have been associated with sensitivity to ionizing radiation and defective cell-cycle checkpoints. Interestingly, Nua4 dependent acetylation of the H4 tail is inhibited by serine 1 phosphorylation of the same tail (Utley et al., 2005). However, temporally H4 acetylation precedes S1 phosphorylation which in turn is correlated with deacetylation. Consistent with these results the serine 1 kinase CK2 was found to be associated with the histone deacetylase complex Sin3/Rpd3 (Utley et al., 2005), which has also been linked to DNA DSB repair (Jazayeri et al., 2004). Taken together, these data suggest that Nua4 substrates are deacetylated by the Sin3/Rpd3 complex recruited along with the CK2 kinase which then phosphorylates H4 S1 thereby preventing Nua4 from using the H4 tail as a further substrate for reacetylation. Additional support for this model comes from the report that waves of acetylation and

deacetylation of both the H3 and H4 have been observed during DSB repair in *S. cerevisiae* (Tamburini and Tyler, 2005). Thus, the ability of the cells to survive DNA damage seems to be dependent on the temporal regulation of covalent modifications. It has been suggested that the role of this dynamic regulation of histone modifications might be to restore chromatin to its original state and terminate checkpoint activity after the repair process has been completed (Downs and Cote, 2005; Downs et al., 2007).

Acetylation of lysine 56 on newly synthesized histone H3 just upstream of its histone fold domain, is another abundant modification that plays an important role in DNA repair (Masumoto et al., 2005; Ozdemir et al., 2005). Accordingly, mutation of K56 leaves cells sensitive to genotoxic agents. In *S. cerevisiae* the modification is mediated by the HAT Rtt109 together with the histone chaperone Asf1 and is incorporated throughout the genome during replication (Driscoll et al., 2007; Recht et al., 2006). Although K56 acetylation normally disappears in G2, in the presence of DNA damage the H3 K56 deacetylases Hst3 and Hst4 are downregulated and acetylation is maintained in a Rad9 dependent manner (Celic et al., 2006; Maas et al., 2006; Masumoto et al., 2005). It has been proposed that the DNA damage function of this modification is mediated through the key structural position of the lysine, which contacts the phosphodiester backbone at the entry and exit points of the nucleosome core. Consistent with this idea, it has been reported that incorporation of histones with acetylation mimicking mutation K56Q into nucleosomes renders chromatin hypersensitive to micrococcal nuclease digestion (Masumoto et al., 2005). This argues that acetylation of K56 facilitates remodeling of chromatin structure by directly weakening histone H3-DNA interactions, thereby creating a chromatin environment suitable for efficient DNA damage repair.

Methylation

Methylation of lysine and arginine residues is the third most abundant post-translational mark of histones. Histones can be mono-, di- or tri-methylated on lysines and mono- and di- (symmetrically or asymmetrically) methylated on arginines (Lachner et al., 2003; Lee and Stallcup, 2009). Depending on the type of methylation and the residue involved, methylation has been correlated with both gene activation and silencing. For example, methylation of H3 K4, H3 K36 and H3 K79 is often associated with transcriptional activation, while methylation of H3 K9, H3 K27 and H4 K20 is often involved in transcriptional repression. Two of these modifications, methylation of H3 K79 and H4 K20, have also been implicated in the response to UV irradiation. In contrast, arginine methylation has not been studied as well as lysine methylation and no involvement of this modification to the DNA damage response has been found to date.

Methylation of lysine 79 of histone H3 by the *S. cerevisiae* methyltransferase Dot1 (disruptor of telomeric silencing 1), has been shown to have a role in the DNA-damage checkpoint regulation (Huyen et al., 2004). Mutations in *dot1* and the modification site itself which disrupt methylation, result in G1 and intra-S phase checkpoint deficiency and hypersensitivity to UV (Bostelman et al., 2007; Wysocki et al., 2005). Trimethylation of K79 by Dot1 depends on prior ubiquitylation of histone H2B at K123 by the Rad6/Bre1 complex, further demonstrating the intricate interplay between different histone modifications (Briggs et al., 2002). In fact, the regulation of K79 methylation by H2B K123 ubiquitylation was one of the first demonstrations of a unidirectional 'trans-tail' cross-talk where a covalent modification of one histone tail is dependent on a different histone tail. Accordingly, mutations involved in the K123 ubiquitylation pathway also cause checkpoint defects (Giannattasio et al.,

2005). Another unique aspect of K79 methylation is that among the several histone H3 methylation sites identified to date, it is the sole methylation site located in the histone fold domain. Surprisingly, there is no evidence for either global or DSB–specific changes in H3 K79 methylation in response to DNA damage, suggesting that its DNA damage function is likely mediated by increased accessibility of this otherwise buried constitutively methylated site at DSB sites. Indeed, DNA damage dependent exposure of the methylated K79 at DSBs facilitates recruitment of checkpoint and repair machinery.

Methylation of histone H4 at K20 by the histone methyltransferases Set9, and Suv4-20h, has also been implicated in the DNA damage response in fission yeast and mammalian cells respectively (Sanders et al., 2004; Schotta et al., 2008). Similar to K79 methylation, disruption of H4 K20 methylation, by *set9* or K20 mutations, causes UV sensitivity and a mild impairment in DNA-damage checkpoints in fission yeast. In particular, although mutant cells are capable of successfully initiating checkpoint arrest, they are unable to maintain the checkpoint. Also, mice with conditional null alleles for the two Suv4-20h histone methyltransferase genes, which mediate K20 di- and tri- methylation in mammalian cells, are perinatally lethal and have lost nearly all H4K20 di- and tri- methyl states (Schotta et al., 2008). The genome-wide transition to an H4 K20 monomethyl state results in increased sensitivity to damaging stress, since in the chromatin is less efficient for DNA DSB-repair and prone to chromosomal aberrations. Like K79 methylation, the levels of H4 K20 methylation do not change in response to DNA damage arguing that similar mechanisms of exposing the modified region of the histone after DNA damage are likely to exist. Once exposed the methylated K20 presents a docking site for checkpoint proteins.

Ubiquitylation

Conjugation of a one (monoubiquitylation) or multiple (polyubiquitylation) 8.5 kDA ubiquitin peptides to lysine residues is the largest post-translational modification of proteins. It usually occurs via a three step enzymatic reaction carried out by ubiquityl –activating (E1), -conjugating (E2), and –ligating (E3) enzymes. Ubiquitylation can either target its substrate for proteosomal degradation or serve to modify protein function, and only recently it has been linked to DNA repair. Although all four core histones appear to be ubiquitylation substrates, ubiquitylation of histone H3 and H4 is least abundant. Nevertheless, a temporary H3 and H4 ubiquitylation is induced by UV irradiation, catalyzed by the CUL4-DDB-Roc1 complex. It has been suggested that H3 and H4 ubiquitylation facilitates assembly of NER factors by modulating chromatin structure (Wang et al., 2006).

The main histone ubiquitylation substrate in mammalian cells is histone H2A, and the modification is specifically induced during DNA damage in response to UV irradiation (Bergink et al., 2006). In contrast to mammalian cells, mono-ubiquitylation of histone H2B at K123 by the Rad6/Bre1 E1/E2 complex is the most abundant histone ubiqutylation mark in *S. cerevisiae* (Robzyk et al., 2000). Although there is no evidence that H2B ubiquitylation is induced upon DNA damage, it is nevertheless required for proper response to several DNA damaging sources, including UV. Indeed, absence of this modification affects activation of checkpoint kinases Rad53 directly, and Rad9 indirectly through its effect on H3 K79 methylation (Giannattasio et al., 2005).

Recruitment of effector proteins

In addition to their direct effect on chromatin structure by the 'cis' mechanism, histone modifications indeed play an important role in DNA repair

by facilitating chromatin association of DNA damage response proteins via the 'trans' effector binding mechanism. In the past decade, a number of conserved histone modification-specific binding domains have been identified, many of them found in proteins involved in the cellular DNA damage response. Bromodomains were the first protein modules shown to selectively interact with a covalent histone modification, and remain the only known protein fold that recognizes acetylated lysines in sequence-specific contexts (Dhalluin et al., 1999). These domains are present in many transcriptional regulators with histone acetyltransferase activity such as Gcn5, PCAF and $TAF_{II}250$, and components of chromatin remodeling complexes such as RSC and Swi/Snf.

In contrast to bromodomains, histone methylation targeting modules define a broader group of recognition modules, organized into different classes. The largest class of evolutionarily conserved methyl-binding protein folds known as the Royal superfamily, includes chromodomains, malignant brain tumor (MBT) domains and tudor domains (Maurer-Stroh et al., 2003; Taverna et al., 2007). Increasing evidence within the past five years, has demonstrated a role for methylation-dependent tudor domain interactions in the DNA damage response. For example, the mammalian checkpoint protein 53BP1 (53 binding protein 1) and Rad9, its functional homolog in budding yeast, contain tandem tudor domains that bind to methylated K79 on histone H3. Interestingly, 53BP1 has DNA damage sensor properties and localizes to DSBs *in vivo* in a K79 methylation-dependent manner. Indeed, mutations within the tudor domain which abrogate 53BP1 interaction with methylated lysines, as well as suppression of Dot1, the enzyme responsible for K79 methylation, abolish 53BP1 recruitment to DSB sites *in vivo* (Huyen et al., 2004). Recent experiments suggest that 53BP1 also binds dimethylated H4 K20 *in vitro* and methylation of this residue by the mammalian PR-SET7 methyltransferase which shows a preference

for carrying monomethylation, is required for irradiation-induced foci formation in mammalian cells (Botuyan et al., 2006). Given that methylation of H3 K79 and H4 K20 localize to different chromatin domains, it is likely that they both contribute to 53BP1 recruitment depending on the specific chromatin context. Similarly, initial recruitment of the fission yeast checkpoint protein Crb2, which contains a noncanonical tudor fold related to that of 53BP1, is also dependent on recognition of the histone H4 K20 methylation, via the double tudor domains (Botuyan et al., 2006; Sanders et al., 2004).

In addition to the royal superfamily class, several other methyl-binding folds have been identified including WD40 repeats (Wysocka et al., 2005) and plant homeodomain (PHD) fingers (Wysocka et al., 2006). Although they primarily function in transcriptional regulation, there are few reports linking these modules to the DNA damage response. For example, it's been shown that the PHD finger protein ING2 tethers the repressive Sin3a-HDAC1 complex to highly active, proliferation specific genes after the exposure to DNA-damaging agents (Pena et al., 2006; Shi et al., 2006). Similarly, the PHD finger of the ING1 tumor suppressor is required for the DNA repair and apoptotic activities of ING1 (Pena et al., 2008).

Numerous phosphate-binding modules have also been described, however mainly for non-histone proteins. In fact, this phosphate-mediated effector-recognition has been a paradigm for signal transduction pathways (Seet et al., 2006). Phospho-histone dependent interactions on the other hand, have only been identified for two types of effectors and only one of them is directly involved in the DNA damage response. The first phospho-serine histone binding module is the 14-3-3 family of proteins, which has seven distinct isoforms involved in regulation of signal transduction, chromosome condensation and apoptotic cell death (Dougherty and Morrison, 2004; Seet et al.,

2006). 14-3-3 isoforms interact with histone N-terminal H3 tails in a phophorylation-dependent manner (Macdonald et al., 2005).

BRCT (breast cancer susceptibility protein C-terminal) domains on the other hand, appear to be histone-specific γH2A.X binding modules. They are found in several proteins involved in the DNA damage response including the 53BP1 fission yeast homologue, Crb2. Although recruitment of Crb2 to damage foci is also dependent on the tudor domain interaction with H4 K20 methylation, the accumulation of Crb2 at damage foci is independently regulated by γH2A.X as well (Nakamura et al., 2004). It is likely that BRCT γH2A.X-binding domain interaction with this damage induced phosphorylation site may be stabilized via the recognition of the H4 K20 methylation. Mediator of DNA damage checkpoint protein 1 (MDC1, also known as NFBD1), is another BRCT domain-containing protein that is a key regulator of the DNA damage response in higher eukaryotes (Stucki and Jackson, 2004). Consistent with the BRCT being a γH2A.X phospho-recognition module, MDC1 localizes to DNA-damage induced foci in a γH2A.X-dependent manner (Peng and Chen, 2003). Structural studies have accordingly revealed a direct interaction between the γH2A.X phospho-epitope and the tandem repeats of MDC1 (Lee et al., 2005; Stucki et al., 2005).

Additional γH2A.X-dependent protein interactions have also been observed although the specific binding modules have not been identified. For example, the Nua4 HAT complex associates specifically with γH2A.X-phospho peptides and this interaction is dependent on at least one Nua4 subunit, the actin related protein 4, Arp4 (Downs et al., 2004). Arp4-dependent Nua4 complex recruitment to the DSBs *in vivo* is also established, however the structural basis for this Arp4-γH2A.X interaction remains unclear. Interestingly, Nua4 recruitment to chromatin as well as its histone acetyltransferase activity are also required and temporally precede recruitment of chromatin remodeling

complexes Ino80 and Swr1 to DSB sites (Downs et al., 2004). However, specific bromodomain-containing factors potentially responsible for the Nua4-dependent recruitment of chromatin remodeling complexes have not been identified to date.

ATP-dependent chromatin remodeling

Histone modification-mediated effector recruitment can also target ATP-dependent chromatin remodeling complexes as another mean of inducing function specific alterations of the chromatin fiber. ATP-dependent chromatin remodeling complexes use the energy of ATP hydrolysis to physically manipulate chromatin structure, either by repositioning or removing nucleosomes, or by exchanging histone components and thereby altering nucleosome composition. The catalytic subunits of these energy-dependent multi-subunit complexes are ATPases of the large superfamily of Swi2/Snf2 helicases. Based on the presence of a distinct motif outside the ATPase region, the superfamily is divided into the following four classes: (1) Swi/Snf class which contains a bromodomain, (2) Iswi, characterized by a DNA binding – SANT domain, (3) Chd class has both a chromodomain and a DNA binding capacity, and (4) Ino80. Members of the Ino80 class, which includes Swr1, do not possess any known domains and are characterized by an insertion that splits the ATPase domains in two segments. Recent work has demonstrated that the ATP-dependent remodeling complexes, such as NURF (nucleosome remodeling factor), are involved in transcriptional gene regulation. In particular, through their association with histone post-translational modifications (Wysocka et al., 2006), recent studies have revealed an additional, transcription-independent role for four chromatin remodeling complexes in the DNA damage response. Indeed, Ino80, Swr1, as well as the Swi/Snf class members Rsc and the founding member Swi/Snf itself, have been shown to mediate large-scale reconfiguration of

chromatin surrounding the break site thereby facilitating access to repair and checkpoint proteins to DNA lesions (Bennett et al., 2001; Mizuguchi et al., 2004; Shen et al., 2000; Shim et al., 2005). Consistent with their role in the DNA damage response, mutations in several of the subunits belonging to these complexes render cells hypersensitive to DNA break-inducing agents.

The DNA damage response function of the chromatin remodeling complexes appears to be mediated by their recruitment to DNA DSBs. Chai and colleagues found that Rsc and Swi/Snf remodelers localize to DNA DSB sites *in vivo,* suggesting that they play a direct role in DNA repair (Chai et al., 2005). In their study, Rsc was found to appear very early after DSB induction, followed by the appearance of Swi/Snf. The DNA repair proteins Mre11 and Ku70 are recruited with the same kinetics as two of the Rsc members, Rsc8 and the catalytic subunit Sth1. The Sth1 recruitment is dependent on the presence of Mre 11 and Ku70, as absence of Mre11 abolishes Rsc recruitment to the break. Accordingly, a physical interaction has been seen between the Rsc subunit Rsc1 and the Mre11 and Ku80 proteins (Shim et al., 2005). Swi/Snf has also been associated with NER as its *in vitro* activity is dependent on the presence of NER factors XPC, XPA and RPA (Hara and Sancar, 2002). *In vivo*, two of the *S. cerevisiae* Swi/Snf subunits, Snf5 and Snf6 have been shown to enhance NER and the silent locus after UV irradiation. Interestingly, Snf5 and Snf6 copurify with NER factor Rad4 (*S. cerevisiae* homologue of XPC) and Rad23, and this binding to the Rad4-Rad23 complex is the likely a mechanism for Swi/Snf recruitment to DNA lesions (Gong et al., 2006).

Components of the Ino80 and Swr1 complexes were found to accumulate at HO-induced DSBs in *S. cerevisiae* in a γH2A.X-dependent manner (Downs et al., 2004). This observation represents a wonderful example that the mechanisms that modulate chromatin dynamics, namely histone variants, histone post-

Accordingly, absence of a functional Tip60 complex, leads to failure to acetylate H2Av and accumulation of phosphorylated H2Av in response to DSBs induced by ionizing radiation. Based on these findings it is likely that in budding yeast acetylation of γH2A.X by Nua4 near DSBs may stimulate replacement of γH2A.X with H2A.Z through the recruitment of the chromatin remodelers Ino80 and Swr1.

Interestingly, *S. cerevisiae* Swr1, essentially a subcomplex of *Drosophila* Tip60, has been shown to preferentially associate with Htz1, a homologue of the mammalian histone variant H2A.Z and catalyze nucleosomal histone exchange of H2A/H2B dimers with Htz1/H2B dimers *in vitro*. *In vivo* Swr1 catalyzes the incorporation of Htz1 into chromatin in order to prevent heterochromatin spreading (Krogan et al., 2003; Mizuguchi et al., 2004). A report by the Peterson and colleagues indicates that Swr1 functions in a similar fashion during DNA damage by depositing Htz1 into chromatin near an HO-induced DSB (Papamichos-Chronakis et al., 2006). Indeed, nucleosomes displacement has been observed from regions flanking HO breaks in order to facilitate DNA break processing and efficient repair (Tsukuda et al., 2005). This eviction however, is independent of swr1, which appears to antagonize Ino80 function by replacing Ino80 evicted nucleosomes with their Htz1 containing counterparts to presumably restore chromatin structure after repair. Nevertheless, the Swr1 dependent Htz1 enrichment in DSB regions is only observed in strains lacking a functional Ino80 and it is correlated with depletion of γH2A.X at sites of DSB. Given that Ino80 also shares subunits with Tip60, taken together, these results strongly indicate that Ino80, Swr1 and Nua4 complexes function together to facilitate Htz1 and γH2A.X exchange at lesions, mimicking the larger Tip 60 complex in mammalian cells. In summary, the current chromatin remodeling model holds that during DNA damage in budding yeast, Nua4 acetylation of

histones at DSBs facilitates downstream displacement of γH2A.X by Ino80 followed by the Swr1 dependent replacement with H2A.Z at sites of DNA damage.

Meiosis

The information obtained from DNA damage DSB-repair studies, has implications on other biological processes involving physiological DSBs, such as meiosis. Meiosis is a cellular division program characterized by a single round of genome duplication followed by two successive rounds of chromosome segregation to produce haploid gametes from diploid germ cells. The key to this reductional nuclear division is the reciprocal exchange of genetic information between the homologous parental chromosomes that occurs during prophase of the first meiotic division, a process that requires the recognition and alignment of the homologues, formation of synaptonemal complex – a protein assembly that connects the homologues, and subsequent meiotic recombination.

Meiotic recombination is initiated through the introduction of programmed DNA DSBs by a topoisomerase-like protein known as Spo11, which is conserved from yeast to humans (Keeney et al., 1997). In most organisms these DSBs are crucial for initiating the intimate pairing of the parental chromosomes, termed synapsis, which in turn facilitates their subsequent repair (Mahadevaiah et al., 2001; Roeder, 1997). During repair, the DSBs are processed in a 5′–3′ direction, resulting in the formation of 3′ single-stranded DNA overhang that invades an intact nonsister chromatid homologous donor template for its repair, a process referred to as crossover. Ultimately, the successful resolution of the crossover intermediates results in a reciprocal exchange of chromatid arms. DSBs therefore appear to be an early step in the meiotic recombination process

and a prelude to the reshuffling of the maternally and paternally derived genomes during meiosis.

As such, it is not surprising that histone post-translational modifications that mediate the damage DSB response might also play critical roles in facilitating meiotic recombination. Indeed, Spo11-dependent γH2A.X formation associated with meiotic DSBs on all chromosomes has been observed in mouse spermatocytes during early stages of meiotic prophase I (Mahadevaiah et al., 2001). However, the same study also identified a second wave of sex chromosome-specific Spo11-independent γH2A.X accumulation during later stages of meiotic prophase revealing a novel meiotic role for γH2A.X. An interesting feature of the sex chromosome, or the X-Y body as it is commonly referred to, is the remarkable condensation that occurs during meiotic prophase to form macrochromatin body within which X- and Y- linked genes are transcriptionally repressed (Solari, 1974). The kinetics of the massive Spo11-independent accumulation of γH2A.X throughout the X-Y chromatin closely correlates with the chromatin condensation of the X-Y body arguing that γH2A.X plays a causal role in heterochromatinization of the sex body during meiosis. Evidence for such physiological role of the γH2A.X association with sex chromosomes, came from a subsequent study whereby the X and Y chromosomes of histone H2A.X-deficient spermatocytes failed to condense to a sex-body, did not initiate meiotic sex chromosome inactivation and exhibited severe defects in X-Y pairing (Fernandez-Capetillo et al., 2003). While the sex-body-specific γH2A.X function is independent of Spo11 meiotic recombination-associated DSBs, it remains a mystery whether Spo11-independent DSBs are involved in triggering the γH2A.X-mediated heterochromatinization of the XY-chromosome. Several recent reports argue that the γH2A.X-mediated chromatin condensation of the sex-body might be actually a response to unpaired

translational modifications and ATP-dependent chromatin remodeling, are functionally linked. Accordingly, the recruitment of Ino80 and Swr1 is impaired in strains lacking the γH2A.X kinases Mec1 and Tel1, as well as the phospho-acceptor site itself (Morrison et al., 2004; van Attikum et al., 2004). The association of Ino80 and Swr1 complexes with the chromatin surrounding DSBs has been show to occur through their Nua4-shared subunit, Arp4, which directly interacts with γ-H2A.X (Downs et al., 2004). However, localization of Ino80 and Swr1 subunits is delayed relative to Nua4 appearance at DNA DSBs, suggesting that the Arp4 - γH2A.X interaction is not the sole mechanism by which these complexes accumulate at sites of DNA damage. In fact, Morrison and colleagues found that another Ino80 specific subunit, Nhp10, is also necessary for stable Ino80 association with γH2A.X *in vitro* and for the recruitment of Ino80 to DNA DSBs *in vivo* (Morrison et al., 2004). Given that Ino80 complexes isolated from *nhp10* mutants lack both Nhp10 and Ies3 subunits, it is likely that Nhp10 and Ies3 subunits facilitate the Arp4-mediated Ino80 - γH2A.X interaction.

Although γH2A.X has emerged as a central player in assembly of chromatin remodeling complexes at DSBs, Ino80 and/or Swr1 enrichment at DNA lesions is not solely influenced by γH2A.X interactions. As already mentioned, Nua4 mediated histone acetylation has also been shown to play a role in the process (Downs et al., 2004). Indeed, the DSB association of the Rvb1 component of Ino80 and Swr1 is impaired by mutations in the Nua4 catalytic subunit Esa1, arguing that chromatin needs to be acetylated before remodelers can be efficiently recruited to the break. Also consistent with this hypothesis is the fact that the *Drosophila* HAT/chromatin remodeling complex Tip60, an orthologue of both *S. cerevisiae* Swr1 and Nua4, preferentially binds and acetylates a phosphorylated histone H2A.Z/H2A.X fusion variant in *Drosophila*, known as H2Av, and exchanges it for unmodified H2Av (Kusch et al., 2004).

chromosomes i.e. asynapsis of the non-homologous sex chromosomes, to ensure transcriptional silencing of asynapsed chromosomes or chromosome regions (Baarends et al., 2005; Sciurano et al., 2007; Turner et al., 2006; Turner et al., 2005).

There is already a precedent for heterochromatin element involvement in meiosis, such as the role of centromeres and telomeres in controlling the position of meiotic recombination events (Loidl, 1990; Scherthan, 2001; Yamamoto and Hiraoka, 2001). Moreover, numerous studies in different organisms have identified an increasing number of repressive histone modifications that play a critical role in the meiotic process. For example, the *C. elegans* HIM-17 protein, which is required for H3 K9 methylation, was shown to be necessary for the formation of DSBs that initiate meiotic recombination (Reddy and Villeneuve, 2004). Additionally, histone H2A ubiquitylation, was found to localize to unpaired and silenced chromatin regions, including the X-Y body in male meiotic prophase of mouse, rat and human (Baarends et al., 2005). It would be interesting to find out whether additional histone modification might be playing a role in meiosis. Such studies would also help define the events of meiotic prophase and shed some light on the mechanism of synapse formation and the importance of DSBs in the process. For my thesis I chose to study DSBs and their involvement in meiosis in the ciliate *Tetrahymena thermophila*, especially because synaptonemal complexes have not been observed in this organism and otherwise very little is known about the process in this system.

Tetrahymena thermophila

Tetrahymena is a member of the ciliated protozoa, a group of unicellular eukaryotes that inhabit freshwater environments. It is a motile, relatively large organism, about 50 μm long and 20 μm wide. Although unicellular, *Tetrahymena* exhibits evolutionary features similar to multicellular organisms. These features

include a clear separation of the germ-line and soma, exemplified by the possession of two related but functionally distinct genomes. One of the most distinctive features of ciliates and therefore *Tetrahymena* is that the two genomes are carried in separate nuclei present within a single cell, a phenomenon referred to as nuclear dimorphism. The germ-line in *Tetrahymena* is stored in the smaller diploid micronucleus, whereas the somatic genome is contained within the polyploid macronucleus. The transcriptionally inert micronucleus, which is capable of both mitosis and meiosis, contains two complete haploid genome sets arranged on 5 chromosomes. In contrast, the macronuclear genome is made up of multiple (~45) copies of rearranged micronuclear subset of genes and is responsible for all gene expression thus determining the cell's phenotype. In addition to germ-line/soma separation, *Tetrahymena* possesses a typical eukaryotic life cycle, including a vegetative stage limited to the diploid phase of the cell cycle, and conventional meiosis followed by internal fertilization through union of exchanged haploid gamete nuclei, which is restricted to the sexual stage of the life cycle.

Tetrahymena life cycle

During the asexual, vegetative stage of the life cycle, *Tetrahymena* cells reproduce exclusively by binary fission, as long as they are maintained in rich media (see stage 7, Figure 1.6). The doubling time is ~2 hours, during which the micronucleus divides by conventional mitosis and the macronucleus divides amitotically by elongating and pinching into two during cytokinesis.

Conjugation is the sexual stage of *Tetrahymena* life cycle and can be induced with high efficiency and synchrony by mixing sexually mature cells of complementary mating types which have been nutritionally starved for several hours. Citologically, conjugation consists of meiotic prophase, three prezygotic

nuclear divisions, two post-zygotic nuclear divisions and macronuclear development. The nuclear events of conjugation (Orias, 1998), depicted in Figure 1.5, can be readily visualized by fluorescent staining with DNA-specific dye DAPI. Under stationary conditions the cells begin to pair within 30 min after mixing, and achieve 85-90% pairing efficiency within 2 hours post initiation (see 1, Figure 1.6). As soon as stable pairs are formed, the micronuclei in each conjugating partner move away from the macronucleus and meiotic prophase I is initiated. During this stage the micronuclei begin to elongate, increase in length over 50-fold and adopt a semi-circular crescent shape. This stage is similar to the horsetail stage of meiosis in *S. pombe* (Nimmo et al., 1998; Yamamoto and Hiraoka, 2001) when homologous chromosomes are aligned and presumably undergoing meiotic crossing over. The crescent micronucleus features a side-by-side alignment of the ten bivalent chromosomes as parallel bundles, and this polarized arrangement resembles a classical bouquet with most of the telomeres assembled near one end (Loidl and Scherthan, 2004) and centromeres occupying the opposite end (Mochizuki et al., 2008). This parallel arrangement of the chromosomes is stabilized through the spatial constraints imposed by the elongated meiotic micronuclear shape. The crescent also ensures juxtaposition of homologous regions and facilitates homologous recombination in the absence of synaptonemal complex which has not been observed in *Tetrahymena.* Based on the stage of elongation or contraction of the micronucleus, the meiotic prophase I has been divided into six stages (Cole et al., 1997; Martindale et al., 1982; Sugai and Hiwatashi, 1974). Stage I begins when the micronucleus moves away from the macronuclear pocket where it resides during interphase. During stage II the micronucleus begins to elongate, with the maximum micronuclear elongation into full crescent represented by stage IV when the five bivalent chromosomes are in parallel arrangement. After stage IV the micronucleus begins to contract

back to its original shape and the bivalent chromosomes begin to separate which is accomplished during the last stage of meiotic prophase I, stage VI.

Following meiotic prophase I the micronuclei complete two meiotic divisions to yield four haploid nuclei (see 2, Figure 1.6). The nuclei undergo a process referred to as 'nuclear selection' in which three of the haploid nuclei disintegrate and the only remaining functional nucleus divides mitotically, producing two genetically identical gametic pronuclei. One of the pronuclei, designated as the 'stationary pronucleus' remains in the cell of origin, while the other, 'migratory pronucleus' is reciprocally exchanged between the cells of the mating pair (see 3, Figure 1.6). The migratory pronucleus fuses with the stationary micronucleus of the recipient cell forming a diploid zygotic nucleus (see 4, Figure 1.6). The new zygote nucleus is the progenitor of both the micronucleus and the macronucleus of the developing cell. Following the fusion event, the nucleus immediately undergoes two rounds of mitosis, giving rise to four genetically identical diploid nuclei (see 5, Figure 1.6). In the last stage, defined as macronuclear development, the two posterior nuclei are maintained as micronuclei, whereas the two anterior nuclei differentiate into macronuclei. At this stage the developing macronuclei, also referred to as anlagen, undergo extensive DNA rearrangements of the germ-line-derived chromosomes whereby ~15% of the micronuclear genome is eliminated. Meanwhile, the old parental macronucleus is destroyed by an apoptotic-like mechanism, characterized by the production of oligonucleosome-sized DNA fragments (Davis et al., 1992). Finally, conjugation is completed by exconjugates' separation and restoration of normal nuclear composition through one round of binary fission.

Figure 1.6: Ciliate life cycle

(0) Vegetative cells. Small and large circles are micronucleus (MIC) and macronucleus (MAC) respectively. (1) Two paired cells, homozygous for alternative alleles at one locus. (2) MICs undergo meiosis, and four haploid nuclei are produced. Only the anterior meiotic product remains functional; the other three disintegrate. This is the stage at which meiotic crossing-over, used for genetically mapping the MIC genome, occurs. (3) Mitotic division of functional meiotic product yields genetically identical migratory (anterior) and stationary (posterior) gamete pronuclei. (4) Migratory pronuclei are reciprocally exchanged and fuse with stationary pronuclei of the recipient cell, forming the zygote nucleus, which is diploid and, in this instance, heterozygous. (5) The zygote nucleus undergoes two mitotic divisions, giving rise to four genetically identical diploid nuclei. (6) Two of those nuclei (checkerboard-filled) have differentiated into macronuclei; the other two (solid and white halves) remain diploid micronuclei. The old MACs (at the bottom of each conjugant) are being resorbed and will be lost. This is the stage at which chromosome fragmentation and other site-specific DNA rearrangements occur in the differentiating MAC. The two exconjugants have separated and undergo their first binary fission, restoring the normal nuclear composition (back to stage 0). (7) Vegetative cell dividing by binary fission. The diploid MIC has divided mitotically; the polyploid MAC is undergoing "amitotic division," pinching off into roughly equal halves. This life cycle scheme is highly conserved among ciliates, although differences of detail occur in particular groups and species (adapted from Orias, 1998).

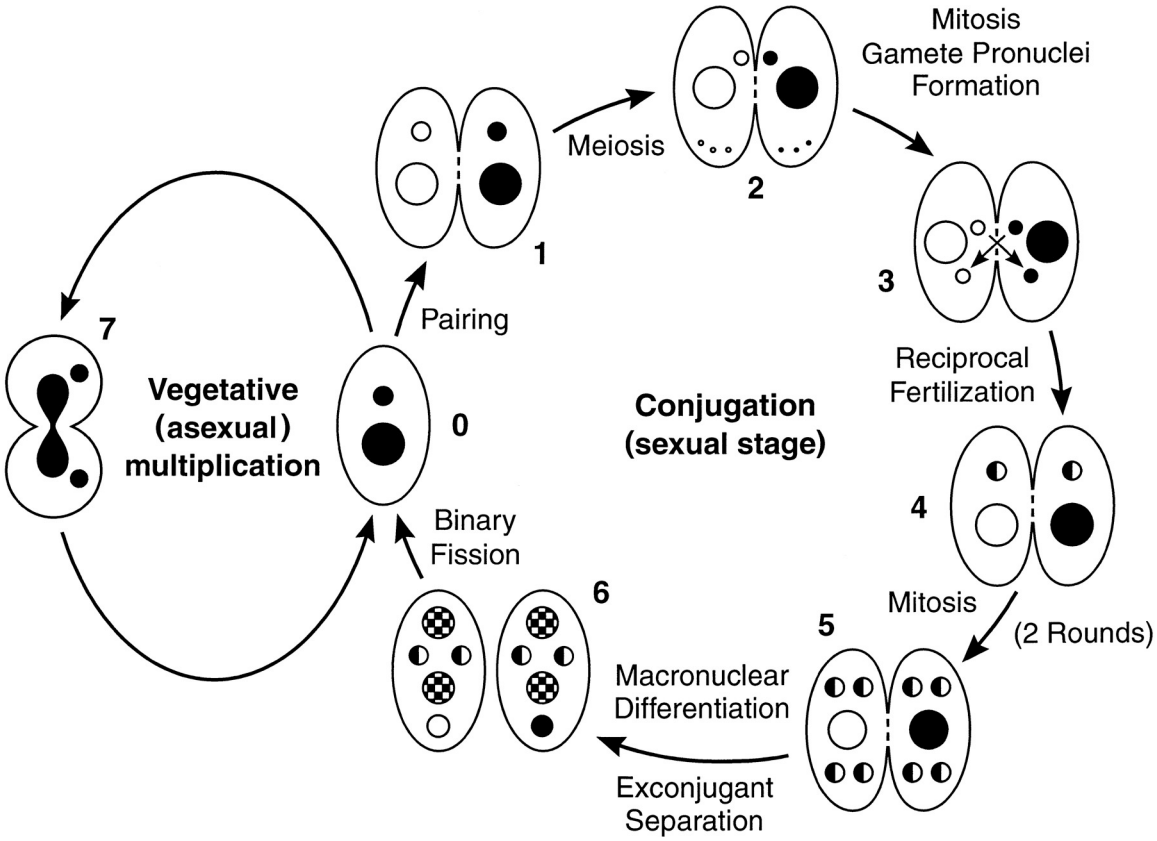
Mitosis
Gamete Pronuclei
Formation
Meiosis
2
1
3
Reciprocal
Fertilization
Pairing
7
Vegetative
(asexual)
multiplication
0
Conjugation
(sexual stage)
4
Binary
Fission
6
Mitosis
(2 Rounds)
5
Macronuclear
Differentiation
Exconjugant
Separation

Tetrahymena as a model organism

Tetrahymena offers several advantages that make it a specially useful experimental system for biological research. Its large size facilitates detailed morphological investigations and its rapid doubling time of ~2.5 hours at 30°C allows for quick culturing to high population densities (10^6 cells/ml). *Tetrahymena* genome has also been recently sequenced providing additional utility for the use of this organism in genetic research.

As a result, *Tetrahymena* has offered many insights into general features of eukaryotic biology such as the discovery of dynein (Gibbons and Rowe, 1965), self-splicing RNA (Kruger et al., 1982) and telomerase (Collins et al., 1995; Greider and Blackburn, 1985, 1989). Additionally, the macronuclear differentiation process has revealed a role for small RNAs in whole-genome rearrangements (Mochizuki et al., 2002; Taverna et al., 2002) which are mechanistically similar to the RNA-directed establishment of silent chromatin (Volpe et al., 2002). The compartmentalization of the gene expression states reflected by the two distinct nuclei in *Tetrahymena* has also provided a fertile ground for the study of the function of chromatin proteins and their modifications in epigenetic regulation. In fact, new chromatin regulators such as the first histone acetyltransferase (HAT) type A (Brownell and Allis, 1995; Brownell et al., 1996) as well as some of the histone variants were first identified in *Tetrahymena* by comparative analyses of the germline and somatic nuclei (Allis et al., 1980; Allis et al., 1979).

Specifically, transcriptionally active macronuclei in *Tetrahymena* contain two primary sequence variants absent from the micronuclei. One of them is the minor histone H2A variant, hv1, encoded by a single gene, HTA3. Evidence suggests that this variant performs an essential function (Liu et al., 1996) presumably through its association with transcriptionally competent chromatin

(Allis et al., 1982; Stargell et al., 1993). The other macronuclear specific minor histone variant, hv2, is also encoded by a single gene, HHT3, and differs in 16 amino acids from the major histone H3 proteins. Much like the H3.3 replacement variants of multicellular eukaryotes, which it closely resembles, hv2 is constitutively expressed i.e. it is synthesized and deposited in macronuclei of non-growing as well as growing cells (Bannon et al., 1983).

The most striking differences in the histone proteins between the *Tetrahymena* macronuclei and the micronuclei are in the linker histones. The only macronuclear histone H1, encoded by a single gene, HHO, is a highly positively charged, 163 amino acid small protein, missing its central, hydrophobic domain. The micronuclear linker histones however, consist of 4 proteins, α, β, γ and δ, a proteolytic processing products of a polypeptide precursor X, also encoded by a single gene, MLH.

As opposed to the minor variants and the linker histones, biochemical analyses of purified histones and of cloned histone genes demonstrate that a standard complement of highly conserved core histones, each encoded by two genes, is present in both *Tetrahymena* nuclei. Both of the primary histone H3 proteins as well as histone H4 proteins encoded by their respective dual gene copies are identical. The two histone H2B genes however, encode for somewhat divergent proteins. Similarly, the two major histone H2A proteins encoded by their respective genes, HTA1 and HTA2, also slightly differ from each other, with H2A.S being the larger, slower migrating form on SDS gels, and H2A.F, a 5 amino acid shorter, faster migrating form. Neither of the two genes encoding the major H2A histones is essential, and each can substitute for the other during vegetative growth (Liu et al., 1996). Intriguingly however, although both major H2A histones are expressed in roughly equimolar amounts in the macronucleus, the steady-state levels of the two histones show enrichment of H2A.S in the

micronucleus (Allis et al., 1980). Given the unique role of the otherwise transcriptionally silent micronucleus in the conjugation process described above, it is plausible that the differences in relative levels of the two H2A proteins between nuclei could reflect a conjugation-specific functional role for H2A.S, a hypothesis I explored in my thesis research covered in Chapter 2.

CHAPTER 2

PHOSPHORYLATION OF HISTONE H2A.S AT THE SQ MOTIF IS REQUIRED FOR DNA REPAIR AND MEIOSIS IN *TETRAHYMENA THERMOPHILA*

Introduction

DNA double strand breaks (DSBs) represent deleterious lesions which can either be caused by extrinsic sources such as ionizing radiation and mutagens; or produced endogenously by stalled replication forks, oxygen radicals, and as intermediates of programmed cellular events including meiosis, V(D)J recombination, mating type switching and apoptosis. Inefficient repair of these lesions can lead to mutations, aberrant chromosomal rearrangements, or loss of genetic information, which ultimately can result in diseases such as cancer. As such, the repair of DNA DSBs is critical for maintenance of genomic stability and cells have evolved mechanisms for detecting the presence of the break and restoring the integrity of the DNA. Since DNA repair functions in the context of chromatin, it is not surprising that histone modifications have been found to play an important role in this process.

One of the earliest chromatin-associated events that occurs at DSBs is phosphorylation of the histone H2A variant H2A.X on a serine within a conserved C-terminal SQ motif, producing a modified protein designated as γH2A.X (Rogakou et al., 1998). Within minutes of DSB, γH2A.X spreads over 50-100 kilobase domains flanking DSB in budding yeast, where H2A.X is the major form of H2A (Shroff et al., 2004). Likewise, in mammalian cells where the H2A.X variant represents ~10% of the total H2A population, ATM/ATR induced γH2A.X extends over megabase regions surrounding the DNA break induced by

ionizing radiation (Rogakou et al., 1999). γH2A.X is involved in processes involving programmed DNA DSBs intermediates such as V(D)J rearrangement during lymphocyte development in mammals (Chen et al., 2000), as well as meiotic recombination in mice germ cell development (Mahadevaiah et al., 2001). Therefore γ-H2A.X is thought to serve as a general signal for the presence of a DSB and has been shown to be required for efficient DNA repair in budding yeast and mammalian cells (Bassing et al., 2002; Downs et al., 2000; Redon et al., 2003) where it mediates localization of numerous break-recognition and repair factors to the DSB sites (Downs et al., 2004; Fernandez-Capetillo et al., 2002; Nakamura et al., 2004; Strom et al., 2004).

Despite the significant progress in defining the function of γH2A.X in higher eukaryotes, the presence of this variant has not been well studied in lower eukaryotes. Interestingly, a sequence analysis of the H2A family members of the ciliated protozoa *Tetrahymena thermophila,* revealed that the slower-migrating isoform of the two major types of *Tetrahymena* histone H2A, hereafter referred to as H2A.S, contains a C-terminal SQ motif reminiscent of the conserved H2A.X motif in other organisms (Figure 2.1A). I then sought to investigate whether the *Tetrahymena* histone H2A.S is phosphorylated at the suspected SQ motif, and if so, whether this phosphorylation event is functionally important in processes that involve this isoform, but not the faster migrating form, H2A.F. Indeed, using a γH2A.X-specific monoclonal antibody, I established that *Tetrahymena* H2A.S is phosphorylated at the SQ serine 134 in response to DSBs induced by chemical agents and during meiosis. In collaboration with Qinghu Ren and Xiaoyuan Song in the laboratory of Dr. Martin Gorovsky at the University of Rochester, NY, we found that H2A.S S134A mutation abolishes the phosphorylation of the SQ motif and although not lethal, it leads to meiotic defects in *Tetrahymena* cells. These results demonstrate that one of the

Tetrahymena major histone H2As functions as a typical H2A.X and for the first time establish its presence in ciliated protozoa. In addition, they establish that γH2A.X is important for maintaining genomic stability during different stages of *Tetrahymena* life cycle. Most importantly, this study provides the first evidence for the existence of meiotic DSBs in *Tetrahymena* and defines the time interval of meiotic recombination in this organism.

Results

Tetrahymena thermophila H2A.S is phosphorylated in response to induced DSBs

Conservation of the C-terminal SQ H2A.X sequence motif within the C-tail of histone H2A.S, one of the two major histone H2As in the ciliate *Tetrahymena thermophila,* prompted an investigation into whether *Tetrahymena* H2A.S is phosphorylated in response to DSBs. For that purpose, DNA damage was induced by a 4-hour treatment of *Tetrahymena* cultures with 5 mM methyl methanesulfonate (MMS), an alkylating agent that introduces DNA lesions, subsequently converted to DSBs. A species cross-reactive mouse monoclonal antibody (Upstate Biotechnology, cat. # 05-636) raised against mammalian γ-H2A.X epitope, was then used for immunofluorescence (IF) analysis of the MMS treated *Tetrahymena* cells. The antibody specifically detected a signal in micronuclei, and to a lesser extend, also macronuclei of MMS treated cells (Figure 2.1B). The difference in γH2A.X staining intensity in micronuclei versus macronuclei from MMS-treated cells could reflect differential activities of the phosphorylation machinery in different nuclei, or else it could be due to previously observed enrichment of H2A.S in the micronucleus (Allis et al., 1980). In contrast, micronuclear γH2A.X staining was absent in untreated cells, demonstrating that the antibody signal is specific to DSBs induced by the DNA-damaging agent.

Tetrahymena thermophila H2A.S is phosphorylated during meiosis

As previously observed histone steady-state levels in *Tetrahymena* show enrichment of H2A.S in the micronucleus (Allis et al., 1980), it is plausible that these differences in relative levels of the two H2A forms between nuclei reflect distinct functional roles for the different H2As. In particular, higher levels of micronuclear H2A.S could be due to the specialized function of the micronucleus

Figure 2.1: Double strand break (DSB)-induced phosphorylation of the conserved C-terminal SQ motif in *Tetrahymena thermophila* detected by anti γH2A.X specific antibody

A. Amino acid sequences of histone H2A from various organisms were obtained from GenBank (http://www.ncbi.nlm.nih.gov). The accession numbers are as follows: human_H2A.1, NP_254280; human_H2A.X, NP_002096; mouse_H2A.1, NP_783591; mouse_H2A.X, NP_034566; *D. melanogaster*_H2AvD (H2A.Z homologue), NP_524519; *S. pombe*_H2A.2, NP_594421; *S. cerevisiae*_H2A.1, NP_010511; *S. cerevisiae*_H2A.2, NP_009552; *S. cerevisiae*_H2A.Z, NP_014631 (also known as htz1; *T. thermophila*_H2A.S (also known as H2A.1), AAC37291; *T. thermophila*_H2A.F (also known as H2A.2), AAC37292, *T. thermophila*_H2A.Z (also known as hv1), CAA33554. Only the C-terminal regions are shown. Alignment was generated with ClustalW identity algorithm. The conserved SQ motif is highlighted. The suspected phosphorylation site in the SQ motif is labeled in red. The putative *Tetrahymena* H2A.X homologue is enclosed by a red box. Alignment gaps are indicated with a hyphen (-).

B. Immunofluorescence (IF) analysis of wild type vegetatively growing *Tetrahymena* cells treated with 5 mM MMS for 4 hrs to induce double strand breaks (DSBs). Shown are the macronucleus (MAC) and the micronucleus (MIC) stained with a specific monoclonal antibody (Upstate Biotechnology, cat. # 07-636) raised against the phosphorylated C-terminal peptide KATQA[pS]QEY of human H2A.X (red signal).

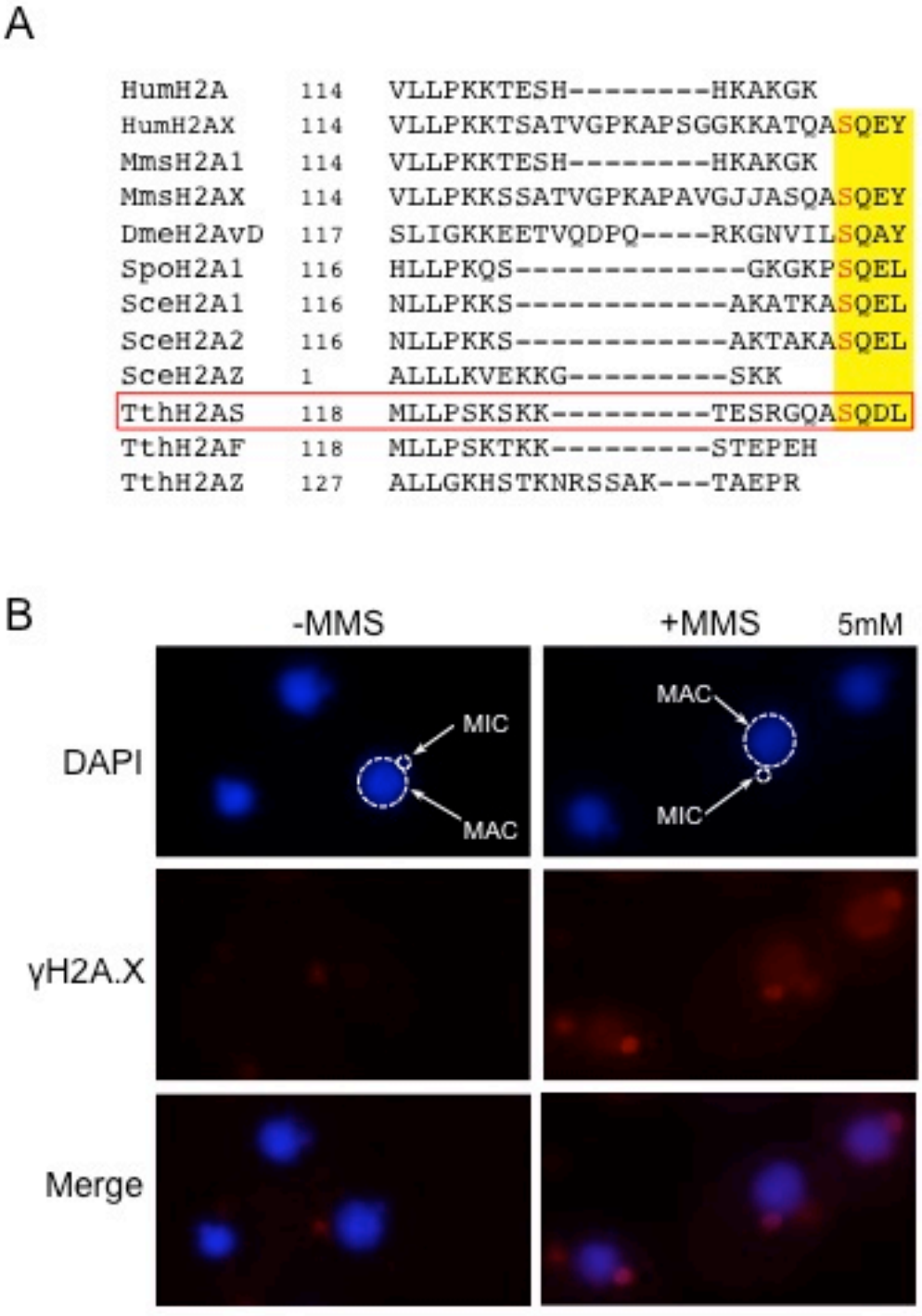
A
HumH2A 114 VLLPKKTESH--------HKAKGK
HumH2AX 114 VLLPKKTSATVGPKAPSGGKKATQASQEY
MmsH2A1 114 VLLPKKTESH--------HKAKGK
MmsH2AX 114 VLLPKKSSATVGPKAPAVGJJASQASQEY
DmeH2AvD 117 SLIGKKEETVQDPQ----RKGNVILSQAY
SpoH2A1 116 HLLPKQS----------GKGKPSQEL
SceH2A1 116 NLLPKKS----------AKATKASQEL
SceH2A2 116 NLLPKKS----------AKTAKASQEL
SceH2AZ 1 ALLLKVEKKG---------SKK
TthH2AS 118 MLLPSKSKK---------TESRGQASQDL
TthH2AF 118 MLLPSKTKK---------STEPEH
TthH2AZ 127 ALLGKHSTKNRSSAK---TAEPR
B
-MMS
+MMS
5mM
DAPI
MIC
MAC
MAC
MIC
γH2A.X
Merge

Figure 2.1

To investigate whether H2A.S phosphorylation functions during *Tetrahymena* meiosis, the γH2A.X specific antibody was used to immunostain *Tetrahymena* cells fixed at the meiosis-specific stage of conjugation. Indeed, strong γH2A.X signal was detected in the elongated micronuclei during the crescent stage, at ~2.5 hours of conjugation, which corresponds to meiotic prophase I (Loidl and Scherthan, 2004; Sugai and Hiwatashi, 1974) (Figure 2.2A). These observations were supported by immunoblotting analysis of acid extracted histones from micronuclei and macronuclei purified by sucrose sedimentation at unit gravity, isolated from either vegetative cells or cells undergoing meiotic prophase I. Only micronuclear histones from cells undergoing meiotic prophase I, collected around 2.5 hours of conjugation, contained substantial amounts of γH2A.X (Figure 2.2B). The signal was absent from macronuclear histones derived from cells collected during the same conjugation time point, consistent with the fact that meiosis in *Tetrahymena* is a micronuclear-specific developmental process. When histones from meiotic micronuclei were resolved on a longer SDS gel containing higher percentage polyacrylamide which allows separation of the two H2A isoforms, the γH2A.X signal was consistent with the slower migrating H2A isoform corresponding to histone H2A.S (Figure 2.2C).

Based on the morphological division of *Tetrahymena* meiotic prophase into six stages, immunofluorescence analysis of various stages during *Tetrahymena* conjugation, showed that γH2A.X signal appears in the meiotic micronucleus as early as stage II of meiotic prophase when the micronuclei just begin to elongate (Figure 2.3b). Taken together these results suggest that the γH2A.X signal is specific to histone H2A.S and this phosphorylation event marks early stages of meiotic chromatin in *Tetrahymena*. Moreover, these observations have greater implications for the understanding of the specific events of *Tetrahymena* meiosis, a process not well studied in this organism. Given the documented association

during conjugation i.e. its potential to undergo homologous recombination during meiosis.

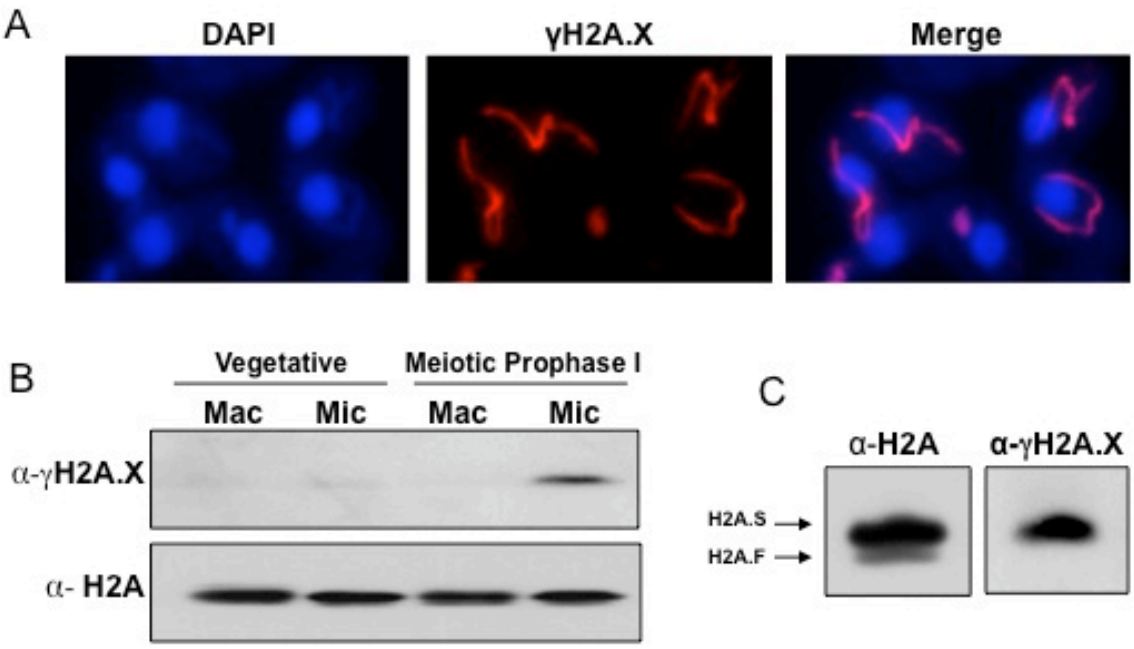

Figure 2.2: Anti- γH2A.X antibody detects meiotic DSB phosphorylation in *Tetrahymena thermophila*

A. Immunofluorescence (IF) analysis of *Tetrahymena* during meiotic prophase I stage of conjugation. Shown are the macronucleus (MAC) and the micronuclear crescent (MIC) stained with anti- γH2A.X antibody (red).
B. Immunoblotting analysis of differentially purified nuclei from vegetative and meiotic prophase I conjugation stage of *Tetrahymena* separated on a short 10 x 8 cm 12% SDS-PAGE and probed with anti- γH2A.X and anti-H2A antibodies.
C. Immunoblotting analysis of differentially purified micronuclei from the meiotic prophase I conjugation stage. The two different *Tetrahymena* H2A isoforms are separated on a longer 10 x 12 cm 15% SDS-PAGE and probed with anti- γH2A.X and anti-H2A antibodies.

of γH2A.X with DSBs (Rogakou et al., 1998), and the fact that DSBs are considered to be essential intermediates in the meiotic recombination process (Cao et al., 1990; Mahadevaiah et al., 2001; Sun et al., 1989), the observed meiotic prophase I-specific γH2A.X signal presents a first evidence for existence and temporal regulation of meiotic DSBs and meiotic recombination in *Tetrahymena*.

H2A.S is phosphorylated in developing macronuclei undergoing DNA rearrangement, but not during programmed nuclear death of parental macronuclei

DNA DSBs are also known to occur during two additional stages of *Tetrahymena* conjugation: during chromosome fragmentation and DNA elimination in the developing macronucleus (Yao and Chao, 2005), and also during breakdown of the parental macronucleus, a process thought to be related to apoptosis whereby the DNA is degraded producing oligonucleosome-sized DNA fragments (Davis et al., 1992). Since γH2A.X has been shown to accompany other DNA DSB-mediated events in eukaryotes such as with V(D)J recombination (Chen et al., 2000) and apoptosis in mouse cells (Lu et al., 2006), the presence of γH2A.X staining during DSB-associated stages of *Tetrahymena* conjugation was examined using the γH2A.X specific antibody. Interestingly, γH2A.X signal was very abundant in late-stage developing macronuclei at a time when programmed DNA rearrangements were taking place (Figure 2.3e,f). In contrast, the parental macronucleus was devoid of γH2A.X throughout all stages of conjugation including late stages of DNA fragmentation corresponding to nuclear breakdown.

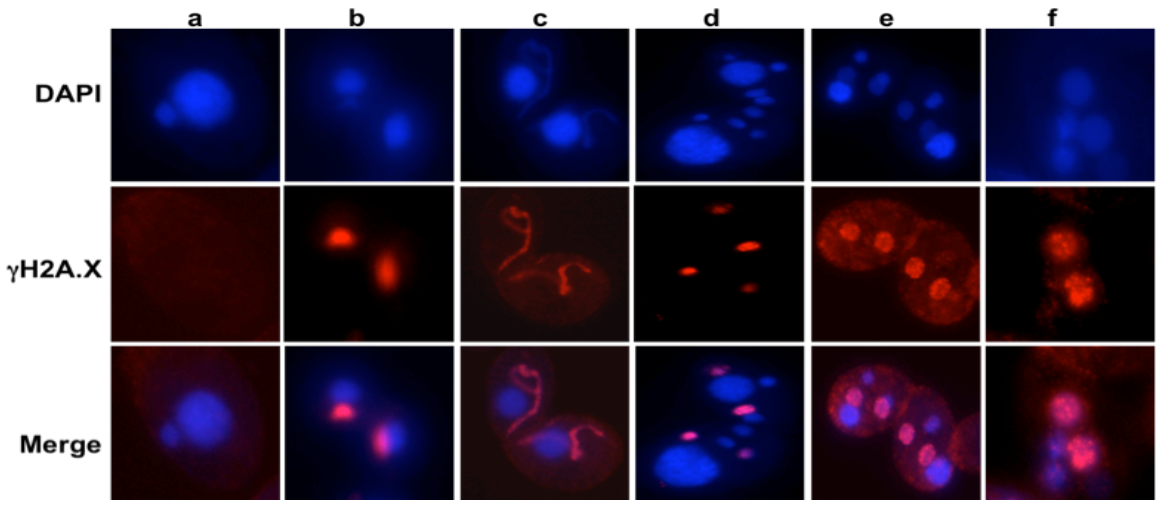

Figure 2.3: ***Tetrahymena*** **histone H2A.S is phosphorylated in developing macronuclei undergoing DNA rearrangement, but not during programmed nuclear death of parental macronuclei**

Immunofluorescence (IF) analysis of H2A.S phosphorylation during various stages of *Tetrahymena* conjugation probed with anti- γH2A.X antibody (red). Conjugation stages scored include: Initiation – before cell pairing (a); Meiotic prophase I stage II – micronucleus begins to elongate (b); Meiotic prophase I stage IV – full crescent (c); Meiosis II completed – 4 micronuclei stage (d); Macronuclear development II (e); Pair separation (f).

H2A.S phosphorylation occurs on the C-terminal S134

The γH2A.X phosphorylation site was then mapped in collaboration with Qinghu Ren and Xiaoyuan Song in the laboratory of Dr. Martin Gorovsky at University of Rochester, NY. To that end a site directed mutagenesis approach was used followed by a separation of charged histone isoforms on acid-urea (AU) acrylamide gel. AU gels developed by Panyim and Chalkley (Panyim and Chalkley, 1969), cleanly separate histones, histone variants and differently modified histone isofoms (such as acetylated and phosphorylated histones) on the basis of differences in their charge (Shechter et al., 2007). Since wild-type

H2A.S in *Tetrahymena* is known to exhibit phosphatase resistant isoforms due to charge-altering N-terminal lysine acetylations (Allis et al., 1980; Ohba et al., 1999; Ren and Gorovsky, 2003), an H2A.X 5R mutant strain in which these acetylation sites were eliminated was used for this study. In addition, S1, a potential phosphorylation site in H2A.S which can also be blocked by N-terminal acetylation, a conserved process that adds an acetyl group to the first amino acid of many histone peptides, was replaced with alanine in order to further reduce the complexity of the charged isoforms observed (Figure 2.4A). AU acrylamide gel analysis of histones isolated from this low complexity H2A.S S1A+5R strain, exhibited only three phosphatase-sensitive isoforms (Figure 2.4B), suggesting that three phosphorylation sites exist in growing cells under normal conditions. These isoforms disappeared when phosphorylation was abolished by mutation of four potential H2A.S C-terminal phosphorylation sites, namely S122, S124, T127 and S129, to their non-phosphorylatable alanine analogues. The resulting H2A.S S1A+5R+$(AAAAS)_c$ strain produced viable progeny and developed normally, indicating that although three of the four mutated sites in H2A.S are phosphorylation targets under normal conditions, this phosphorylation is dispensable for growth and its function is yet to be determined. However, when the histone H2A.S S1A+5R+$(AAAAS)_c$ strain was treated with 5 mM of MMS for 4 hours, a novel, single phosphatase-sensitive isoform was detected upon AU gel analysis, suggesting a presence of additional, DNA-damage dependent, phosphorylation site in H2A.S (Figure 2.4B). Interestingly, S134 within the highly conserved SQ motif is the only remaining phospho-acceptor in the C-terminus of the H2A.S S1A+5R+$(AAAAS)_c$ strain, suggesting it might be responsible for the observed DSB-induced phosphorylation event. To test this possibility, an HTA.S S134A point mutation was introduced in a double *Tetrahymena* H2A knockout heterokaryons, to produce a viable progeny in which

Figure 2.4: Histone H2A.S C-terminal S134 is the substrate for the γH2A.X – detected DSB-induced phosphorylation in *Tetrahymena*

A. N- and C-terminal tail sequences of *Tetrahymena* histone H2A.S. The lysines within the N-terminal tail, known acetylation substrates, are labeled green. The serine in the conserved SQ motif, and the four serine/threonine residues upstream of the SQ motif, are labeled in red. Denoted below are the two strains carrying mutations of the N-terminal tail that eliminate acetylation in an otherwise wild type background, or in the presence of alanine substitutions (in blue) of the four C-terminal serines/threonines. All of the mutations generated viable transformants.
B. Western blot of an AU-PAGE separating nuclear histones from wild type strains and strains containing indicated H2A.S point mutations, probed with anti-H2A antibody. The figure is courtesy of Dr. Qinghu Ren from the laboratory of Dr. Martin Gorovsky at the University of Rochester, New York.
C. Immunofluorescence (IF) analysis of wild type and S134A mutant cells during meiotic prophase I of conjugation probed with anti-γH2A.X antibody (red). The arrows point to the macronucleus (MAC) and the micronucleus (MIC) in each mating pair.

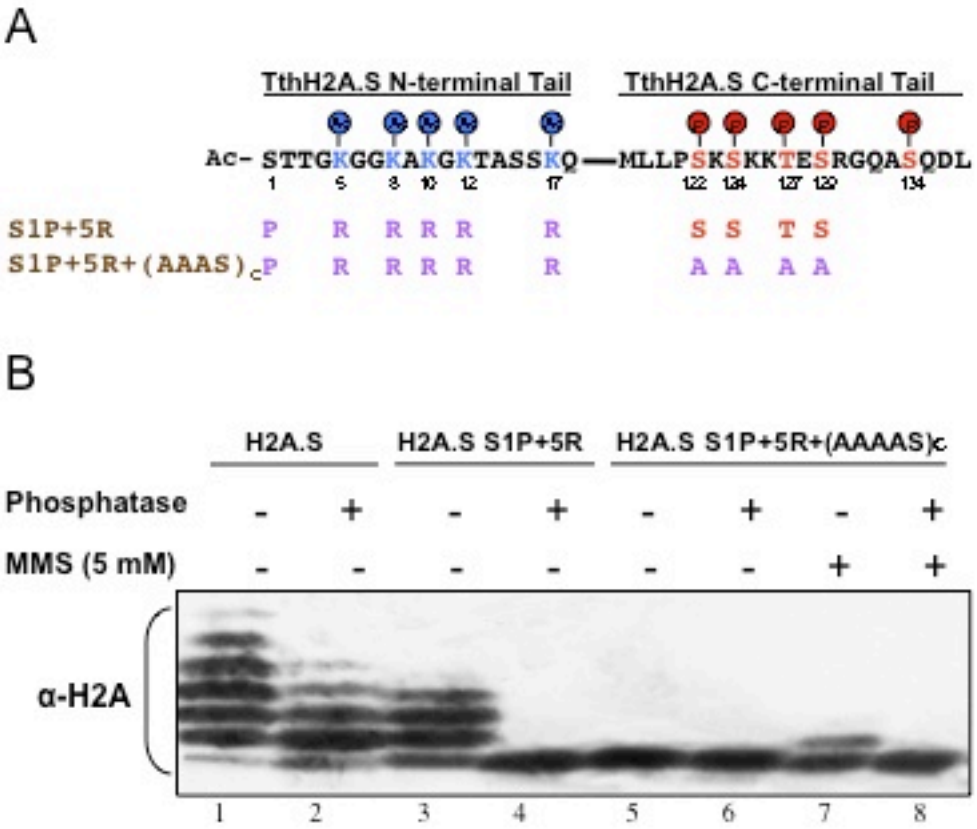
A
TthH2A.S N-terminal Tail
TthH2A.S C-terminal Tail
Ac- STTGKGGKAKGKTASSKQ—MLLPSKSKKTESRGQASQDL
1 5 8 10 12 17
122 124 127 129 134
S1P+5R P R R R R R S S T S
S1P+5R+(AAAS)c P R R R R R A A A A
B
H2A.S
H2A.S S1P+5R
H2A.S S1P+5R+(AAAAS)c
Phosphatase - + - + - + - +
MMS (5 mM) - - - - - - + +
α-H2A
1 2 3 4 5 6 7 8
C
DAPI
γH2A.X
Merge
WT
MAC
MIC
S134A
MIC
MAC

Figure 2.4

both major H2A genes are deleted from the genome, and the mutated S134A in the somatic macronucleus is the only source of H2A.S.

Immunofluorescence analysis of the S134A mutant cells during conjugation using the γH2A.X specific antibody strongly supported the conclusion that S134 is likely the exclusive site for DSB-induced phosphorylation of H2A.S. The single S134A point mutation specifically abolished the γH2A.X staining in meiotic prophase crescent micronucleus (Figure 2.4C), confirming that S134 in H2A.S is the major, if not the exclusive, site of meiotic DSB phosphorylation.

Absence of H2A.S S134 phosphorylation leads to meiotic defects

The γH2A.X deficient S134A strain was next used to determine the functional significance of meiotic S134 phosphorylation of histone H2A.S during conjugation. For that purpose, conjugation was initiated with either a wild-type H2A.S or S134A somatic heterokaryon strains and the process was examined in order to establish whether absence of S134 phosphorylation during homologous recombination results in conjugation defects. The different developmental stages during *Tetrahymena* conjugation, derived from the changes in nuclear morphology depicted in Figure 2.5B, were visualized by staining of the conjugating cells with DAPI. The cell fractions at different developmental stages were then scored during various time points after initiation of conjugation.

Wild-type H2A.S somatic heterokaryons advanced through all stages of conjugation to the final pair separation to give 34% of exconjugants 24 hours after the process was initiated, showing they were able to complete conjugation with a transformed wild-type H2A.S gene in the macronucleus. In contrast, matings between S134A mutant cells were unable to complete conjugation.

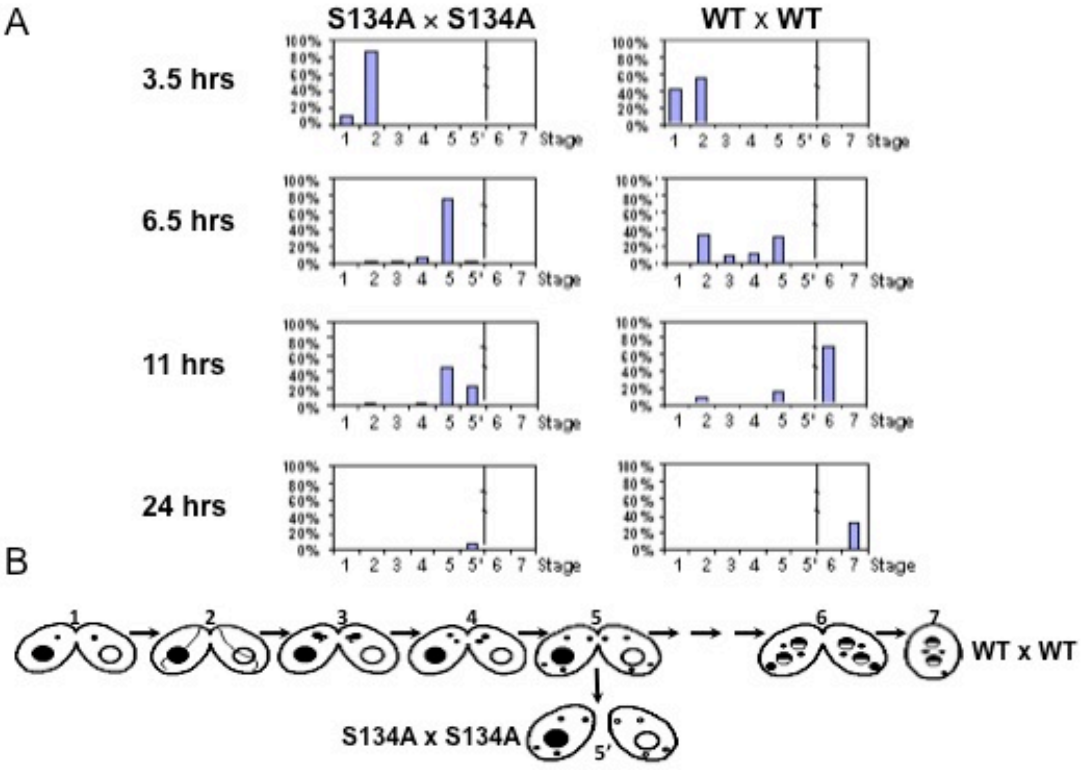

Figure 2.5: Disruption of S134 phosphorylation leads to premature termination of conjugation after meiosis II

The figure is courtesy of Dr. Qinghu Ren and Dr. Xiaoyuan Song from the Laboratory of Dr. Martin Gorovsky at the University of Rochester, New York.

A. Developmental profiles of wild type and mutant H2A.S S134A during conjugation. Seven different stages of conjugation (depicted in panel B) were scored by DAPI staining of samples removed at 3.5, 6.5, 11 and 24 hours after mixing.

B. Conjugation stages scored in panel A above include: 1. Pair formation; 2. Meiotic prophase I – crescent stage; 3. Chromosome condensation; 4. Meiosis I completed – two micronuclei stage; 5. Meiosis II completed – 4 micronuclei stage; 6. Developing macronuclei (anlagen); 7. Pair separation.

Discussion

Phosphorylation of the C-terminal SQ motif that defines H2A.X variants is required for efficient DNA DSB repair in diverse organisms (Redon et al., 2002), but has not been studied in ciliated protozoa. This study for the first time establishes the presence of a typical H2.X in lower eukaryotes such as the ciliate *Tetrahymena thermophila.* It shows that *Tetrahymena* histone H2A.S can be phosphorylated at S134 within the conserved SQ motif in response to DSBs induced by damaging agents and during micronuclear meiosis. It also demonstrates that S134 phosphorylation is important for normal micronuclear meiosis as S134A mutation that abolishes phosphorylation, causes meiotic defects. These results clearly establish that *Tetrahymena* H2A.S can function like histone H2A.X in vertebrates.

Interestingly however, although γH2A.X is essential for proper meiosis in *Tetrahymena* and it appears very early in the crescent meiotic prophase I stage, its absence in the S134A mutant cells only leads to premature cessation of conjugation after meiosis II and contrary to expectations there was no evidence of cell arrest directly at meiotic prophase I. The observed cell cycle delays following meiosis II suggest it is unlikely that the lack of prophase I arrest could be due to an adaptation mechanism. Otherwise operational in *S. cerevisiae* (Malkova et al., 1996; van Vugt and Medema, 2004; Xie et al., 2005), the adaptation process permits cells to entirely escape checkpoint arrest and allows unimpeded cell cycle progression despite unrepaired DSBs. Instead, in the S134A mutant, the cell cycle block indeed exists, albeit at later stages of conjugation following meiosis II, and is likely due to activation of a mitotic DNA damage checkpoint in response to unrepaired breaks that persist past meiosis II. This observation suggests that unlike other organisms, the recombination checkpoint (Hochwagen and Amon, 2006) that monitors meiotic DSBs and

allows for break repair by delaying the cell cycle progression in prophase I, is either weak or non-existent in *Tetrahymena,* and instead, cells arrest in response to a later mitotic checkpoint. This checkpoint mechanism ensures proper meiosis before the fertilization process can occur.

In vegetative S134A cells however, the mitotic checkpoint must be subject to adaptation as the cell growth is unimpeded in the mutant cells despite visible defects in micronuclear mitosis during the vegetative cycle (data not shown, (Song et al., 2007). In fact, the S134A mutant strain is viable suggesting that *Tetrahymena* can tolerate unrepaired DSBs during vegetative growth. Consistent with this observation, mutations that abolish SQ phosphorylation or knock out H2A.X in other organisms are also not lethal (Celeste et al., 2002; Downs et al., 2000). In addition, most previously described mutations that affect *Tetrahymena* micronuclei are not lethal as well (Mochizuki and Gorovsky, 2005; Wei et al., 1999), which is likely due to the lack of micronuclear transcriptional activity during vegetative growth. At this stage of the life cycle the micronuclei are transcriptionally inert and therefore the damage accumulated in the vegetative micronucleus will not have a major phenotypic effect until the next round of conjugation when the germline micronucleus gives rise to both, the macronucleus and the micronucleus of the daughter cells. In fact, it might have been evolutionary advantageous to eliminate the mitotic DNA damage checkpoints in vegetative cells to allow *Tetrahymena* to indefinitely replicate even in the absence of functional micronucleus.

The macronuclei on the other hand, are transcriptionally active and responsible for the phenotype of the vegetative cells. However, the macronuclei of S134A mutant cells are capable of compensating for DSBs because of the gene redundancy, namely there are ~45 copies of each chromosome enabling cells to survive unrepaired breaks because other copies of the gene might still be intact.

This study also sheds new light on the unique nature of the programmed degradation of the parental macronucleus during conjugation. Previous studies suggested that the parental macronucleus is destroyed by a process that resembles apoptosis in higher eukaryotes and is accompanied by the production of oligonucleosome-sized DNA ladders (Davis et al., 1992). However, apoptosis in higher eukaryotes is also accompanied by H2A.X phosphorylation, which was clearly absent from *Tetrahymena* degenerating parental macronuclei.

Finally, the results demonstrate a timeline for meiotic recombination in *Tetrahymena.* Meiotic recombination events in mouse and yeast are well established and γH2A.X appearance in these organisms precedes and is spatially distinct from synapsis (Mahadevaiah et al., 2001; Roeder, 1997; Zenvirth et al., 1992). In *Tetrahymena,* micronuclei undergo meiosis during conjugation adopting a highly elongate crescent shape, which then shortens and condenses at metaphase I. The crescent stage is thought to be analogous to most of meiotic prophase I because it precedes the meiotic divisions and it also exhibits some other features of meiotic prophase found in other organisms, such as bouquet-like clustering of both telomeres (Loidl and Scherthan, 2004) and centromeres (Cui and Gorovsky, 2006). However, unlike other organisms, synaptonemal complexes (SCs) have not been identified (Loidl and Scherthan, 2004; Wolfe et al., 1976) in *Tetrahymena* making it difficult to correlate stages of micronuclear meiotic prophase to key events in meiosis such as chromosome pairing and homologous recombination. The results in this study show that despite the lack of observed SCs, *Tetrahymena* γH2A.X follows a similar timeline as DSB-associated meiotic H2A.X phosphorylation in higher eukaryotes because it appears early before the micronucleus starts elongating and before pairing of homologous chromosomes in the crescent stage (Figure 2.3b). As such, this

study provides the first evidence for the existence of meiotic DSBs in *Tetrahymena* and defines the time interval of meiotic recombination in this organism by demonstrating that DSBs occur in the very early prophase of meiosis I, and persist until the end of the crescent stage, when meiotic crossing-over is likely completed.

CHAPTER 3

THE AMINO-TERMINAL SRS MOTIF OF *SACCHAROMYCES CEREVISIAE* HISTONE H2A IS IMPORTANT FOR PROPER DNA DAMAGE RESPONSE

Introduction

To accommodate the length of the DNA and its proper segregation during cell division, eukaryotic cells package their genomes in a nucleoprotein complex known as chromatin. The basic unit of DNA compaction within chromatin is the nucleosome which consists of 147 base pairs of DNA wrapped around an octamer composed of two copies of each of the four core histones H2A, H2B, H3 and H4 (Luger et al., 1997; Richmond and Davey, 2003). Even at this level of lowest compaction, the DNA is relatively inaccessible to the factors required for gene transcription, DNA replication, recombination and repair. In order to surmount the repressive compaction barrier eukaryotes have developed mechanisms that regulate chromatin accessibility. These mechanisms include: (1) ATP-dependent chromatin remodeling, (2) incorporation of histone variants into nucleosomes and (3) covalent histone modifications, such as phosphorylation, methylation, acetylation and ubiquitylation. Histone modifications have thus far been extensively studied mainly in the context of transcriptional regulation. Lately however, there's been a growing body of evidence linking an increasing number of histone modifications to DNA repair, their functions ranging from (1) lesion markers, (2) recruitment of repair machinery components to (3) facilitating the action of these components reviewed by (Downs et al., 2007). An overview of all histone modifications associated with DNA damage detection and repair is given in Table 1.

Although they were able to enter meiosis II and the micronuclei of each pair were able to divide and produce four meiotic products, these nuclei were not able to undergo further divisions, nuclear exchange and fertilization. Conjugation of the S134A mutant cells was aborted at the meiosis II stage and the pairs separated prematurely with four or fewer meiotic micronuclei (Figure 2.5A and 2.5B, stage 5'). S134A cells appeared cytologically normal through meiotic prophase I, however abnormalities such as DNA fragmentation and chromosome loss as well as chromosome segregation defects were observed during metaphase I and anaphase I (Song et al., 2007). These results demonstrate that loss of H2A.S S134 phosphorylation leads to meiotic defects and premature termination of conjugation and suggest that phosphorylation of the H2A.S SQ motif is required for proper meiosis in *Tetrahymena*.

Table 1: Covalent histone modifications that influence DNA-damage responses

Histone	*S. cerevisiae*			*S. pombe*			Mammals		
	Mark	Enzyme	Reference	Mark	Enzyme	Reference	Mark	Enzyme	Reference
H2A	S129ph	Mec1, Tel1	Downs et al, 2000	S129p	Rad53	Nakamura et al, 2004	-	-	-
H2A.X	-	-	-	-	-	-	S139ph	ATM, ATR, DNA-PK	Rogakou et al, 1998
H2B	S10ph	Ste20	Ahn et al, 2005	ND	ND	-	S14ph	Mst1	Cheung et al, 2003
	K123ub	Rad6, Bre1	Giannattasio et al, 2005	ND	ND	-	K123ub	RAD6	Wu et al, 2009
H3	K14ac	Hat1	Qin et al, 2002	ND	ND	-	ND	ND	-
	K23ac	Hat1	Qin et al, 2002	ND	ND	-	ND	ND	-
	K56ac	Rtt109	Masumoto et al, 2005	K56ac	Rtt109	Xhemalce et al, 2007	K56ac	CBP/p300	Das et al, 2009
	K79me	Dot1	Wysocki et al, 2005	ND	ND	-	K79me	DOT1L	Huyen et al, 2004
H4	S1p	CK1	Cheung et al, 2005	ND	ND	-	ND	ND	-
	K5ac	Esa1	Bird et al, 2002	ND	ND	-	K5ac	Tip60	Kusch et al, 2004
	K8ac	Esa1	Bird et al, 2002	ND	ND	-	K8ac	Tip60	Kusch et al, 2004
	K12ac	Esa1, Hat1	Bird et al, 2002	ND	ND	-	K12ac	Tip60, MOF	Kusch et al, 2004
	K16ac	Esa1	Bird et al, 202	ND	ND	-	K16ac	Tip60	Kusch et al, 2004
	ND	ND	-	K20me	Set9	Sanders et al, 2004	K20me	PR-SET7	Tardat et al, 2007

ND, not determined; ph = phosphorylation; ub = ubiquitylation; ac = acetylation; me = methylation.

*Adapted from a review by Downs JA, Nussenzweig MC and Nussenzweig A, 2007

In order to assess the contributions of additional histone residues in DNA damage recognition and repair, I surveyed *S. cerevisiae* cells lacking specific N- and C-terminal histone tails for survival in the presence of a range of DNA damaging agents, such as the alkylating agent methyl methanesulfonate (MMS), hydroxyurea (HU), and following exposure to ultraviolet (UV) radiation. I found that deletion of the H2A amino terminus imparts significant sensitivity to all DNA damaging agents tested. Specifically, a DNA damage survival property exists in a conserved SRS region spanning residues 17-19 of the H2A tail. This region lies within a domain previously identified as a Histone H2A Repression (HAR) domain (Parra and Wyrick, 2007) or a 'knuckle' (Luger and Richmond, 1998) which is a single turn α-helix preceding the H2A α1 helix (Figure 1.1). Here, I show that point mutations within the SRS region that change the surface charge of residues, such as H2A S17E and H2A S19E phospho-mimics which introduce a negative charge, as well as H2A R18A which neutralizes the positive charge of arginine, render cells sensitive to all DNA damage agents tested and account for the broad spectrum of damage sensitivity of the H2A N-terminal deletion strain.

Finally, a subtle DNA damage sensitivity to MMS only, was contributed by the three lysines present in the H2A N-tail. Using mass spectrometry (MS) in collaboration with Hillary Montgomery in the laboratory of Dr. Donald Hunt at the University of Virginia, we demonstrate that *in vivo* two of the lysines, H2A K4 and H2A K7, are acetylated individually as well as together, and identified the third lysine, H2A K13, as a novel acetylation site.

Results

Deletion of the amino-terminal tail of S. cerevisiae histone H2A confers sensitivity to DNA damaging agents

Given the increasing number of histone covalent modifications recently associated with DNA damage recognition and repair, it is plausible that there are additional histone contributions to the DNA damage response. To determine whether other histone residues play a role in the cell's ability to cope with DNA damage, a 'plasmid shuffle' strategy was used to introduce mutations within the histone genes of interest. The strategy developed by Boeke and colleagues, is a genetic method which allows mutagenesis of essential genes in *S. cerevisiae* (Boeke et al., 1984). It relies on expression of a wild type copy of a gene of interest from a 'resident' plasmid to support viability of strains carrying a deletion of the respective gene. Upon introduction of a plasmid-born mutant copy of the gene maintained by a different selectable marker, the URA3 auxotrophic marker-containing 'resident' plasmid is lost by counter-selection with the pyrimidine analogue, 5-fluoro-ortic acid (5-FOA). The method offers an experimental advantage over lengthy procedures required for introducing genomic mutations and has already proven to be a useful approach for histone genetic studies (Bird et al., 2002; Megee et al., 1990; Recht et al., 1996; Sun and Allis, 2002).

A schematic illustration of the histone shuffle experimental system used in this study is depicted in Figure 3.1. In particular, a plasmid-borne copy of various histone H2A and H2B tail deletions was introduced in a haploid *S. cerevisiae* 'shuffle' strain in which both copies of the chromosomal H2A and H2B loci had been disrupted. The histone deletion strains were then analyzed for their ability to survive in the presence of a range of genotoxic factors, such as methyl methanesulfonate (MMS), hydroxyurea (HU) and ultraviolet (UV)

radiation, which inflict different types of DNA damage repaired by distinct mechanisms. At the concentrations used, 0.05% and 150 mM respectively, both MMS and HU, create replication-dependent double strand breaks repaired primarily by homologous recombination. Alternatively, UV irradiation produces intrastrand photoproducts through crosslinking of adjacent cytosine and thymine bases. The resulting pyrimidine dimers are substrates for nucleotide excision repair pathways, which create single-strand lesions.

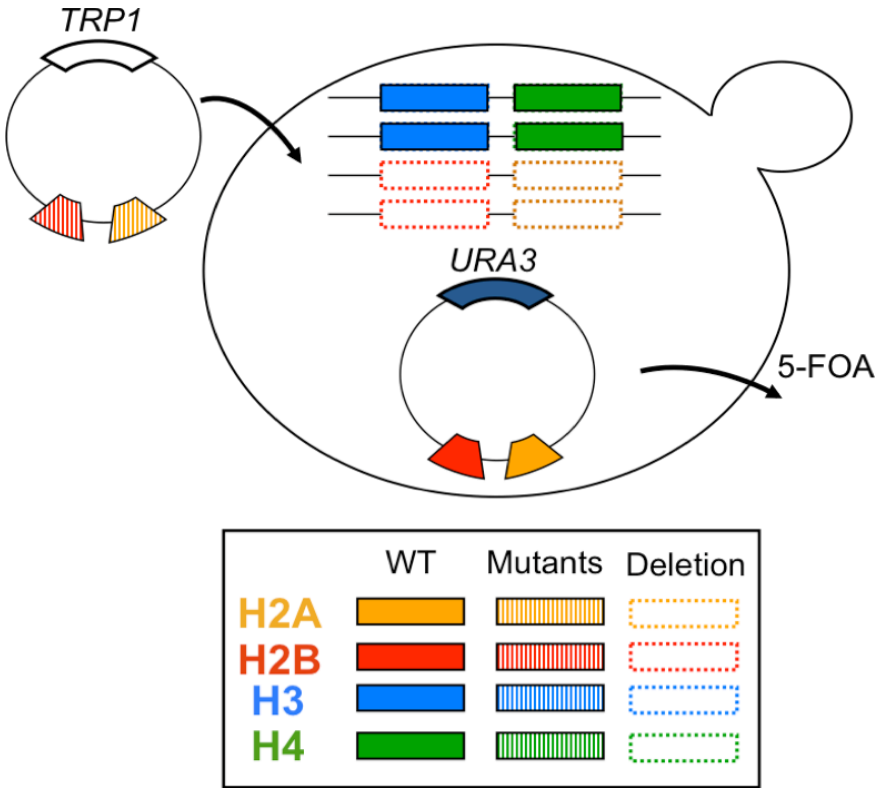

Figure 3.1: *S. cerevisiae* H2A-H2B histone plasmid-shuffle strain
Both copies of the chromosomal H2A and H2B loci are disrupted in a haploid *S. cerevisiae* strain in which survival is supported by a 'resident' URA3 plasmid-borne wild type copy of histone H2A and H2B. The strain is useful for testing histone point mutations and tail truncations *in vivo* by counter-selecting against the 'resident' URA3 plasmid after introduction of a plasmid-born mutant copy of histone H2A and H2B maintained by a different selectable marker, in this case TRP1. The strain and figure are courtesy of Dr. Judith Recht.

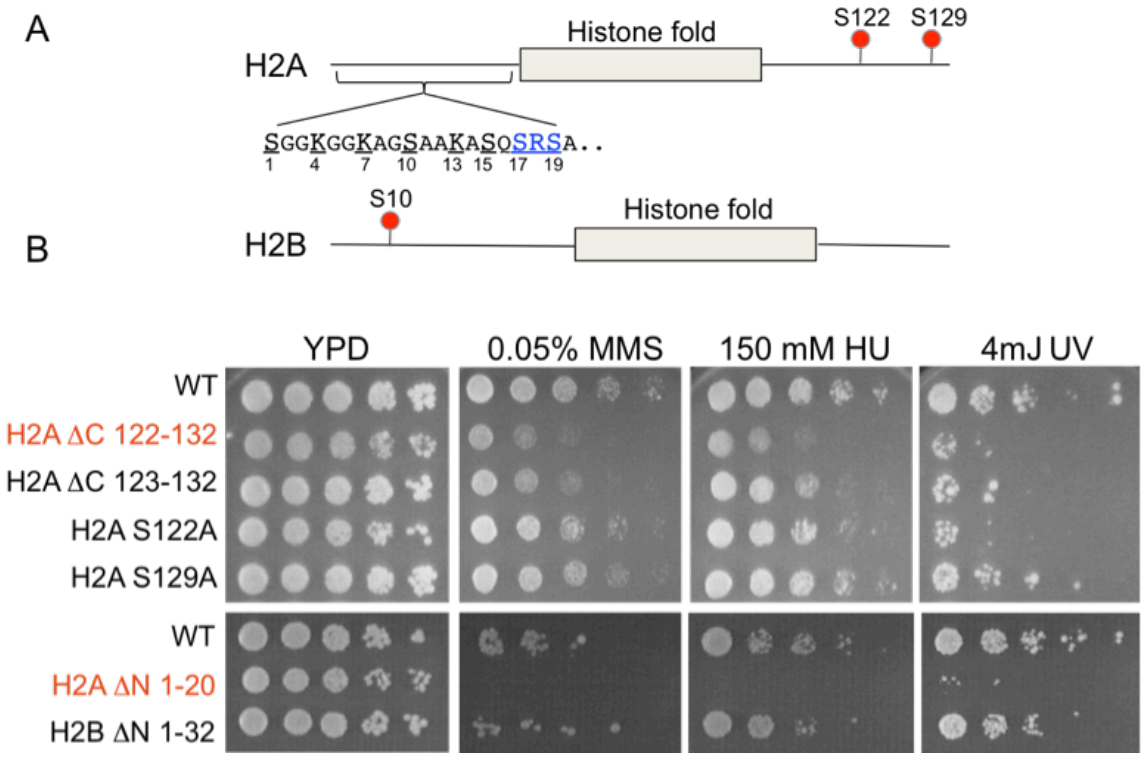

Figure 3.2: N-terminus of histone H2A, but not histone H2B is required for growth during DNA damage

A. Schematic representation of the amino acid sequence of the *S. cerevisiae* histone H2A N-terminal tail 1-20 truncation. All potentially modifiable residues are underlined and represented in larger case. The conserved SRS motif within the tail is shown in blue. DNA damage associated-serine phosphorylation sites contained within the other tail deletions constructs tested are also indicated in the diagram.

B. Five fold serial-dilutions of cells containing the indicated histone tail deletions or were spotted on YPD plates containing the indicated concentration of methyl-methane sulfonate (MMS) and hydroxyurea (HU). A third set of YPD plates was exposed to ultraviolet (UV) irradiation. All plates were incubated at 30°C and photographed after 3 days. Strains exhibiting DNA damage sensitivity are labeled red.

When the growth of the histone 'shuffle' strains carrying tail deletions (Figure 3.2A) was examined on plates containing MMS, HU or after UV radiation, only the histone H2A 20 amino acid-terminal tail deletion strain was found to be markedly hypersensitive to all three DNA-damaging factors tested (Figure 3.2B). An H2A carboxy-tail deletion strain, containing the hallmark DNA damage γH2A.X site, S129, as well as a longer C-tail deletion strain which also included S122, another phosphorylation site linked to DNA repair (Harvey et al., 2005) showed a subtle, but increasingly more sensitive phenotype as a function of the increasing length of the tail removed. In contrast, the growth and survival of the histone H2B amino-terminal deletion strain, which removes a 'cell death'-inducible phosphorylation mark within the tail, was unaffected during DNA damage. The observed sensitivity of the H2A N-tail deletion strain to all damaging conditions tested did not appear to be an indirect effect of general growth deficiencies of the strain as its growth rate in the absence of damage is indistinguishable from the wild-type. These results suggest that the histone H2A amino-terminus or residues within it are important for survival in the presence of DNA damage.

Histone H2A N-terminal acetylation mapped by mass spectrometry confers subtle sensitivity to MMS

The observed DNA damage hypersensitivity imparted by the deletion of the H2A N-terminus could be a consequence of its effect on histone modification status of residues within the N-tail. To that end, the histone post-translational modifications within the H2A amino-terminal tail were mapped by mass spectrometry (MS) in collaboration with Hillary Montgomery in the laboratory of Dr. Donald Hunt at the University of Virginia. Acid extraction from cultured wild type cells before and after 2-hour treatment with 0.05% MMS was used to

Figure 3.3: Purification of *S. cerevisiae* histone H2A for mass spectrometry analysis of the post-translational modification profile

Acid extracted proteins from wild type *cerevisiae* strains before (A) and after (B) treatment with 0.05% MMS for 2 hrs were separated by RP-HPLC on an acetonitrile gradient and the resulting traces are shown. (C) Fractions containing histone H2A were identified by immunoblotting after separation on a 15% SDS-PAGE. Arrow heads denote, and fraction numbers labeled red contain histone H2A.

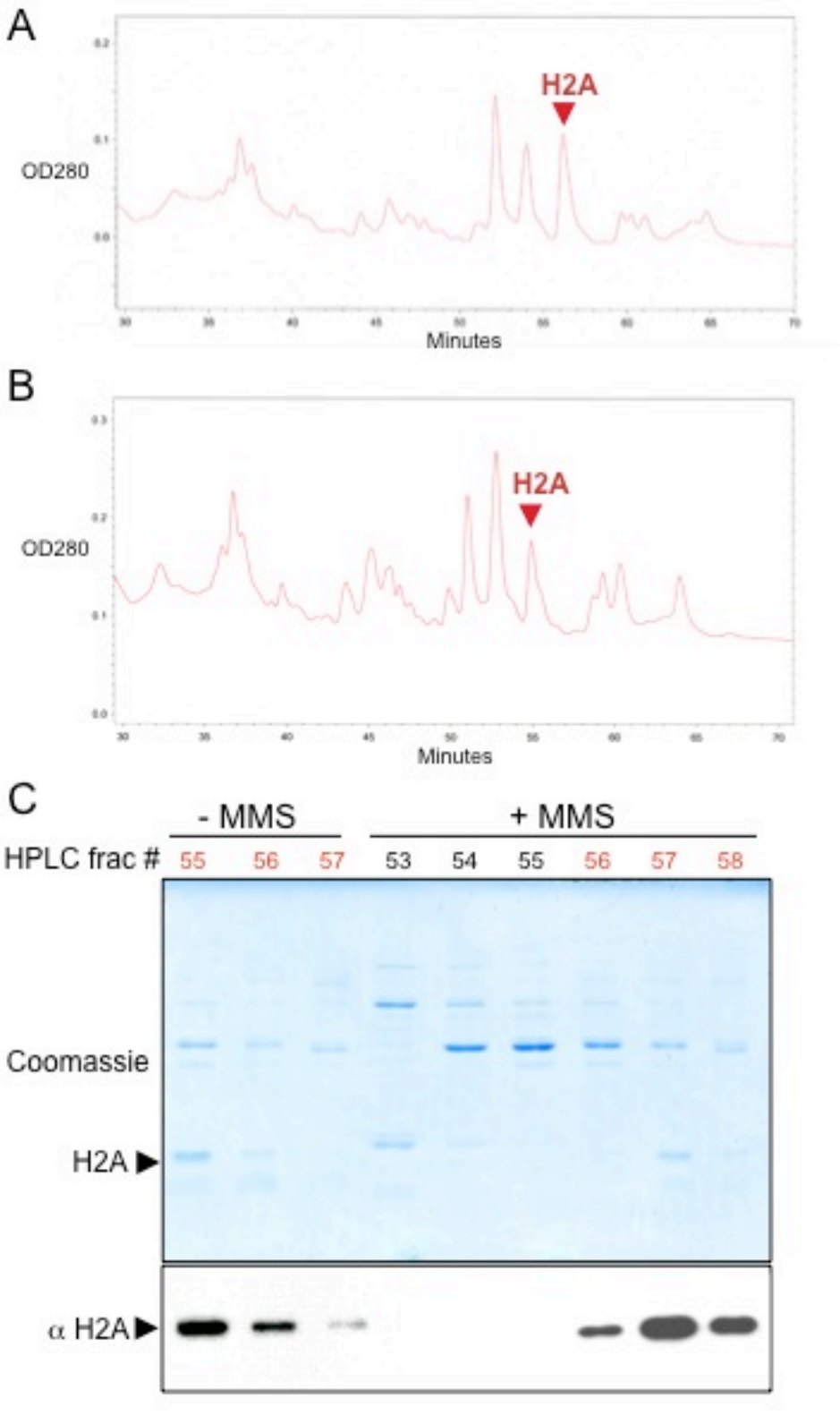
A
H2A
OD280
Minutes
B
H2A
OD280
Minutes
C
- MMS
+ MMS
HPLC frac #
55
56
57
53
54
55
56
57
58
Coomassie
H2A
α H2A

Figure 3.3

isolate endogenous histone H2A which was subsequently purified by separation on a reversed phase HPLC. Histone H2A containing fractions were run on SDS-PAGE gel and the protein was identified by immunoblotting (Figure 3.3). The MS analysis of the RP-HPLC purified histone H2A, detected acetylation on all three tail lysines: K4, K7 and a novel acetylation site previously not observed in *S. cerevisiae*, K13. Acetylation was present in both the MMS treated and the untreated sample and there were no significant changes in abundance before and after MMS treatment. To ensure DNA damage conditions induced a proper response, C-terminal H2A tryptic peptides were examined for the presence of the DNA damage γH2A.X mark. Indeed, a γH2A.X peptide was observed in the MMS-treated sample. The analysis also revealed presence of coexisting modifications within the intact N-terminal 18 amino acid peptide, product of the tryptic digest of H2A. Interestingly, ~1% of the sample population contained a dual K4/K7 acetylation species (Figure 3.4) which has not been observed before.

To test the requirement for H2A N-terminal lysine acetylation in the DNA damage response, each of the three tail lysines was mutated individually and in combination to either arginine (R) or an acetyl-mimic glutamate (Q), and survival was scored on plates containing the same set of DNA damaging reagents: MMS, HU and after UV radiation. Only strains carrying K4,7R and K4,7Q double mutations, as well as strains with triple mutations, K4,7,13R and K4,7,13Q displayed modest sensitivity to MMS, but not the other DNA damage agents tested (Figure 3.5). These results argue that the requirements for lysine acetylation during DNA damage are likely dynamic. However, the damage phenotype observed with the lysine mutants was not strong enough to attribute for the severity of the N-tail deletion phenotype indicating that other tail segments are responsible for the role of H2A in cellular viability during damage.

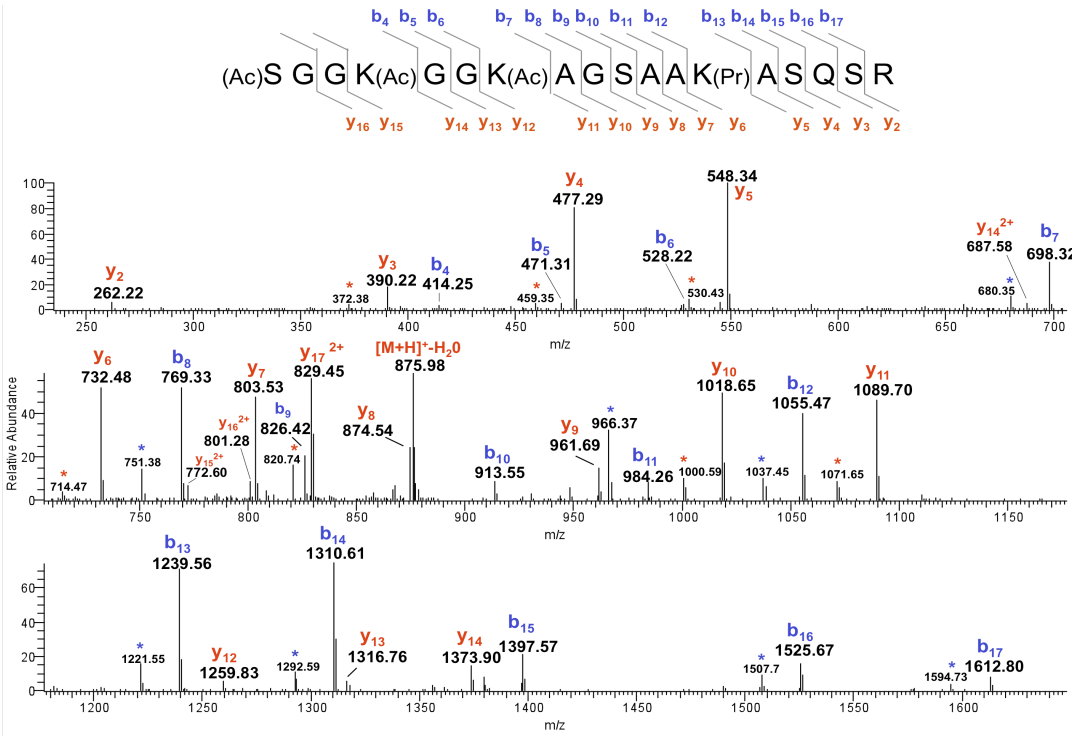

Figure 3.4: Tandem mass spectrum of a doubly acetylated *S. cerevisiae* histone H2A amino-terminal peptide

Tandem mass spectrum (MS/MS) of a doubly acetylated (Ac) wild-type *S. cerevisiae* histone H2A N-terminal peptide, residues 1-18, prior to treatment with methyl-methane sulfonate (MMS), fragmented by collision activated dissociation (CAD). The N-terminal N-acetylated peptide was generated from an in-solution digest with trypsin after derivatization of unmodified or monomethylated lysine residues with propionic anhydride (Pr). A fraction of the resulting peptide mixture was analyzed by online nanoflow high performance liquid chromatography micro-electrospray ionization tandem mass spectrometry (nHPLC-μESI MS/MS) on a Finnigan LTQ –FT mass spectrometer operated in a data-dependent manner. The instrument cycled through the acquisition of a full-scan mass spectrum (MS) and the top 10 most abundant masses in this initial MS scan were sequentially chosen for MS/MS. The spectrum shows that the H2A peptide is acetylated at both lysines 4 and 7 together. It also confirms the existence of acetylation at the N-terminal serine *in vivo*. b and y fragment ions are denoted in blue and red, respectively. Doubly-charged fragment ions are designated as 2+, and ions corresponding to the neutral loss of water are denoted with asterisks (*). (Figure courtesy of Hillary Montgomery).

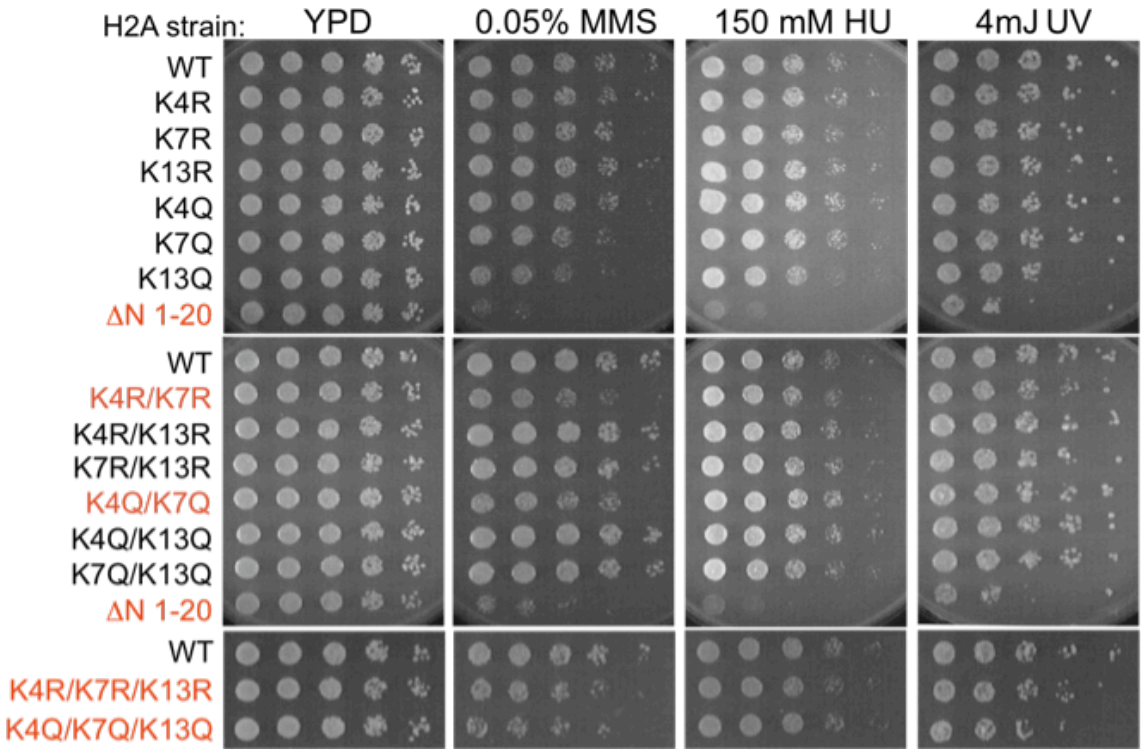

Figure 3.5: Amino-terminal lysine point mutations in *S. cerevisiae* histone H2A confer subtle sensitivity to MMS

Five fold serial-dilutions of cells containing the indicated histone H2A N-terminal lysine point mutations to either arginine (R) or acetylation-mimic glutamate (Q), were spotted on YPD plates containing the indicated concentration of methyl-methane sulfonate (MMS) and hydroxyurea (HU). A third set of YPD plates was exposed to ultraviolet (UV) irradiation. All plates were incubated at 30°C and photographed after 3 days. Strains exhibiting DNA damage sensitivity are labeled red.

The DNA damage-survival property of histone H2A amino-terminal tail is encoded in the 'knuckle' region

To assess the contributions of each residue within the H2A N-terminal tail to the damage sensitivity of the N-tail deletion, a series of H2A mutant strains were next generated by site directed mutagenesis of the remaining modifiable residues within the H2A amino-terminus. For that purpose, each of the five potential

serine (S) phospho-acceptors in the H2A N-terminal tail, was individually replaced with either alanine (A) to eliminate the phosphorylation potential of the serine, or glutamic acid (E), a constitutive phospho-mimic. Strains carrying single serine to alanine substitutions showed no obvious sensitivity to any of the damaging conditions tested (Figure 3.6). Similarly, the growth of most of the

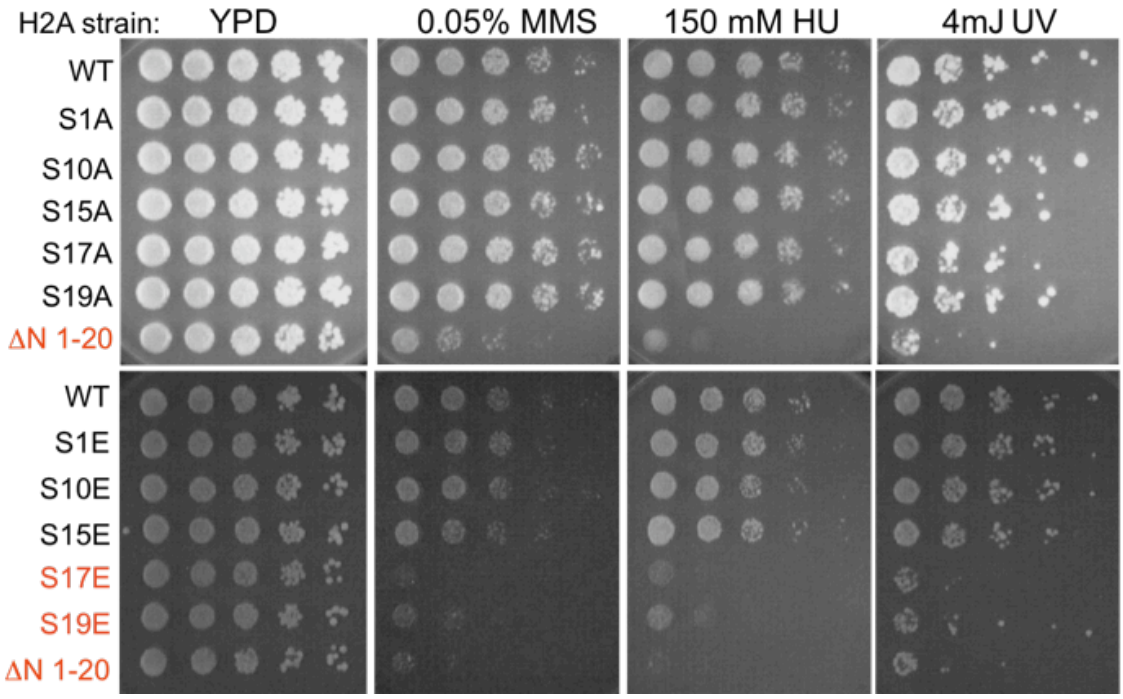

Figure 3.6: DNA damage sensitivity survey of *S. cerevisiae* strains containing H2A amino-terminal serine point mutations

Five fold serial-dilutions of cells containing the indicated H2A N-terminal tail serine point mutations to either the unphosphorylatable alanine (A) or the phospho-mimic glutamic acid (E), were spotted on YPD plates containing the indicated concentration of methyl-methane sulfonate (MMS) and hydroxyurea (HU). A third set of YPD plates was exposed to ultraviolet (UV) irradiation. All plates were incubated at 30°C and photographed after 3 days. Strains exhibiting DNA damage sensitivity are labeled red.

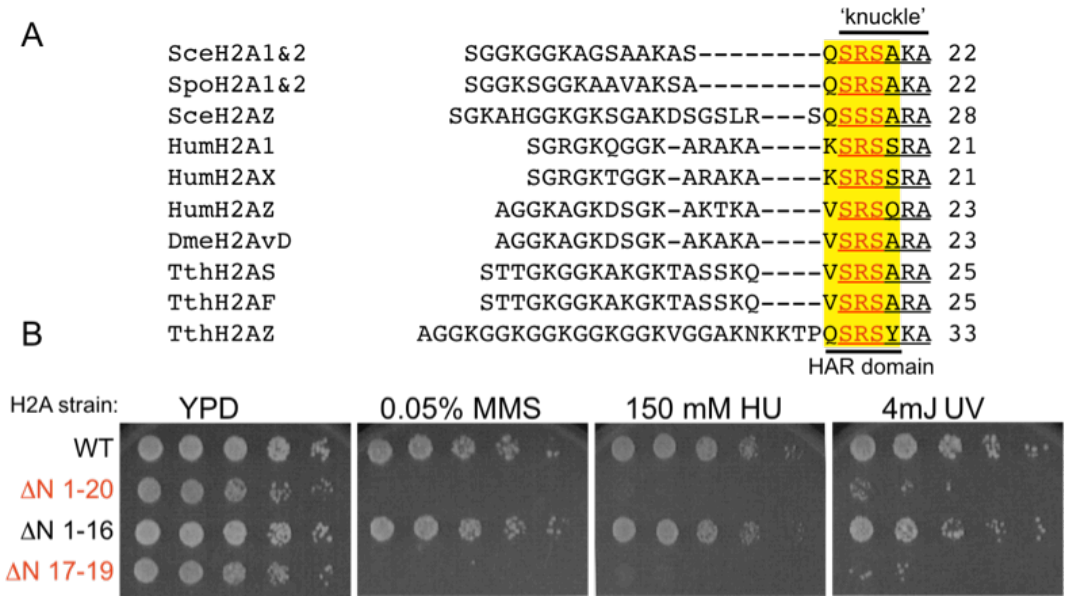

Figure 3.7: The conserved amino-terminal SRS region of within the histone H2A 'knuckle' is important for survival after DNA damage

A. Amino acid sequence alignment of histone H2A N-terminal tails from various organisms. Sequences were obtained from GenBank. The accession numbers are as follows: human_H2A.1, NP_254280; human_H2A.X, NP_002096; *D. melanogaster*_H2AvD (H2A.Z homologue), NP_524519; *S. pombe*_H2A.2, NP_594421; *S. cerevisiae*_H2A.1, NP_010511; *S. cerevisiae*_H2A.2, NP_009552; *S. cerevisiae*_H2A.Z, NP_014631 (also known as htz1); *T. thermophila*_H2A.S, AAC37291; *T. thermophila*_H2A.F, AAC37292, *T. thermophila*_H2A.Z, CAA33554. Alignment was generated with ClustalW identity algorithm. The conserved SRS motif is labeled in red. Residues that comprise the Histone H2A Repression (HAR) domain are highlighted. Residues that comprise the 'knuckle' single turn α helix are underlined. Alignment gaps are indicated with a hyphen (-).

B. Five fold serial-dilutions of cells containing the indicated H2A N-terminal tail deletions were spotted on YPD plates containing the indicated concentration of methyl-methane sulfonate (MMS) and hydroxyurea (HU). A third set of YPD plates was exposed to ultraviolet (UV) irradiation. All plates were incubated at 30°C and photographed after 3 days. Strains exhibiting DNA damage sensitivity are labeled red.

glutamic acid phospho-mimic strains was unaffected by any type of DNA damage. However, when either S17 or S19 were individually replaced with glutamic acid, the resulting strains were severely impaired for growth on MMS- or HU- containing plates, as well as following UV radiation. The observed phenotypes of the S17E and S19E strains, correlate with the location of these residues in the nucleosome, namely both of them map within the H2A N-tail structured region designated as the 'knuckle' (Luger and Richmond, 1998) (Figure 3.7A). Indeed, when an H2A N-tail deletion spanning 'knuckle' residues 17 through 19 was introduced into the 'shuffle' strain, it fully recapitulated the broad DNA-damage hypersensitivity of the H2A 1-20 tail deletion (Figure 3.7B).

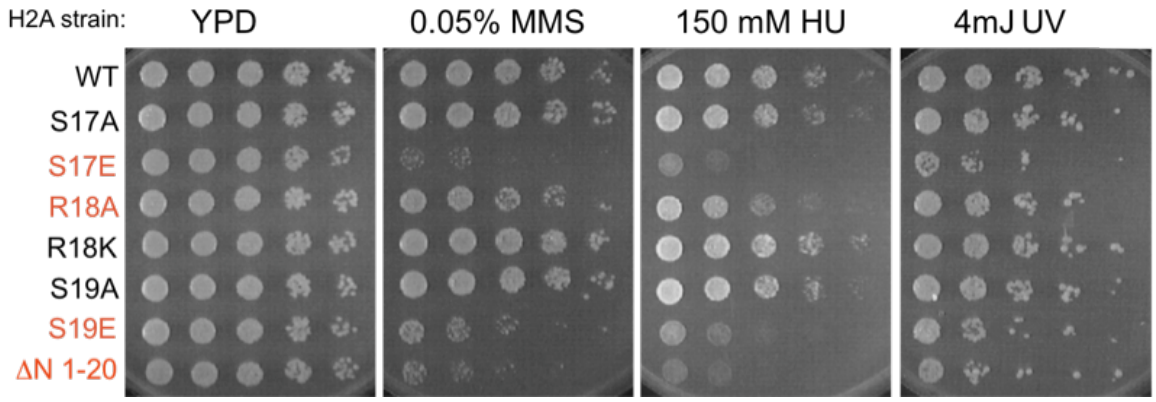

Figure 3.8: Histone H2A 'knuckle' region charge-altering point mutations confer DNA damage sensitivity

Five fold serial-dilutions of *S. cerevisiae* cells containing the indicated H2A 'knuckle' point mutations of serines (S) to either alanine (A), or glutamic acid (E), and arginine to either alanine (A) or lysine (K) were spotted on YPD plates containing the indicated concentration of methyl-methane sulfonate (MMS) and hydroxyurea (HU). A third set of YPD plates was exposed to ultraviolet (UV) irradiation. All plates were incubated at 30°C and photographed after 3 days. Strains exhibiting DNA damage sensitivity are labeled red.

The sensitivity to DNA damage is not only limited to the S->E 'knuckle' point mutations, as R18 'knuckle' substitution to a charge-neutralizing alanine, but not lysine had a similar, although more subtle effect (Figure 3.8). These observations land further support to the idea that the DNA damage survival property of the H2A N-terminal tail is encoded almost entirely by the 'knuckle' region. The property, although broad in its effect as it mediates response to DNA damage inflicted by various mechanisms, seems to be indeed DNA damage specific, as no obvious growth phenotypes were seen in under normal conditions.

Expression of wild-type histone H2A suppresses damage sensitivity of strains containing 'knuckle' point mutations

In the context of the nucleosome, the histone octamer contains two H2A copies. Although structurally each H2A component of the octamer constitutes a dimer with histone H2B, functionally the nucleosome can be viewed as a homozygous H2A dimer. In circumstances where a mutant H2A histone can be incorporated into the nucleosome in the presence of a wild-type H2A copy, it is possible that it might adversely affect the normal function of the wild-type component. In such cases, the mutation in one of the H2A constituents of the histone octamer might cause a dominant negative phenotype, as nucleosomes would be missing one of its functional H2A components. To examine whether H2A proteins carrying 'knuckle' mutations can still efficiently incorporate into nucleosomes together with the wild-type H2A gene product and whether this incorporation interferes with the normal DNA damage function of the wild-type nucleosome, sensitivity to the previously used palette of genotoxic agents was assayed in H2A 'knuckle' heterozygous strains.

Heterozygous 'knuckle' strains were generated in the 'shuffle' background by keeping the wild-type resident plasmid histone H2A copy along with the newly introduced plasmid carrying the H2A 'knuckle' mutations. When the growth of these strains heterozygous for either S17E, R18A or S19E, was examined on plates containing either MMS, HU or after UV exposure, each of the strains was able to grow as well as the homozygous wild-type strain (Figure 3.9). These results demonstrate a lack of a dominant negative phenotype of 'knuckle' mutations as the presence of a wild-type histone H2A copy is able to suppress the DNA damage sensitivity of each 'knuckle' point mutant. A likely interpretation of this observation is that wild-type histone H2A is a preferred nucleosomal component and in its presence histones with 'knuckle' mutations are not incorporated into chromatin or their incorporation is simply less efficient.

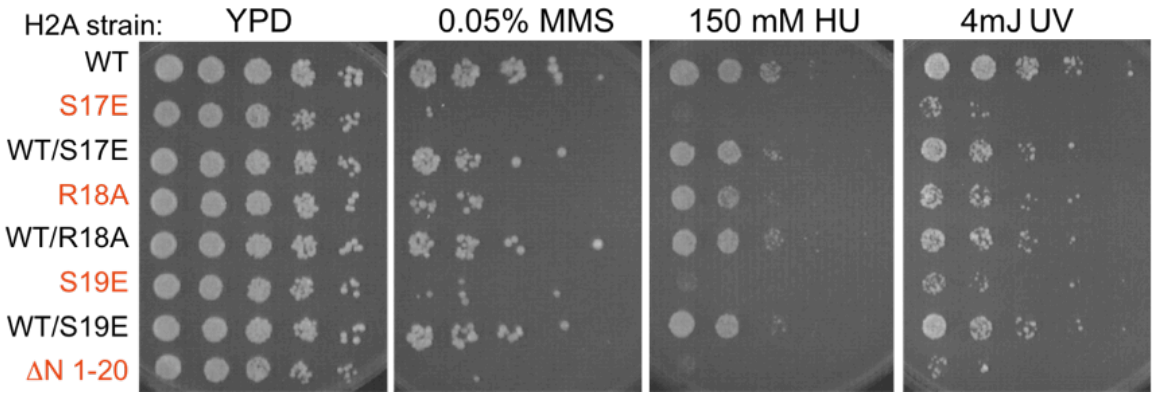

Figure 3.9: Expression of wild-type histone H2A suppresses damage sensitivity of *S. cerevisiae* strains with 'knuckle' point mutations

Five fold serial-dilutions of cells containing the indicated H2A 'knuckle' point mutations in the presence of a wild-type histone plasmid, were spotted on YPD plates containing the indicated concentration of methyl-methane sulfonate (MMS) and hydroxyurea (HU). A third set of YPD plates was exposed to ultraviolet (UV) irradiation. All plates were incubated at 30°C and photographed after 3 days. Strains exhibiting DNA damage sensitivity are labeled red.

If indeed incorporation efficiency of the mutant H2A is only reduced and not completely suppressed in the heterozygous strains, then the results suggest that presence of a wild-type H2A component in each nucleosome, or some fraction of them, is sufficient for the normal DNA damage function of H2A and can fully compensate for the sensitivity conferred by the 'knuckle' mutations.

Discussion

Post-translational modifications of all core histones have been implicated in the cellular response to DNA damage in eukaryotes (Bird et al., 2002; Downs et al., 2004; Harvey et al., 2005; Qin and Parthun, 2002; Tamburini and Tyler, 2005; Wyatt et al., 2003; reviewed by (Downs et al., 2007). Here, I uncover a unique and previously unrecognized role for the H2A N-terminal tail in the DNA damage response in *S. cerevisiae*. This function is limited to the conserved SRS motif spanning residues 17-19 within the H2A 'knuckle' region and is broad in its effect as it mediates response to DNA damage inflicted by various mechanisms. A lesser contribution, specific to MMS inflicted damage, is provided by the three H2A amino-terminal lysines which appear to be functionally redundant as sensitivity to MMS is observed only with double K4,7R/Q as well as triple, but not individual tail lysine mutations. Using a mass spectrometry (MS) approach to map post-translational modifications of the H2A amino terminus, we demonstrate that *in vivo* two of the lysines, H2A K4 and H2A K7, are acetylated individually as well as together, and identified the third lysine, H2A K13, as a novel acetylation site in *S. cerevisiae*.

It is unclear however, whether the DNA damage sensitivity imparted by the H2A amino-terminal lysine mutations is mediated through the MS detected acetylation of these sites. The broad substrate specificity of many histone modifying enzymes, including histone acetyltransferases and deacetylases, makes it difficult to discern specific contributions of individual modifications. In this particular case, both H2A K4 and K7 are substrates for the catalytic subunit of the Nua4 histone acetyltransferase complex, Esa1 (Clarke et al., 1999; Roth et al., 2001; Suka et al., 2001). Interestingly, Esa1 also acetylates N-terminal lysines in histone H4 (Allard et al., 1999; Bird et al., 2002), and it has been previously

established that the Esa1-dependent H4 lysine acetylation is required for DNA repair in *S. cerevisiae* (Bird et al., 2002). The broad range of Esa1 substrates, some of which have already been linked to the DNA damage response, makes an enzyme-targeting strategy an unfeasible approach when evaluating whether Esa1-dependent acetylation of individual histone H2A target sites contributes to DNA damage sensitivity. Nevertheless, if the DNA damage function of the histone H2A tail lysines is indeed mediated through acetylation, its overall contribution to cell viability during DNA damage appears to be minor as the observed phenotype of even triple H2A N-tail lysine to glutamate substitutions is subtle. It is therefore reasonable to speculate that the mild DNA damage sensitivity of the triple H2A N-tail lysine mutation is likely due to a redundant function of the H2A and H4 lysine acetylation during the DNA damage response. In fact, in addition to the pairwise preference of Esa1 for histones H2A and H4 there are other pairwise similarities between the N-terminal tails of these two histones, providing further support for the functional redundancy hypothesis (Cheung et al., 2000). For example, the N-terminal tails of both histone H2A and H4 are shorter than those of H3 and H2B and as opposed to H3 and H2B, both H2A and H4 have a serine at the N-terminal starting position. Consistent with the functional redundancy prediction for histone H2A and H4, deletion of both H2A and H4 amino-terminal tails in *S. cerevisiae* is lethal (Arthur Hsu unpublished results). Nevertheless, the functional redundancy hypothesis can be tested by monitoring progression of DNA damage sensitivity phenotypes when individual, pairwise double or triple histone H2A N-tail lysine mutations are combined with histone H4 N-tail deletion or H4 N-tail lysine mutations.

The DNA damage sensitivity of the strains carrying 'knuckle' mutations could also be mediated by altering modification states of 'knuckle' amino acids. Alternatively, 'knuckle' mutations might have a direct effect on nucleosome and

chromatin structure. The former doesn't seem very likely as the MS analysis of the post-translational modification status of the conserved SRS motif within the *S. cerevisiae* histone H2A 'knuckle,' before and after MMS treatment, did not reveal phosphorylation of the serines or methylation of the arginine within this region. In addition, acid-urea electrophoresis separation of *S. cerevisiae* H2A isoforms before and after MMS treatment did not reflect a damage-dependent loss of histone H2A charged species in the strains containing non-phosphorylatable amino acid analogues in 'knuckle' positions (data not shown). Although it is possible that transient modification states might not have been captured by these methods, the damage sensitivity phenotype imparted by the charge-altering mutations within the 'knuckle' region is likely a direct consequence of changes in chromatin structure rather than changes in modification states of residues in this region.

Interestingly, Boeke and colleagues recently screened a systematic library of individual histone alanine substitutions for mutations that impair response to DNA damaging agents camptothecin (CPT), methyl methanesulfonate (MMS), hydroxyurea (HU) and ultraviolet radiation (UV) (Dai et al., 2008; Huang et al., 2009). Unfortunately, phospho-mimic mutations such as serine to glutamic acid substitutions were not included for histone H2A in their study. Nevertheless, consistent with their results, the serine to alanine substitutions mapping to the 'knuckle' region did not elicit a DNA damage phenotype in my experiments (Dai et al., 2008; Huang et al., 2009). The only phenotypic discrepancy pertains to the R18A mutation which appears to have a subtle DNA damage sensitivity in my hands as opposed to the absence of a phenotype in the published data, however this could be due to differences in the assay protocol, or different methods used for scoring for the severity of the phenotype.

The hypothesis that 'knuckle' mutations might have a direct effect on nucleosome and chromatin structure is supported by the location of the 'knuckle' residues within the nucleosome crystal structure, namely S17 and R18 face the DNA minor and major grooves respectively, whereas the S19 is oriented toward the central axis of the α1 helix and likely serves to stabilize the structure by 'capping' the helical dipole (Figure 3.10). Substitution of S17 with the negatively charged glutamic acid might simply pose a charge interference problem with the like, negatively charged DNA, in addition to the steric hindrance issue introduced by the bulkier replacement. Alanine point mutation of the arginine at position 18 that neutralizes its positive charge might destabilize nucleosome structure as well, by eliminating favorable long distance interactions with the negatively charged DNA. In the case of S19, the polarity of the serine is directly responsible and necessary for its 'capping' role and it is reasonable to expect that a bulkier charged glutamic acid can interfere with the normal helix stabilizing function of the serine. The proposed effect of 'knuckle' mutations on nucleosome stability underscores the importance of the 'knuckle' structure preservation, specifically for the cell's capacity to cope with DNA damage. Based on the absence of a dominant negative phenotype, this effect of the 'knuckle' mutations on the nucleosome structure likely reduces the efficiency of 'knuckle' histone incorporation into chromatin, an event that might have specific consequences during processes that require extensive chromatin remodeling, such as DNA repair, replication or transcription. Otherwise, once incorporated these mutations might further interfere with the favorable chromatin environment that promotes DNA repair and checkpoint signaling through binding of protein factors, or they might indirectly influence these processes through an effect on repair and checkpoint gene expression.

Figure 3.10: Localization and orientation of the conserved SRS 'knuckle' residues within the crystal structure of the nucleosome core particle

Shown are nucleosome crystal structure views (A) perpendicular to the DNA superhlical axis, (B) partial side view rotated roughly 30° around the pseudo-axis passing through the dyad and (C) partial front view through the superhelical axis. The DNA superhelix, shown in brown, is wound around the central histone octamer. Each core histone is represented as a ribbon (H2A blue and purple, H2B yellow and orange, H3 green and pink, H4 white and turquoise). The location of the H2A 'knuckle,' a single turn α-helix shown in purple is indicated. The side chains of each residue within the conserved SRS motif of the 'knuckle' are shown as sticks. S17 and R18 face the DNA minor and major grooves respectively, whereas the S19 is oriented toward the central axis of the α1 helix and likely serves to stabilize the structure by 'capping' the helical dipole.

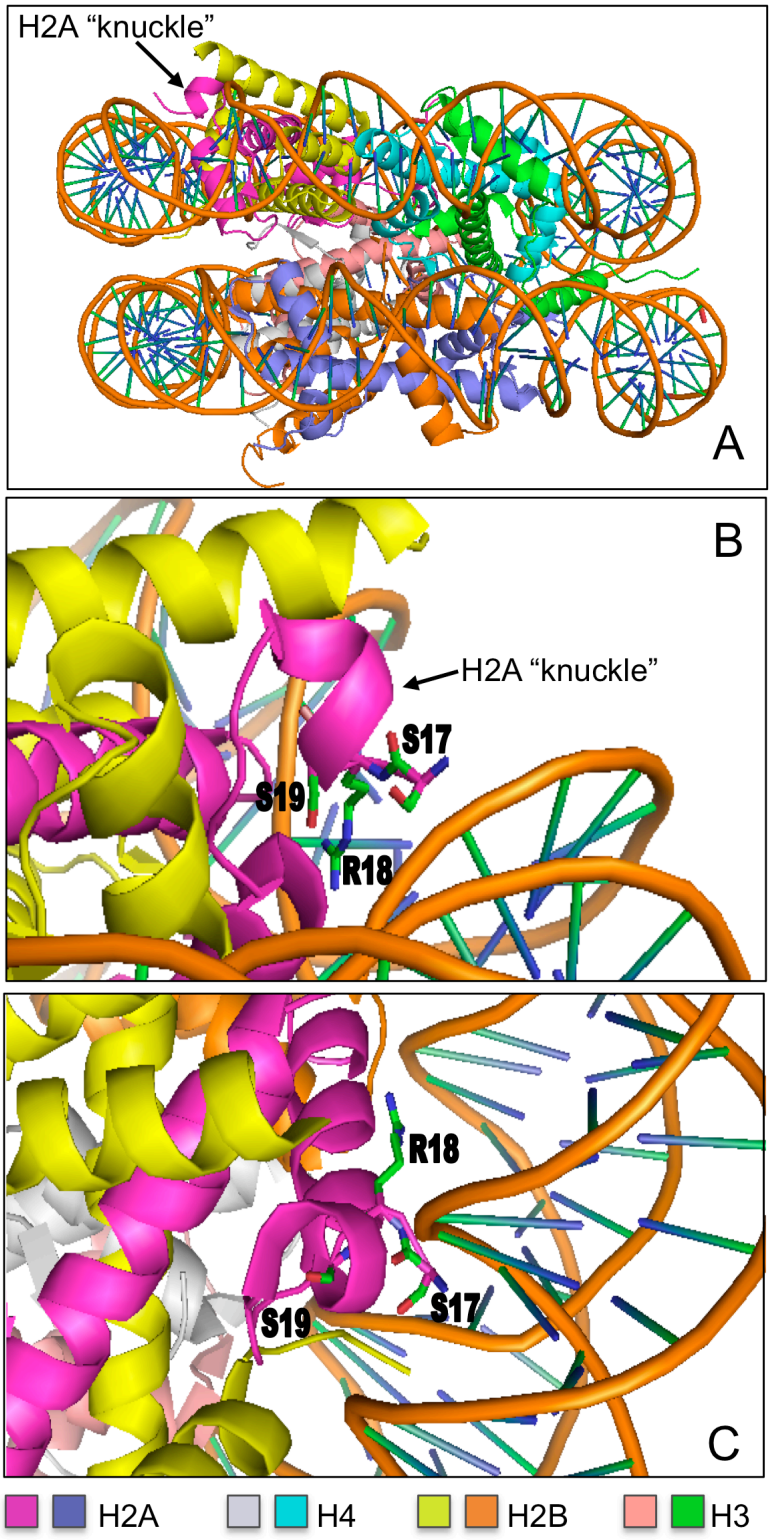
H2A “knuckle”
A
B
H2A “knuckle”
S17
S19
R18
C
R18
S19
S17
H2A
H4
H2B
H3

Figure 3.10

The exact mechanism by which the 'knuckle' structure mediates DNA damage sensitivity is the focus of the studies described in the next chapter. It is safe to speculate that it either involves recognition by a yet unknown histone-binding factor necessary for damage detection and repair, such as a checkpoint protein or a chromatin remodeling histone exchange factor (trans' mechanism), or in contrast, chromatin structure effects resulting from 'knuckle' mutations might directly influence expression of repair and checkpoint genes ('cis' mechanism).

CHAPTER 4

FUNCTIONAL ANALYSIS OF HISTONE H2A 'KNUCKLE' REGION

Introduction

The 'knuckle' region of H2A is a histone-fold extension spanning residues 17-22 within the amino-terminal tail (Figure 3.10). In contrast to the remainder of the histone H2A tail which shows considerable divergence across eukaryotes, the residues comprising the 'knuckle' region, especially the S/T-R-S segment, show remarkable sequence conservation suggesting that they might have important function (Figure 3.7A). Structurally the 'knuckle' represents a single turn α-helix exposed on the surface of the nucleosome. Although not directly involved in histone-DNA interactions it has been proposed that it acts to tether the H2A-H2B dimer to the nucleosome and aids its dissociation from the nucleosome, presumably through recognition of a specific histone-binding factor (Luger and Richmond, 1998).

Initially, the 'knuckle' was functionally defined as a cluster region for a class of H2A mutations causing transcriptional defects of SNF/SWI-dependent genes, such as *SUC2* (Hirschhorn et al., 1995). However, not all of the SNF/SWI-regulated promoters are affected by the 'knuckle'-clustering mutations, suggesting these mutations are phenotypicaly different from the SNF/SWI mutations. Consistent with the distinct transcription promoting function of the 'knuckle,' the defects caused by the mutations are not ameliorated by the suppressor of *snf/swi* mutations, *spt6*, and unlike the *snf/swi* mutations, the chromatin structure of the *SUC2* promoter is in an active conformation in the histone H2A 'knuckle' mutants (Hirschhorn et al., 1995).

A subsequent study (Lenfant et al., 1996) monitoring basal transcription by *GAL1* promoter-driven URA3 reporter construct, ascribed an opposite, repressive transcriptional role for the 'knuckle.' Namely, the 'knuckle,' described as a short region adjacent to the structured α-helical core, was shown to be required for repression of basal, uninduced transcription. Those observations are consistent with a recent genome-wide expression profiling study (Parra and Wyrick, 2007) which confirmed that under standard growth conditions a subset of (~4.8%) genes in the yeast genome is indeed repressed by the H2A N-terminus, and this repression is likely mediated by the 'knuckle' domain as it is largely independent of residues in the remaining portions of the tail. In fact, the 'knuckle' domain of the H2A N-terminal tail, specifically two residues within it, S17 and R18, were shown to be required for the transcriptional repression of the three reporter genes examined, *BNA1*, *BNA2* and *GCY1*. As a result, the 'knuckle' region was designated as a Histone H2A Repression (HAR) domain.

Interestingly, the same study also reported that deletion of the 'knuckle' domain imparts sensitivity to UV irradiation (Parra and Wyrick, 2007). Likewise, a parallel study (Moore et al., 2007) reported that the strain carrying a specific 'knuckle' S17A mutation exhibited significantly reduced survival after UV treatment, and this phenotype is even more pronounced in the H2A amino-terminal tail deletion strain. However, the mechanism by which the 'knuckle' mutations compromised recovery from UV-induced DNA lesions has not been identified.

In the previous chapter I described that a DNA damage survival property indeed exists in the H2A 'knuckle' region, and this property is not only limited to UV damage, but is broad in its effect as it affects response to DNA lesions elicited by various means. The damage specific function of the 'knuckle' is mediated through its structure rather than 'knuckle' post-translational modifications, as it

is appears to be dependent on the charge of each individual residue within the conserved 17-19 SRS sequence. The possible mechanisms by which the 'knuckle' structure regulates DNA damage survival are addressed in this chapter. Consistent with the transcriptional role of the H2A 'knuckle,' a screen for high-copy suppressors of the hydroxyurea (HU) damage phenotype of the S17E mutant revealed genes with metabolic and ribosomal function. In terms of transcription of damage-specific targets, gene expression analysis of a subset of MMS-dependent damage response genes, established opposing 'knuckle'-mediated transcriptional effects for two genes responsible for DNA repair, *RNR2* and *LIG4*. Using HO endonuclease strain background to generate synchronously induced DSBs, it was determined that homologous recombination repair pathway is not affected in strains carrying 'knuckle' mutations. However, consistent with their sensitivity to DNA damage, S17E, R18A and S19E strains exhibit subtle delays in checkpoint termination after repair. Additionally, both, S17A and S17E, as well as the 'knuckle' deletion mutation, impair the efficiency of the NHEJ pathway, by ~40% relative to the wild type strain.

Results

Damage sensitivity to HU conferred by S17E mutation is suppressed by overexpression of genes involved in cellular metabolism and protein synthesis

Suppressor screen, first invented in yeast to identify functions involved in morphogenesis (Bender and Pringle, 1991), is a powerful tool for uncovering more information about a gene or mutation, and identifying other interacting components in a pathway. Therefore, a non-biased screen for high copy suppressors of the hydroxyurea (HU) damage sensitivity of the S17E mutant was performed in an effort to define the pathway that might be affected by HU-dependent damage in the 'knuckle' mutants. For that purpose a high copy ADH promoter-driven cDNA library expressing a URA3 selection marker, was generously provided by the Laboratory of Dr. Mitchell Smith at the University of Virginia. The library was used to screen ~60,000 colonies for their ability to promote survival of the otherwise defective S17E mutant on plates containing 200 mM HU.

The screen yielded 98 positives, out of which ~50% encode a wild type copy of histone H2A which confirms the validity of the method. Contrary to the expectations none of the remaining 'hits' were genes involved in DNA damage detection or repair (Table 2). Instead the isolated suppressors fell in two main categories, metabolic and ribosomal, which is consistent with the role of the 'knuckle' in transcriptional regulation of metabolic genes, such as *SUC2* for example.

Table 2: High copy gene candidates for suppression of HU sensitivity of H2A S17E mutant

Type of gene	Protein encoded
Ribosomal (9)	RPS14B ribosomal protein 59 in the small subunit
	RPS19A protein component of the small (40S) ribosomal subunit
	RPS9B protein component of the small (40S) ribosomal subunit
	RPL25 primary rRNA binding protein of the large subunit
	RPL41A & B ribosomal protein L47 of the large (60S) subunit
	SSB 1&2 cytoplasmic ATPase that is a ribosome associated molecular chaperone
	RPL43A protein component of the large (60S) ribosomal subunit
	EFB1 translation elongation factor 1 beta
	RPPO conserved ribosomal protein PO
Metabolic (6->8)	PDC5 (x2) minor isoform of the pyruvate decarboxylase
	TDH3 (x2) glyceraldehydes 3-phosphate dehydrogenase
	PFK1 alpha subunit of heterooctameric phosphofructo kinase involved in glycolysis
	BCP1 essential protein involved in nuclear export of Mssp4 lipid kinase
	ENO2 enolase II
	GPM1 tetrameric phosphoglycerate mutase
Retrotransposons (1)	Ty1 LTR
Chaperones (1)	SSA1 ATPase involved in protein folding and NLS-directed nuclear transport
Others (2)	CDC5 polo-like kinase that has multiple functions in mitosis and cytokinesis
	YLR257W uncharacterized hypothetical protein
WT H2A (53)	
No insert (24)	
Total (98)	All

Transcription of several DNA damage response genes is affected by mutations in the 'knuckle' region

Considering the documented role of the 'knuckle' in transcriptional regulation, also supported by the results from the suppressor screen, it is possible that mutations that map to this region affect expression of DNA damage response genes and thereby indirectly contribute to the observed DNA damage sensitivity of the histone H2A 'knuckle' mutant strains. Interestingly, the reported subset of the yeast genome repressed by the H2A amino-terminal domain deletion in the Parra and Wyrick study did not include genes known to be involved in the DNA damage response. However, the study was conducted in the absence of damaging agents and therefore it did not evaluate whether deletion of the 'knuckle' region affected damage-dependent expression changes of damage response genes.

To explore the role of histone H2A 'knuckle' region in transcriptional regulation of damage response genes during DNA damage, a small-scale gene expression analysis was conducted before and after 2 hr of 0.02% MMS-induced DSBs in the strains carrying S17E and S19E 'knuckle' mutations. Quantitative PCR was used to assess expression levels of a subset of genes selected based on their previously documented response to 0.02% MMS treatment in a genome-wide expression study of wild-type cells (Gasch et al., 2001). The genes examined in this assay along with their functional description are listed in Table 3. The group includes genes involved in repair by either homologous recombination (HR) or non-homologous end-joining (NHEJ), in addition to damage activated kinases, and damage dependent transcription factors. In wild type cells, all of the genes represented, except *ROX1,* which was repressed, were induced in response to MMS in the Gasch et al study. *SUC2* expression levels were used as a control, based on the established transcriptional defects conferred

by 'knuckle' mutations on this gene (Hirschhorn et al., 1995). The expression values plotted for each gene represent an average of three independent experiments.

Table 3: DNA damage response genes used for gene expression analysis

Gene	Description
RAD51	Strand exchange protein involved in homologous recombination (HR) repair of double strand breaks (DSBs) in DNA during vegetative growth and meiosis, forms a helical filament with DNA that searched for homology
RNR2	Small subunit of ribonucleotide-diphosphate reductase (RNR) complex which catalyzes the rate-limiting step in dNTP synthesis and is regulated by DNA replication and DNA damage checkpoint pathways
RNR3	Large subunit of ribonucleotide-diphosphate reductase (RNR) complex which catalyzes the rate-limiting step in dNTP synthesis and is regulated by DNA replication and DNA damage checkpoint pathways
ROX1	Heme-dependent repressor of hypoxic genes, contains an HMG domain responsible for DNA bending activity
PHR1	DNA damage-induced photolyase involved in photoreactivation and repair of pyrimidine dimers in the presence of visible light
DUN1	Cell-cycle checkpoint serine-threonine kinase required for DNA damage-induced transcription of target genes, phosphorylation of Rad55p and Sml1p, and transient G2/M arrest after DNA damage
YAP1	Basic leucine zipper (bZIP) transcription factor required for oxidative stress tolerance, mediates pleiotropic drug and metal resistance
KU80	Subunit of telomeric Ku complex involved in telomere length meintenance, structure and telomere position effect, relocates to sites of double-strand break (DSB) to promote nonhomologous end-joining (NHEJ) during DSB repair
LIG4	DNA ligase required for nonhomologous end-joining (NHEJ), forms stable heterodimer with required cofactor Lif1p and catalyzes DNA ligation as a part of a complex with Lif1p and Nej1p
***SUC2* (txn control)**	Invertase i.e. sucrose hydrolyzing enzyme which consists of two forms: a secreted, glycosylated form regulated by glucose repression, and an intracellular, nonglycosylated enzyme produced constitutively

Based on the gene expression analysis, transcriptional levels of two out of the nine damage response-related genes examined were consistently affected by both S17E and S19E 'knuckle' mutations (Figure 4.1 and 4.2). Namely, the 'knuckle' region appears to be required for damage specific induction of *RNR2*, a small subunit of the ribonucleotide-diphosphate reductase complex which catalyzes the rate-limiting step in dNTP synthesis required for damage repair. Interestingly, the 'knuckle' region seems to have an opposite effect on the expression of the NHEJ ligase, *LIG4*, as it appears to be necessary for its transcriptional repression, although only in the absence of DNA damage. Surprisingly, *LIG4* was not among the genes reported by Parra and Wyrick as being repressed in a 'knuckle'-dependent manner, possibly because its transcriptional levels were below the arbitrary expression change cut-off imposed in their study. There were no detectable differences in the induction of the remaining genes examined in response to MMS treatment of the 'knuckle' mutants relative to the wild type. These results suggest that the 'knuckle' region is indeed required for transcription regulation of damage response genes, however this effect is rather subtle (less than two fold difference) and limited to a specific set of repair promoters.

H2A "knuckle' is required for efficient DSB repair by the NHEJ pathway

Given the subtle, and opposing effects of the 'knuckle' residues on a limited subset of repair gene expression, it was important to establish whether the defects leading to DNA damage sensitivity of the 'knuckle' mutants are indeed at a level of DNA repair. For that purpose, the repair efficiency of the two major DSB repair pathways, namely homologous recombination (HR) and non-homologous end joining (NHEJ), was examined in the strains carrying 'knuckle' mutations.

Figure 4.1: MMS-dependent expression profile of DNA damage response genes in the S17E and S19E strain

The expression of nine DNA damage-regulated genes was analyzed by quantitative PCR in the wild type and the (A) S17E or (B) S19E strain before and after 2 hr treatment with 0.02% methyl-methane sulfonate (MMS). The genes were selected based on their previously documented response to 0.02% MMS treatment in a genome-wide expression study of wild-type cells conducted by (Gasch et al., 2001) belong to several classes, including repair by both homologous recombination (HR) and non-homologous end-joining (NHEJ), damage activated kinases, and damage dependent transcription factors. The expression was normalized to actin and calculated relative to the levels of the same gene in the untreated wild type control which was set to 100%. Observed expression changes in the mutant strain relative to the wild type, are denoted with a red and blue arrow, for repression and induction respectively. The graph values and standard errors represent an average of three separate experiments.

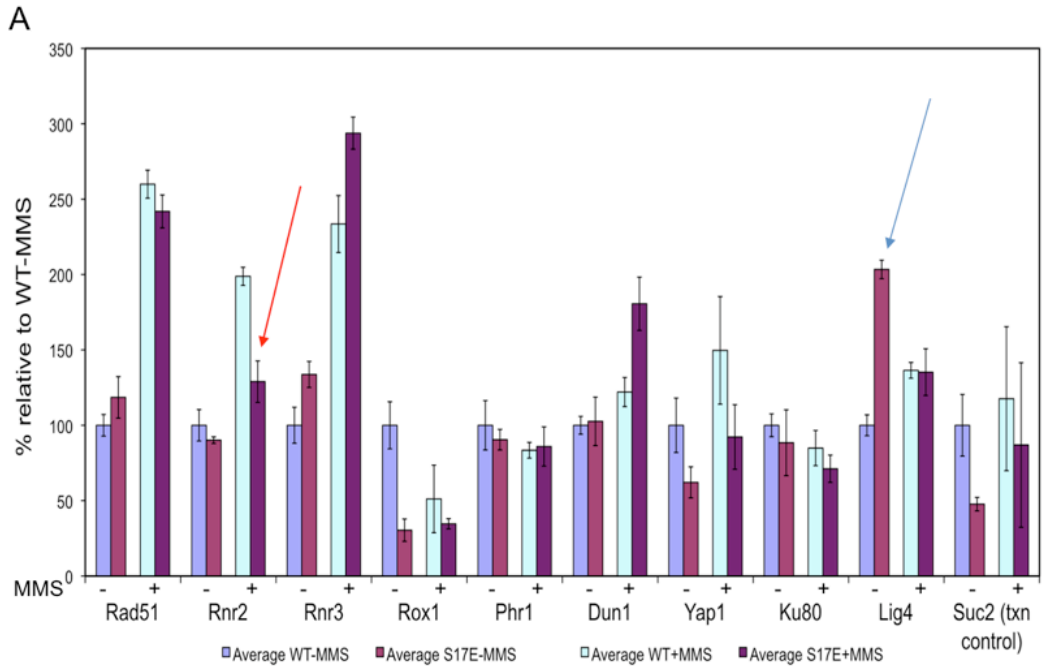
A
% relative to WT-MMS
350
300
250
200
150
100
50
0
MMS
- + - + - + - + - + - + - + - + - + - +
Rad51
Rnr2
Rnr3
Rox1
Phr1
Dun1
Yap1
Ku80
Lig4
Suc2 (txn control)
Average WT-MMS
Average S17E-MMS
Average WT+MMS
Average S17E+MMS

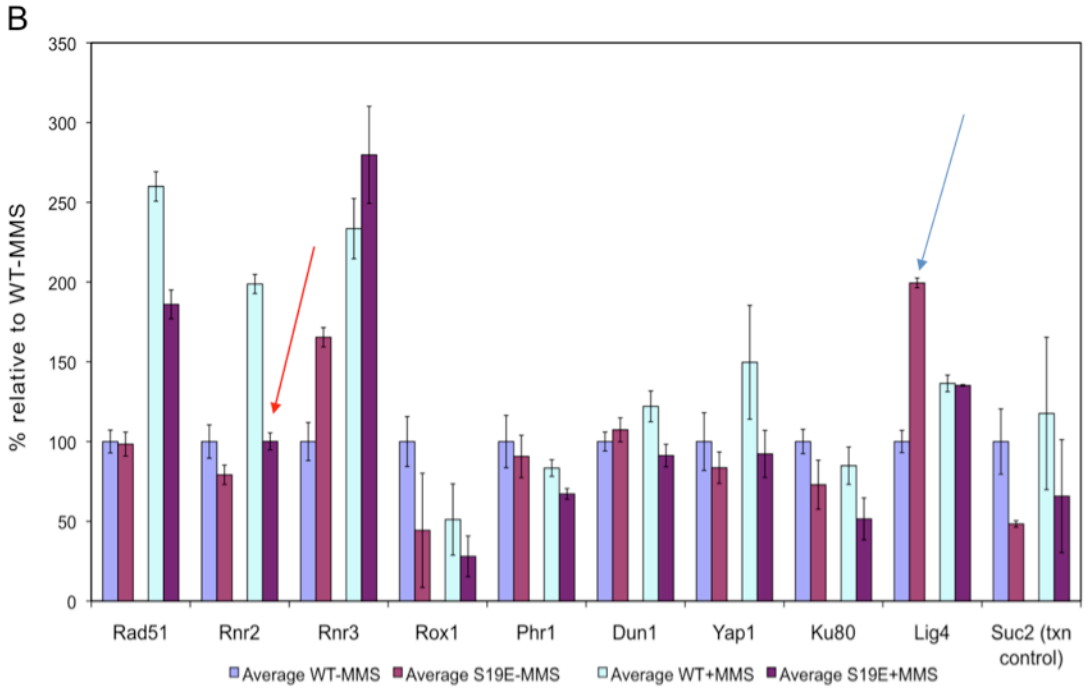
B
% relative to WT-MMS
350
300
250
200
150
100
50
0
Rad51
Rnr2
Rnr3
Rox1
Phr1
Dun1
Yap1
Ku80
Lig4
Suc2 (txn control)
Average WT-MMS
Average S19E-MMS
Average WT+MMS
Average S19E+MMS

A standard plasmid recircularization assay (Boulton and Jackson, 1996) was used in order to determine whether NHEJ pathway was indeed affected by the 'knuckle' mutations. The URA3-containing pRS416 plasmid utilized in this assay had no homology to yeast chromosomes and therefore was incapable of using homologous recombination as a repair mechanism for the DSB generated by linearization of the plasmid by *XhoI* restriction enzyme digestion. Thus, the break encountered when the linearized plasmid was introduced into cells could only be repaired by NHEJ. To ensure expression of the plasmid-encoded URA3 auxotrophic marker, cells had to successfully repair i.e. recircularize the transformed linear plasmids. The efficiency of the NHEJ repair mechanism was then monitored by growth of URA3 expressing colonies, products of recircularized plasmids, on appropriate selective plates. The NHEJ efficiency, scored as a ratio of colony number produced by transformation of linearized vs. intact plasmid, in all strains carrying H2A N-tail or 'knuckle' deletions, as well as S17 mutations, was reduced by ~40% relative to the wild-type (Figure 4.2), suggesting that these mutants were indeed deficient in NHEJ repair.

H2A 'knuckle' residues are not required for DNA DSB break repair by a homologous single strand annealing mechanism

In order to examine whether the homologous repair pathway was also affected by 'knuckle' mutations, each of them was introduced into an HO endonuclease background strain which provides a way to study not only DSB recognition and repair dynamics, but also monitor checkpoint kinetics in *S. cerevisiae*. The advantage of the HO endonuclease system is that synchronous DSBs can be created in nearly all cells of the population by the endonuclease expressed from a

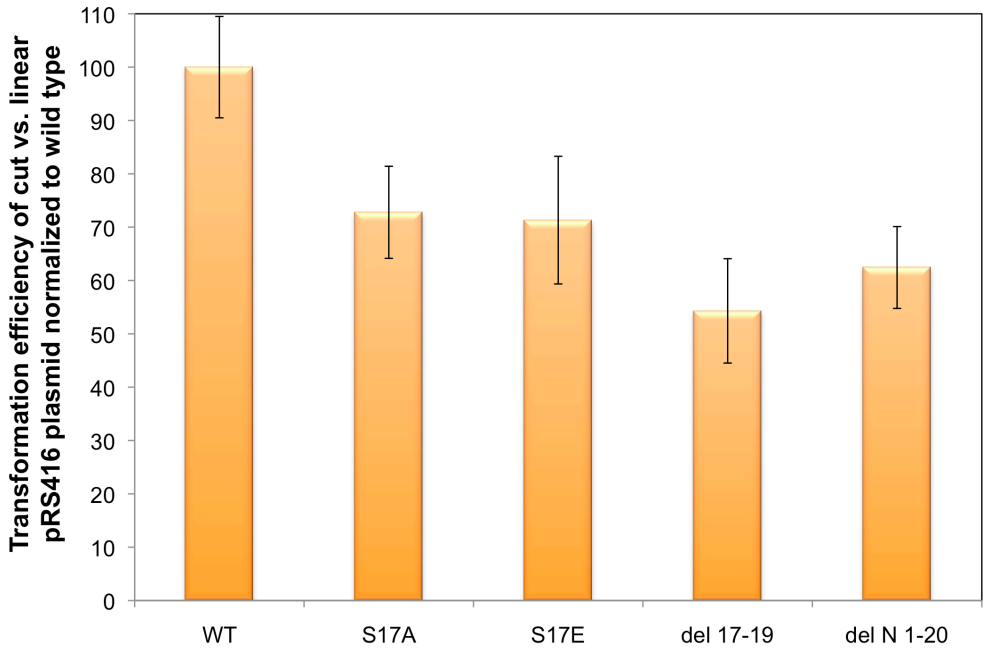

Figure 4.2: Histone H2A 'knuckle' region is required for efficient NHEJ
The indicated H2A *S. cerevisiae* strains carrying a 'knuckle' deletion and S17 point mutations were transformed with uncut or *XhoI*-digested plasmid pRS416. Repair efficiency is expressed as a percentage of colony formation after transformation with linear versus uncut plasmid and normalized to the appropriate wild type control which was set to 100%. The graph values and standard errors represent an average of three separate transformation experiments.

galactose-inducible promoter. In this particular system the endonuclease 24-base-pair recognition cut site is inserted in the Leu2 gene and the break is repaired by single strand annealing (SSA) from a partial duplication of the Leu2 gene located 30 kb away (Fishman-Lobell et al., 1992). The kinetics of DSB repair efficiency in these strains was visualized by a PCR based assay which directly monitors DNA integrity using primers flanking the cut and the repair homologous sequences (Figure 4.3).

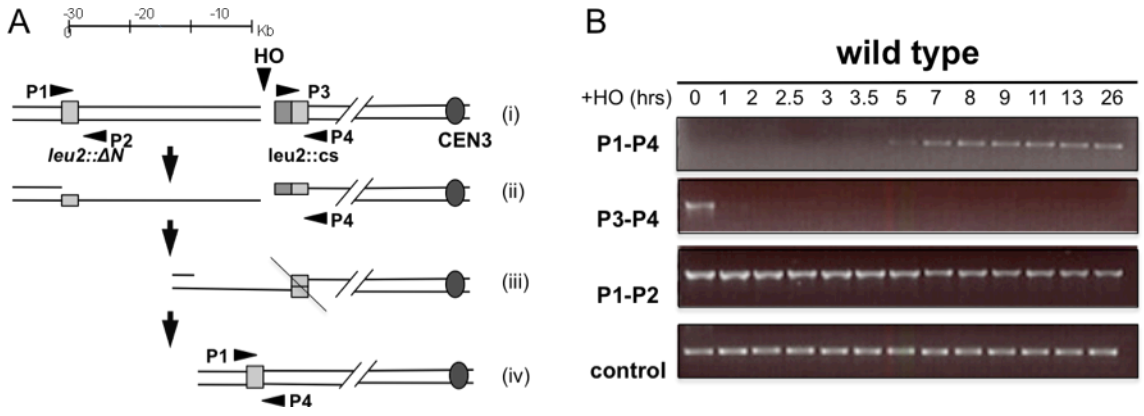

Figure 4.3: Repair dynamics of HO-induced DSB by a single strand annealing (SSA) mechanism

A. Diagram for repair of HO-induced DSB by single strand annealing (SSA) mechanism: (i) Galactose-induced HO cuts at its recognition cut site inserted in the Leu2 locus *(leu2::cs)* on chromosome III. (ii) Processive 5′->3′ resection generates single strand DNA (ssDNA) and eventually reaches a partial Leu2 gene duplication *(leu2::ΔN)* located 30 kb upstream. (iii) The two homologous single strand regions anneal in a Rad52 and Rad1/10-dependent fashion and the non-homologous sequences are excised. (iv) The break is successfully repaired. (adapted from Keogh et al, 2006). Primer sets designated P1-P2, P1-P4 and P3-P4 can be used to monitor the physical integrity of the DNA in the break region by a PCR-based assay. Their location is indicated in the diagram.

B. PCR analysis of genomic DNA from wild type strain with primers P1-P4 was used to monitor HO-induced DSB repair. A primer set amplifying across the cdc13 genomic locus which is on chromosome IV and thereby is not affected by the HO-induced DSB, was used as a DNA loading control. Genomic DNA was collected at each indicated time point following HO induction.

The DSB homologous recombination repair efficiency as determined by PCR did not appear to be affected in any of the strains carrying 'knuckle' mutations as repair products appeared at the same time and developed with the same dynamic in all of the 'knuckle' mutant strains as in the wild type strain (Figure 4.4). This observation indicates that the DNA damage sensitivity of the strains carrying 'knuckle' mutations is not due to defects in the homologous DNA repair pathway.

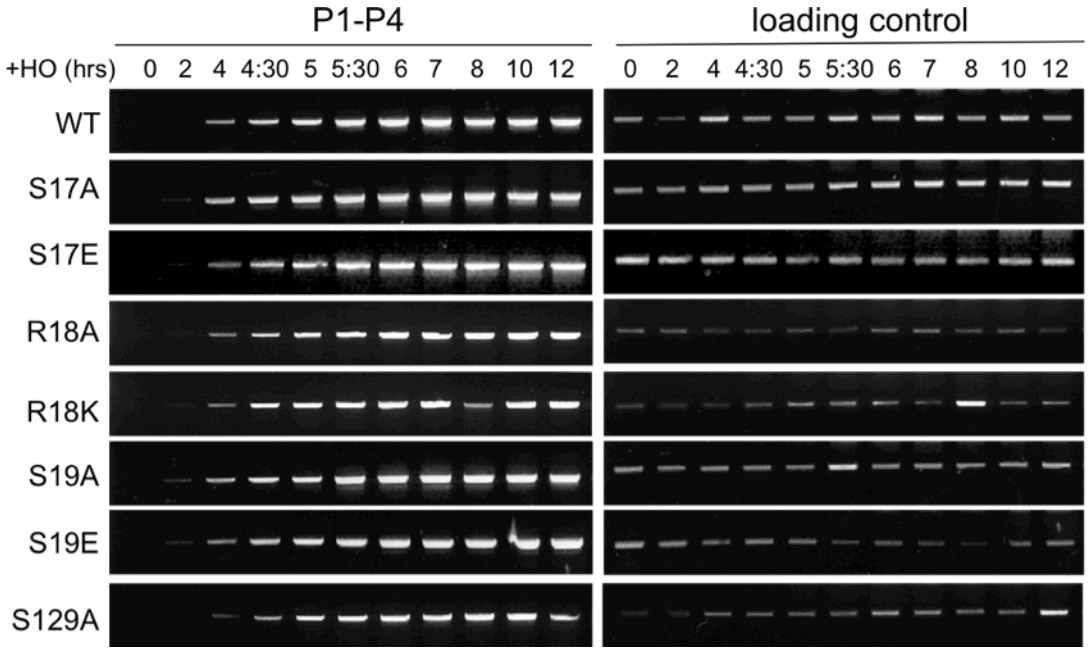

Figure 4.4: H2A 'knuckle' residues are not required for DNA DSB break repair by a homologous single strand annealing (SSA) mechanism

PCR analysis of genomic DNA isolated from *S. cerevisiae* strains containing 'knuckle' point mutations at indicated time points during HO-induced DSB repair. Primer pair P1-P4 flanking the break site and the partial duplication was used for the PCR analysis. A primer set amplifying across the cdc13 genomic locus which is on chromosome IV and thereby is not affected by the HO-induced DSB, was used as a DNA loading control.

Mutations in the H2A 'knuckle' region have checkpoint termination defects

In eukaryotic cells DNA damage generates a checkpoint signal that prevents further cell cycle progression to allow time for DNA repair prior to chromosome segregation. Following repair however, cells need to extinguish the checkpoint arrest signal in order to reenter the cell cycle.

Considering that the DNA damage sensitivity imparted by the 'knuckle' mutations is not related to homologous repair directly, it likely results from a defect in downstream signaling processes required for cell cycle resumption after checkpoint arrest. The mechanism of the HO-induced single-strand annealing repair involves a 5' to 3' resection to form a ssDNA which normally triggers a DNA damage checkpoint-mediated G2/M arrest and phosphorylation of the yeast checkpoint kinase Rad53. To assess whether the 'knuckle' region were indeed required for cell cycle checkpoint responses following DSB repair, cell cycle kinetics of strains carrying 'knuckle' mutations was monitored by flow cytometry during HO-induced DSB repair. The observed dynamics of checkpoint activation in all H2A 'knuckle' mutant strains was comparable to the wild type strain. There was a rapid accumulation of cells with an G2/M phase DNA content within the first few hours. Interestingly however, unlike the wild type strain, which appeared to proceed through M into G1 phase after 7 hours, subtle checkpoint recovery delays of ~1.5 hrs were observed only in the S17E, R18A and S19E mutant strains, consistent with their sensitivity to DNA damage (Figure 4.5). Also consistent with the previously documented requirement for γH2A.X dephosphorylation in checkpoint termination (Keogh et al., 2006), delays were not observed in the non-phosphorylatable H2A S129A mutant strain (Figure 4.6).

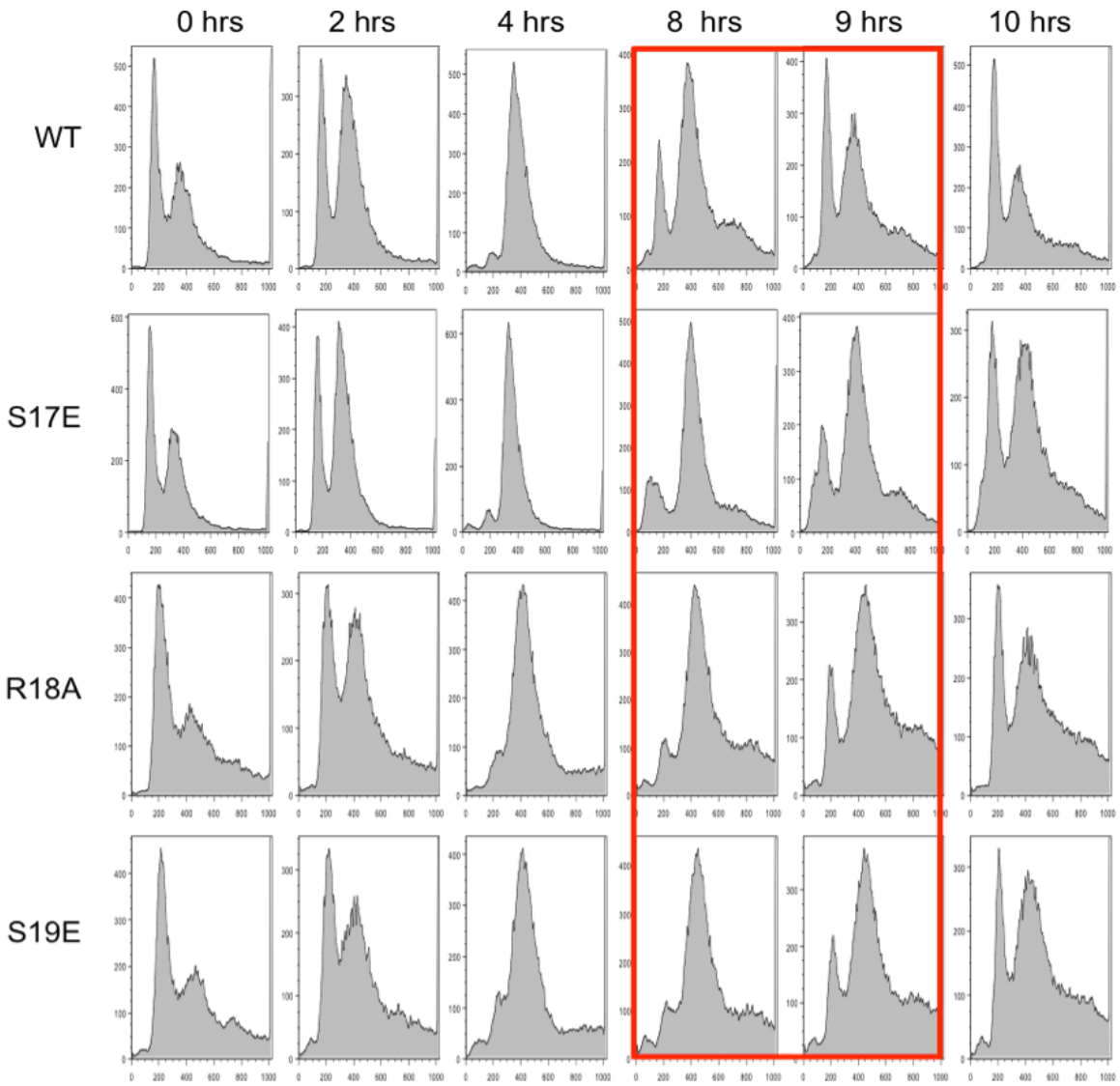

Figure 4.5: Structure-altering mutations of the H2A 'knuckle' region delay efficient cell cycle progression following HO DSB-induced arrest

Cell cycle progression was monitored in response to HO-induced DSBs in indicated *S. cerevisiae* strains containing H2A 'knuckle' structure-altering point mutations. FACS analysis was performed on cells collected at each indicated time point following HO induction and profiles are shown for each individual strain. Time points enclosed in a red box have a delayed cell cycle distribution in the strains with 'knuckle' mutations relative to the wild type strains. The two peaks in the profiles represent cells with 1N or 2N DNA content, corresponding to cells in G1 phase or G2/M phase, respectively.

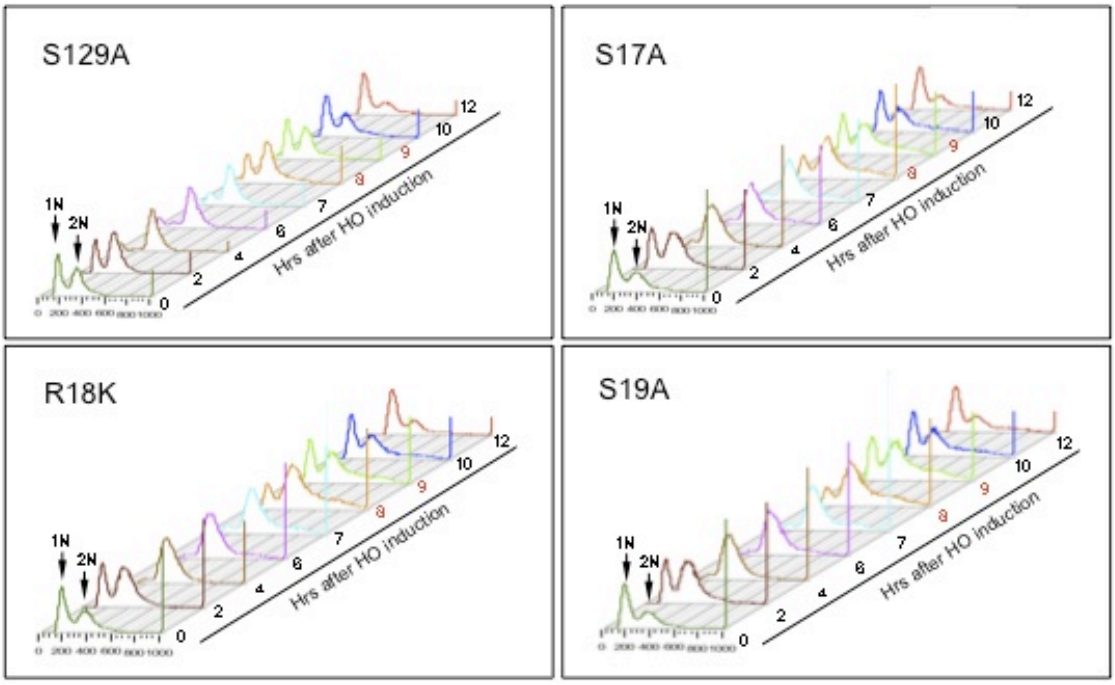

Figure 4.6: Normal cell-cycle progression following HO DSB-induced arrest in strains with non-disruptive 'knuckle' point mutations

Cell cycle progression was monitored in response to HO-induced DSBs in indicated *S. cerevisiae* strains containing H2A 'knuckle' point mutations. FACS analysis was performed on cells collected at each indicated time point following HO induction and profiles are shown for each individual strain. Arrows indicate peaks in the profiles that represent cells with 1N or 2N DNA content, corresponding to cells in G1 phase or G2/M phase, respectively.

The early phosphorylation kinetics of the yeast checkpoint kinase Rad53 after DSB induction is also similar in the 'knuckle' S17 point mutants relative to the wild type. However, whereas Rad53 activity decreased in the wild type strain after 6 hrs, the S17E 'knuckle' mutation prolonged Rad53 activity for ~1.5 hrs (Figure 4.7). The sustained Rad53 phosphorylaton is correlated with the maintenance of G2/M phase arrest observed by FACS, arguing that checkpoint recovery is indeed delayed by DNA damage sensitive mutations in the 'knuckle'

region. Similar Rad53 checkpoint deactivation delays are observed in strains carrying γH2AX phospho-mimic S129E, consistent with the observation that γH2A.X dephosphorylation is necessary for efficient checkpoint recovery.

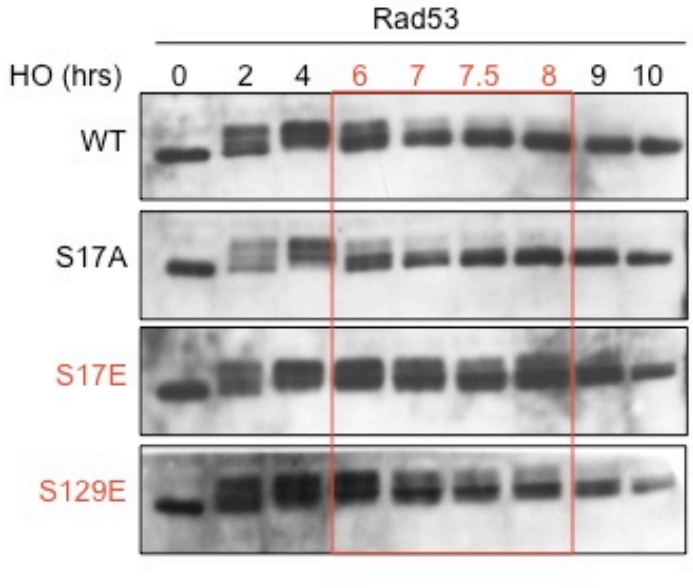

Figure 4.7: S17E mutation has a checkpoint recovery defect
Delayed checkpoint termination in *S. cerevisiae* strains with S17E mutations was monitored by Rad53 checkpoint-dependent autophosphorylation. Whole cell extracts were collected at indicated time points following HO-induction and Rad53 autophosphorylation dynamics was detected by immunoblotting.

Discussion

The conserved SRS motif of histone H2A, spanning residues 17-19 within the 'knuckle' region, encodes a unique and previously unrecognized role for the H2A N-terminal tail in the DNA damage response in *S. cerevisiae*. This study sheds light on the potential mechanisms involved in this function by demonstrating that the H2A 'knuckle' is required for efficient DSB-repair by the NHEJ pathway, but has no effect on the dynamics of homologous single strand annealing (SSA) repair pathway. The 'knuckle' region is also required for efficient recovery from cell cycle arrest following successful repair. The mechanism therefore, by which the H2A 'knuckle' structure mediates the DNA damage response impinges on multiple aspects of chromatin function.

One aspect, which likely indirectly contributes to the DNA damage sensitivity of the 'knuckle' mutations, involves transcriptional regulation. Indeed, transcription of a subset of genes, including some, but not all of the genes involved in DNA repair, such as *RNR2* and *LIG4*, is affected in strains with 'knuckle' mutations. This effect on gene expression is consistent with the model whereby 'knuckle' mutations directly affect nucleosome stability and chromatin structure required for efficient transcription. However, given that histones containing 'knuckle' mutations are the only source of H2A in the cells, and H2A is distributed throughout the genome, it is surprising that the transcriptional effect is specific, and only the expression of a limited subset of promoters is affected in a situation where global 'knuckle' dependent chromatin structure perturbations are expected. Additionally, the effects of the 'knuckle' mutations on the expression of the two affected DNA repair genes are opposing in nature i.e. the 'knuckle' seems to be required for induction of *RNR2* upon damage, but it normally represses expression of *LIG4*. This observation is also consistent with the previously documented contrasting transcriptional role of the 'knuckle' as

both, a repressor of basal uninduced transcription, as well as a region necessary for transcription of SNF/SWI-dependent genes (Hirschhorn et al., 1995; Lenfant et al., 1996; Parra and Wyrick, 2007). A likely explanation for the observed contrasting and limited effects of the 'knuckle' on gene expression, lies within the chromatin environment required for the transcriptional state of a particular gene. In particular, a gene that would require extensive chromatin remodeling for its induction or suppression might be unable to reach its optimal chromatin state necessary for the appropriate transcriptional output in the absence of the 'knuckle' region. These results indicate that chromatin remodeling is at the heart of the transcriptional defects imposed by the 'knuckle' structure perturbations.

The chromatin remodeling model can also explain the difference in observed effects of the 'knuckle' mutations on the repair efficiency of the two distinct repair pathways. Namely, NHEJ repair efficiency appears to be reduced in strains carrying 'knuckle' mutations whereas repair by homologous single strand annealing is not affected. The difference can be explained by the different DNA repair readouts used by the NHEJ and SSA assays. While the SSA repair assay is a PCR-based assay that directly examines the DNA integrity to detect repair, the NHEJ plasmid recircularization assay relies on gene expression as an indirect measure of repaired DNA template. However, repair i.e. efficient physical ligation of DNA ends is not the only prerequisite for normal gene expression, and transcriptional output as already discussed, is directly dependent on the chromatin state of the template after the DNA has been repaired. Thus, it is difficult to discern the specific contributions of DNA repair to the gene expression in the NHEJ assay. If the 'knuckle' mutations are indeed disruptive to chromatin structure and transcription-related chromatin remodeling of the template, gene expression will be affected even after successful DNA repair, which normally happens on naked DNA. Therefore, it is plausible

that NHEJ repair efficiency is not affected by the 'knuckle' mutations, and instead, the results likely reflect reduction of gene expression due to defects in chromatin remodeling required for transcription from the otherwise repaired template.

Finally, the transcriptional defects observed in the strains carrying 'knuckle' mutations are small in magnitude. In other words, the differences in expression levels of the affected promoters are less than two fold, which begs the question whether those changes are sufficient for the observed DNA damage sensitivity of the 'knuckle' mutant strains. It is likely, that is not the case. Although both affected genes *RNR2* and *LIG4*, are involved in DNA repair, there is no clear correlation between the expression and the repair, as SSA and likely NHEJ repair pathways function quite efficiently in these mutants. Instead, the defect in the DNA damage response appears to be downstream of the repair process and at a level of checkpoint signaling after repair has been completed. In particular, delays in checkpoint termination, rather than repair defects per se, seem to be responsible for the DNA damage sensitivity of the strains carrying 'knuckle' mutations, arguing that repair of the DNA lesions itself is not sufficient signal for turning of the DNA damage checkpoint. At this point, it is not clear what the exact signal for checkpoint termination is and while it is possible that 'knuckle' transcriptional defects might indirectly be involved at a level of checkpoint gene expression, it is unlikely that is the case, given the subtle effect the 'knuckle' had on expression of repair genes and on the repair process itself.

One intriguing possibility is that the observed delays in checkpoint termination might be a consequence of the inability of cells carrying 'knuckle' mutations to reinstate an appropriate chromatin structure necessary for checkpoint signaling after repair. There are two, possibly overlapping mechanisms, that might contribute to efficient chromatin reassembly at sites of

DNA lesions. First, 'knuckle' mutations might impose direct structural constrains on efficient chromatin reassembly following DSB repair. Otherwise, and possibly because of the structural constraints, the 'knuckle' mutations might disrupt regulation of histone post-translational modifications necessary for checkpoint termination, such as dephosphorylation of γH2A.X, a process previously linked to checkpoint recovery (Keogh et al., 2006). The misregulation of histone modifications, in turn may prevent efficient restoration of chromatin structure following DSB repair. So again, chromatin remodeling which is required for successful restoration of chromatin structure after DSB repair, is the mechanism likely to be responsible for the observed checkpoint termination defects of the 'knuckle' mutants.

Taken together, the results in this study indicate that in addition to its subtle effect exhibited through transcriptional regulation, the other aspect affected by the 'knuckle' structure mediated modulation of chromatin remodeling, and the one that is likely to be mainly responsible for the DNA damage sensitivity of the strains carrying 'knuckle' mutations, is the efficient chromatin reassembly following DSB break repair.

CHAPTER 5

GENERAL DISCUSSION

The focus of my thesis research has been on histone H2A and its functional domains required for normal response to DNA damage. My work has characterized two conserved regions located within the two different histone H2A tails that play an important role in regulation of the DNA damage response. In particular, I identified an H2A.X variant-specific SQ motif within the C-terminal tail of *Tetrahymena* major histone H2A.S providing the first description of this region in ciliated protozoa. The function of the SQ motif is mediated by post-translational phosphorylation of the conserved serine which is essential for normal progression through *Tetrahymena* life cycle, and in particular, meiosis. I also described another conserved functional domain of histone H2A in budding yeast which also functions in the DNA damage response. This region, also known as the 'knuckle,' is located within the H2A N-terminal tail, and its function appears to be independent of post-translational modifications.

Below I will discuss the significance of these findings in the context of already published results and address their implications for future research.

Carboxy-terminal SQ domain of *Tetrahymena* histone H2A.S

Recombination of the maternal and paternal genomes during the meiotic specialized division cycle requires extensive self-inflicted DNA damage in the form of DNA DSBs. In most organisms these DSBs are crucial for initiating intimate chromosome pairing (synapsis), which facilitates their subsequent repair. A role for the histone variant γH2A.X has been shown in this process in mammalian cells (Fernandez-Capetillo et al., 2003; Mahadevaiah et al., 2001),

however its function has not been closely examined in lower eukaryotes. My studies of this H2A variant in *Tetrahymena thermophila* have revealed a presence of this variant and its hallmark DSB-induced γH2A.X modification for a first time in a ciliate, specifically during the meiotic prophase stage of ciliate development. Here, I will discuss several studies that have expanded on my results in an effort to further characterize the mechanisms by which γH2A.X contributes to *Tetrahymena* meiosis.

Is γH2A.X required for efficient DSB repair in Tetrahymena?

The experimental results presented in Chapter 2 are consistent with a DSB-associated function for γH2A.X in *Tetrahymena.* Nevertheless, the question still remains whether this modification is required for the repair process itself or functions downstream of repair at a level of checkpoint recovery. One way to address this question would be to look directly at the DSB repair machinery and examine its function in the absence of γH2A.X. The limitation of this approach is that there are only a few DSB repair genes characterized in *Tetrahymena.* One of them is Rad51, a recombinase involved in homologous DNA pairing and exchange reaction. Rad51 foci normally emerge soon after the meiotic micronucleus begins to elongate and are maintained beyond the stage of maximal elongation (Loidl and Scherthan, 2004). Preliminary immunofluorescence results, however, looking at the appearance and distribution of Rad51 in γH2A.X mutant S134A in *Tetrahymena* revealed a normal Rad51 dynamics in the absence of γH2A.X (data not shown). Nevertheless it is possible that the distribution rather than kinetics of Rad51 foci is the more accurate read-out for this purpose, and that has yet to be examined. Evidence from other organisms exists however, that Rad51 accumulation at DSB is independent or only partially dependent on γH2A.X (Celeste et al., 2002),

arguing that Rad51 might not be the best choice of repair protein to look at. Proteins such as Nsb1, 53BP1 or Brca1 are more suitable for this analysis however homologues would first have to be identified by searching the *Tetrahymena* genome database.

Dr. Xiaoyuan Song in the laboratory of Dr. Martin Gorovsky, and my collaborator on this project, has been able to address the question with some success, by taking advantage of another approach based on a unique feature of *Tetrahymena* biology, a phenomenon of conjugation-mediated transfer of protein and/or mRNA between mating cells. In this assay a mutant cell is able to receive a wild type protein from its wild type mating partner during the process of conjugation. When γH2A.X S134A mutant cells were used in a mating with a wild-type partner, the γH2A.X staining was observed in the mutant in both nuclei, indicating that DSBs had accumulated prior to conjugation and protein transfer (Figure 5.1). These results indeed unequivocally demonstrate that γH2A.X functions in DSB repair as defects in γH2A.X formation result in inefficient break repair and lead to accumulation of DNA damage.

Is the DSB repair function of γH2A.X required for meiosis in Tetrahymena?

Studies of γH2A.X distribution in mouse spermatocytes have demonstrated two distinct patterns of staining: an early meiotic prophase Spo11-dependent γH2A.X formation associated with meiotic DSBs on all chromosomes, and a later, Spo11-independent staining highly specific for the condensed sex-chromosome (Mahadevaiah et al., 2001). These results, together with the observation that γH2A.X is indeed required for sex-chromosome condensation in mouse spermatocytes, have suggested an additional role for γH2A.X in meiosis, one that is independent of its function in DNA repair (Fernandez-Capetillo et al., 2003). In fact, it's been proposed that γH2A.X might function in transcriptional silencing

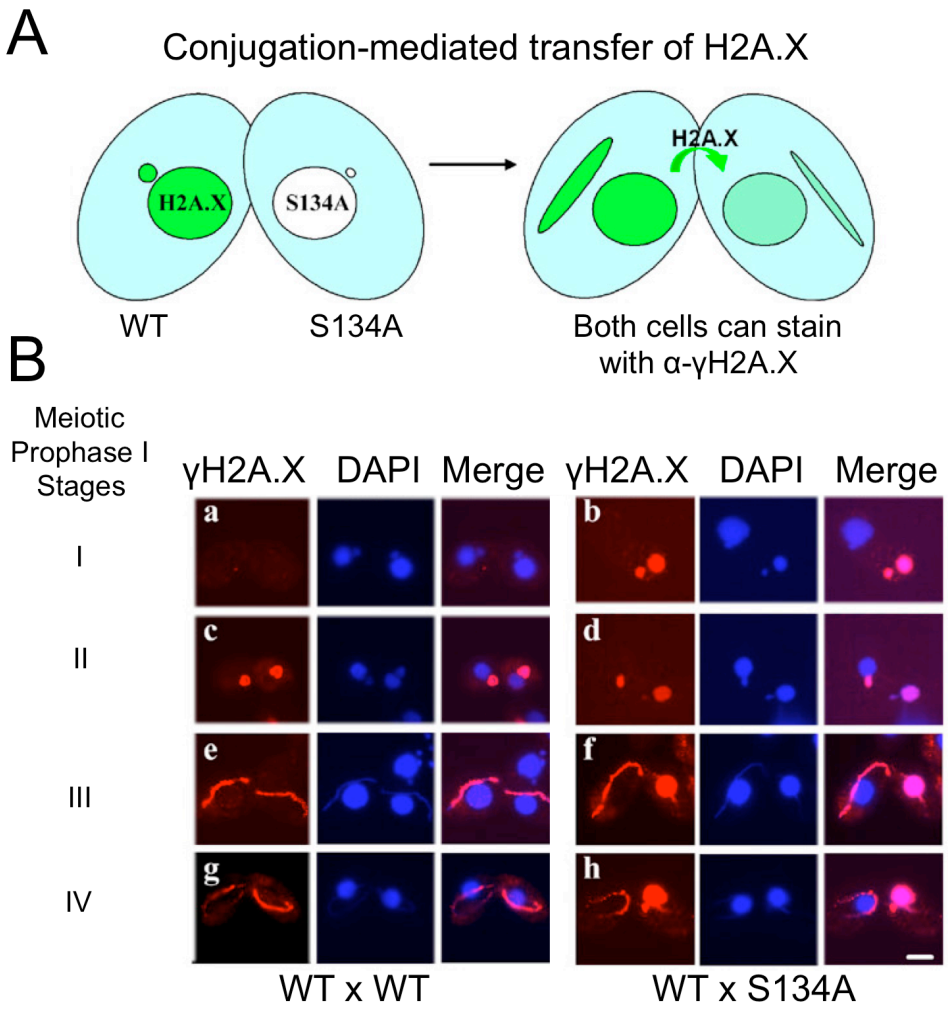

Figure 5.1: H2A.S S134A mutation in *Tetrahymena* macronucleus causes DSB repair defects in both macronucleus and micronucleus

The figure is courtesy of Dr. Xiaoyuan Song from the Laboratory of Dr. Martin Gorovsky at the University of Rochester, New York.

A. Diagram of conjugation-mediated transfer of protein (or mRNA) between two mating partners.

B. Immunofluorescence (IF) analysis of conjugation between wild type and H2A.S rescued cells (rows a, c, e, g) or wild type and S134A rescued cells (rows b, d, f, h) stained with anti-γH2A.X to detect DSB repair defect and damage accumulation. In each mating pair, the wild type cells are on the left.

of unpaired i.e. asynapsed meiotic chromosomes, a function mediated through chromosome condensation (Baarends et al., 2005; Sciurano et al., 2007; Turner et al., 2006; Turner et al., 2005).

It is therefore curious to speculate as to the role of γH2A.X during meiosis in *Tetrahymena*, especially in the light of the fact that synaptonemal complexes (SCs) as a required meiotic recombination intermediates or sequences with obvious homology to genes for SC structural proteins, have not been observed in this organism (Loidl and Scherthan, 2004; Wolfe et al., 1976). Is it possible that the function of γH2A.X during *Tetrahymena* meiosis is independent of its function in DNA repair and meiotic recombination?

Here, I will present several lines of evidence that point to the contrary. First, although *Tetrahymena* micronuclei are transcriptionally silent in vegetatively growing cells, nongenic micronuclear transcription has been detected early during conjugation, when meiotic prophase nuclei adopt the elongate crescent shape (Martindale et al., 1985; Martindale and Bruns, 1983; Sugai and Hiwatashi, 1974). This argues against the role of γH2A.X in meiotic transcriptional silencing, as the only stage marked by micronuclear transcriptional activity is the one that exactly temporally coincides with γH2A.X. A more recent set of experiments further exclude DSB-independent functions for γH2A.X during *Tetrahymena* meiosis. For example, Mochizuki and colleagues have demonstrated that γH2A.X signal during meiotic prophase in *Tetrahymena* is dependent exclusively on the presence of DSBs, meiotic or otherwise (Mochizuki et al., 2008). Namely, the absence of Spo11, a conserved meiosis-specific endonuclease which is required for meiotic DSB formation, abolished γH2A.X during meiotic prophase. In addition *spo11* knockout mutants display aberrant micronuclear elongation, reduced pairing of homologous chromosomes, a complete failure to form chiasmata and exhibit chromosome missegregation.

Interestingly, artificial induction of DSBs by treatment with cisplatin, restores γH2A.X in *spo11Δ* cells, arguing that γH2A.X is indeed dependent on DSB formation, although not Spo11 per se. Taken together these results support the notion that DSBs are the sole requirement for γH2A.X formation during meiotic prophase in *Tetrahymena,* and accordingly, its meiotic function is linked to DSB repair.

Amino-terminal 'knuckle' domain of *S. cerevisiae* histone H2A

A current model for the DNA damage response in the context of chromatin is the concept of 'access-repair-restore' (ARR). The original three-step ARR model was put forth by Smerdon and colleagues to explain how NER might function in the complex chromatin environment of a nucleus (Smerdon, 1991). The model, which has been subsequently extended to other repair systems by studies in *S. cerevisiae* from many laboratories, posits that at sites of DNA damage, chromatin structure is altered to expose DNA lesions to repair factors. Figure 5.2 presents the 'aces-repair-restore' model for DSB repair in *S. cerevisiae.*

In the context of DSB-repair, during access, a Mec1/Tel1 checkpoint–dependent H2A.X phosphorylation at the C-terminal SQ motif following DNA damage, serves as a binding platform for recruitment of histone acetyltransferase Nua4 via its Arp4 subunit. Subsequent Nua4 dependent histone acetylation of H4 N-tail lysines, further assists in recruitment of chromatin remodeling complexes Ino80 and Swr1 to the DSB. Based on my studies of histone H2A in *S. cerevisiae*, it is possible that acetylation of H2A N-terminal lysines, including the novel acetylation site at K13, likely contributes to this step of the damage response in a similar and redundant fashion as H4 acetylation given the shared Nua4 specificity for the substrates (Figure 5.3).

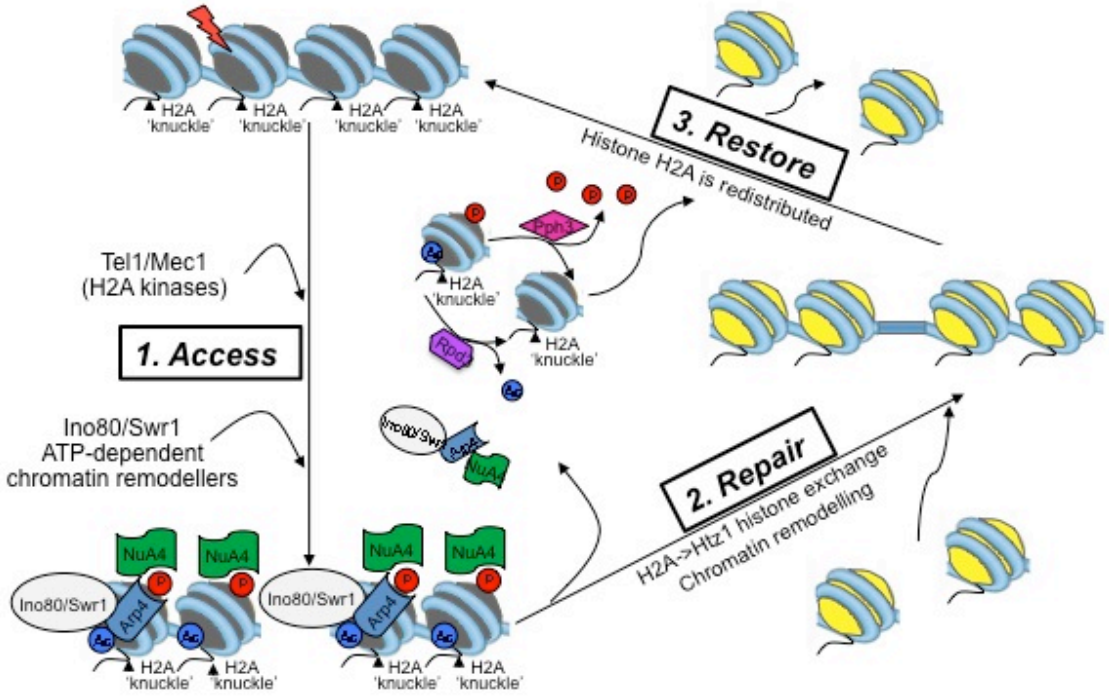

Figure 5.2: The 'access-repair-restore' model for DSB-initiated chromatin dynamics in budding yeast

Functional interplay between histone phosphorylation and acetylation events and different chromatin modifying activities during DSB repair:

1. Access: Mec1/Tel1 – dependent H2A.X phosphorylation at the C-terminal SQ motif following DNA damage serves as a binding platform for recruitment of histone acetyltransferase Nua4. Subsequent Nua4 dependent histone acetylation further assists in recruitment of chromatin remodeling complexes Ino80 and Swr1 to the DSB.

2. Repair: Ino80 dependent nucleosome depletion around DSBs allows for DNA repair followed by Swr1-dependent incorporation of Htz1 containing nucleosomes. γH2A.X is dephosphorylated by the Pph3 phosphatase after nucleosome displacement.

3. Restore: Ino80 dependent histone exchange of Htz1 with dephosphorylated histone H2A.X and subsequent Rpd3 dependent deacetylation of Nua4 substrates in newly assembled chromatin around the DSBs. Rpd3 associated CK2 phosphorylates deacetylated H4 at S1 preventing further reacetylation and restoring chromatin to its original state.

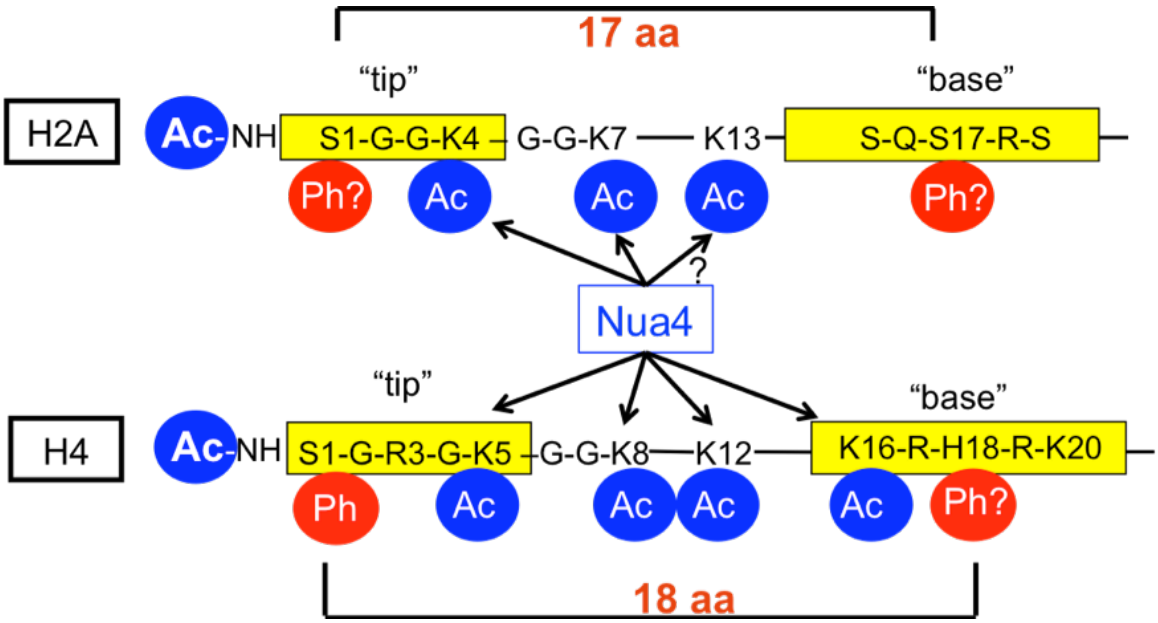

Figure 5.3: Functional redundancy of histone tails

Striking pairwise similarities between the N-terminal tails of histone H2A and H4 (shown are the tails from *S. cerevisiae* histones). For example, both H4 and H2A are the preferred substrates for Esa1p, the catalytic component of the NuA4 complex. Also, the N-terminal tails of both histone H2A and H4 are shorter than those of H3 and H2B, and both, H2A and H4 have a serine at the N-terminal starting position. Ac: acetylation, P: phosphorylation.

During the next stage of the DNA damage response, Ino80-dependent nucleosome depletion around DSBs allows for DNA repair possibly followed by Swr1-dependent incorporation of Htz1 containing nucleosomes. Following nucleosome displacement, γH2A.X is dephosphorylated outside of chromatin by the Pph3 phosphatase. Finally, Rpd3 dependent deacetylation of Nua4 substrates and Ino80 dependent histone exchange of Htz1 with dephosphorylated histone H2A.X restore chromatin around DSB sites. Rpd3 association with the H4 S1 kinase CK2, enables subsequent phosphorylation of deacetylated H4 at S1 preventing further reacetylation until the initiation of the next DNA damage response.

Once DSB repair is complete, cells must extinguish the checkpoint and resume cell cycle progression. This process of turning off the checkpoint has been dubbed 'checkpoint recovery.' There has been a great deal of focus on how the checkpoint is initiated and functions in response to DNA damage, however very little is known regarding its recovery. Here, I show that histone H2A 'knuckle' region is specifically required for efficient checkpoint recovery. In contrast, DNA repair of DSBs by either homologous recombination or non-homologous end joining pathways is not affected, clearly establishing that successful repair is not sufficient for checkpoint recovery. Nevertheless, many questions remain regarding the regulation of checkpoint termination after repair and specifically the mechanism by which the 'knuckle' mediates this process. Below I will discuss some of the possible mechanisms by which 'knuckle' region contributes to checkpoint recovery after DNA repair and the implications that these findings have on the overall understanding of how checkpoint is restored following repair.

Is nucleosome structure affected by 'knuckle' mutations?

In the absence of detectable 'knuckle' modifications by the mass spectrometry methods used, it is probably safe to speculate that charge-altering mutations of the 'knuckle' region affect nucleosome and chromatin structure rather than histone modification status. Consistent with this hypothesis, are observations from Hirschhorn and colleagues where they examined the chromatin structure of SUC2 promoter in an H2A S19F mutant in relation to the transcriptional state of the gene (Hirschhorn et al., 1995). In this study, they looked at MNase sensitivity of H2A S19F mutant DNA by performing an indirect labeling analysis with a SUC2 specific probe on MNase digested chromatin or naked DNA. Their conclusion was that under specific transcriptionally repressing conditions,

chromatin in the S19F mutant fails to adopt a fully repressed structure relative to the wild type.

It would therefore be interesting to test the MNase sensitivity pattern of DNA from strains with 'knuckle' disrupting mutations by running MNase digested genomic DNA on agarose gels. The other assay commonly used for this purpose makes use of a superhelical density pattern of endogenous plasmid. Namely, wrapping of DNA around a histone octamer introduces a negative supercoil into a closed circular plasmid and running the plasmid DNA isolated from either wild type or 'knuckle' strains on a chloroquine-containing gel can provide information about the global chromatin structure based on a difference in degree of plasmid supercoiling in different strains.

Transcriptional regulation - is expression checkpoint recovery genes affected by 'knuckle' structure?

Given that residues within the 'knuckle' region have been shown to function in the transcriptional regulation of certain promoters it is sensible to assume that there is an indirect effect of 'knuckle' mutations on checkpoint gene expression.

One approach to address transcriptional regulation is either a selective checkpoint gene expression study by quantitative PCR, or a microarray analysis of global gene expression levels before and after DNA damage in wild type and 'knuckle' disrupted strains. However, checkpoint gene regulation is not the most favored mechanism for the observed DNA damage sensitivity of 'knuckle' mutations as 'knuckle' effects on repair gene regulation have been subtle and not completely consistent with repair defects. Therefore it is best to examine alternative mechanisms for histone H2A 'knuckle' function in checkpoint recovery.

Is chromatin assembly after repair affected by 'knuckle' structure?

One intriguing hypothesis about the checkpoint function of the 'knuckle' is that mutations that disrupt the structural integrity of the 'knuckle' region reduce the efficiency of nucleosome reassembly after successful repair of double strand breaks (Figure 5.4).

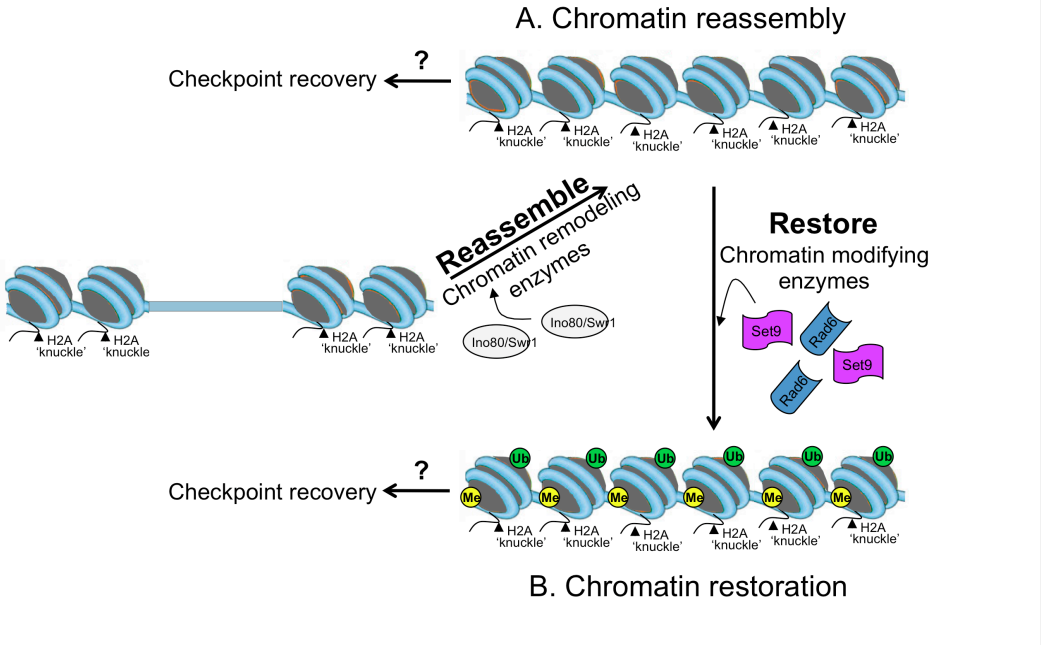

Figure 5.4: Reassembly versus restoration model for checkpoint recovery

Depicted are two potential mechanisms for checkpoint recovery following repair.

A. The chromatin reassembly mechanism posits that nucleosome deposition onto repaired DNA is sufficient to turn off checkpoint signaling. Chromatin reassembly can either signal checkpoint recovery directly or alternatively, histone deposition can displace DNA repair and checkpoint signaling machinery from the vicinity of the repair site resulting in checkpoint inactivation.
B. The chromatin restoration model, suggests that the signal to turn off the checkpoint is a consequence of the entire histone modification pattern established as a result of successful chromatin reassembly following repair.

This kind of scenario would argue that chromatin reassembly, rather than checkpoint gene expression, is the required signal for checkpoint termination. One way this could be accomplished is if nucleosome incorporation following repair directly disrupts the association of checkpoint signaling proteins from the repaired DNA.

Consistent with the chromatin reassembly hypothesis, is the recent demonstration that *asf1* and K56 mutant strains, which are defective in chromatin assembly, display sensitivity to DNA damage, even in the absence of repair defects (Chen et al., 2008; Kim and Haber, 2009). The sensitivity appears to be a consequence of the inability of these strains to recover from DNA damage checkpoint (Kim and Haber, 2009). These results support the hypothesis that in addition to successful repair, efficient nucleosome reassembly on the repaired DNA is required for deactivation of the checkpoint signal and therefore cell survival after DNA damage.

To confirm whether 'knuckle' mutations indeed interfere with the chromatin reassembly efficiency after DSB repair it would be necessary to examine the dynamics of histone incorporation, especially histone H2A-H2B dimer re-deposition, at sites of DSBs. For that purpose, chromatin immunoprecipitation (CHIP), a quantitative method for assaying protein-DNA interactions, has been successfully used to assay kinetics and spatial distributions of chromatin changes and recruitment/deposition of proteins at DSBs (Shroff et al., 2004; Tsukuda et al., 2005). This is best done in a strain where synchronized DSB repair can be induced, such as the HO endonuclease strain previously used for monitoring repair dynamics. CHIP protocol, derived from methodologies originally described by O'Neill and Turner (O'Neill and Turner, 1995), is a useful tool as it gives an *in vivo* snapshot of the protein-DNA interactions by using protein-specific antibodies to precipitate the protein of interest, in this case

histones, that have been cross-linked to the DNA. The DNA can then be amplified by quantitative PCR method to provide information about the level of DNA and accordingly DNA-associated protein represented. The only limitation of the method is availability of protein-specific antibodies. When such antibodies are unavailable, strains can be generated carrying epitope tagged loci. Epitope-tagged histone strains have already been successfully used in *S. cerevisiae* HO-inducible strains to study chromatin remodeling at DSB sites by CHIP (Tsukuda et al., 2005). DNA association of checkpoint signaling molecules following repair can also be monitored by this method.

Reassembly versus restoration - is reinstatement of histone modifications after repair affected by 'knuckle' structure perturbations?

Another possibility for the observed checkpoint recovery defects of the 'knuckle' disrupting mutations, is that the 'knuckle' region might be required for restoration of chromatin to the state that existed prior to DNA damage. In other words, the signal to turn off the checkpoint might be a consequence of 'knuckle'-dependent misregulation of a particular histone modification or entire modification pattern rather than just a problem with chromatin reassembly (Figure 5.4). Of course, both processes are likely related i.e. if the modification is normally established after chromatin is assembled the modification status might depend directly on the chromatin assembly process. It could also be true that histone modification status upstream i.e. before its chromatin incorporation could be affected and important for chromatin assembly downstream, which in turn can affect reinstatement of remaining modifications on the assembled chromatin. This would be true if for example the 'knuckle' disrupting mutations affect the function of the Rtt109 enzyme responsible for K56 acetylation and its subsequent chromatin deposition.

Another potential candidate for pre-deposition modification-associated event is the required dephosphorylation of disassembled H2A.X for checkpoint recovery (Keogh et al., 2006). Although it might be that dephosphorylation is simply necessary for replenishing the unmodified pool of H2A.X in the cell necessary for incorporation into and restoration of chromatin structure after DNA repair, it is also possible that dephosphorylation itself can act as a prerequisite signal for checkpoint recovery. Either way, it would be interesting if 'knuckle' structure is indeed required for the activity of histone modifying enzymes off and on the chromatin after repair.

Testing this model would prove easier if looking at modification levels after chromatin assembly as chromatin immunoprecipitation assays will enable a quantitative measure for modification dynamics around the DSB. Indeed CHIP with histone modification specific antibodies in the HO DSB-inducible *S. cerevisiae* system can be used to monitor the dynamics of individual modifications after repair in the 'knuckle' mutant strains. On the other hand, monitoring of pre-deposition histone modification dynamics might prove more difficult since CHIP method cannot be used for events that are not associated with the DNA. As the checkpoint delays are subtle and the methods available are not quantitative the change in modification levels off chromatin might not be very well resolved. For example, preliminary immunoblotting results monitoring γH2A.X levels during HO-induced DSB repair did not show interpretable delay of γH2A.X dephosphorylation in the S17E 'knuckle' mutant (Figure 5.5).

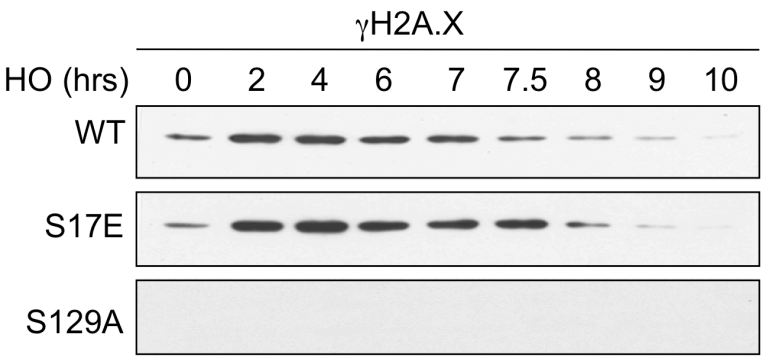

Figure 5.5: Effect of S17E 'knuckle' mutation on γH2A.X dynamics during repair of HO-inducible DSBs

γH2A.X dynamics was monitored in *S. cerevisiae* strains with S17E 'knucke' mutations. Whole cell extracts were collected at indicated time points following HO-induction and γH2A.X was detected by immunoblotting with anti-γH2A.X specific antibody. A γH2A.X point mutant S129A was used as a control for antibody specificity.

How is chromatin reassembly or restoration regulated by 'knuckle' structure?

If the 'knuckle' structure is important for efficient chromatin assembly and/or reinstatement of histone modification patterns after repair, it would be curious how these functions are mediated and interpreted. Binding of chromatin modifying or remodeling 'effector' activities is one of the key mechanisms of controlling chromatin function. And indeed, a 'trans' mechanism of function, whereby the H2A 'knuckle' region might be recognized by a histone-binding factor, has already been proposed, yet the factors have not been identified (Luger and Richmond, 1998).

The HO endonuclease DSB-inducible system can again provide a good method to address 'knuckle'-dependent protein associations at specific time points during checkpoint recovery in *S. cerevisiae* strains carrying 'knuckle' mutations. Histone H2A immunoprecipitation (IP) experiments from either wild type strains or strains with 'knuckle' mutations can provide a differential

snapshot of H2A-associated proteins *in vivo*. Identity of the 'knuckle'-specific protein depletion (or enrichment) can then be examined by mass spectrometry (MS).

In summary, my thesis studies have helped establish a requirement for the conserved SRS motif within the histone H2A N-terminal 'knuckle' region in efficient DNA damage response and define its function in checkpoint recovery in *S. cerevisiae*. However, as with all exciting new work, my results raise many new questions about the exact mechanism of how histone H2A 'knuckle' residues function to maintain a proper DNA checkpoint recovery. It will be very interesting to see how this aspect of DNA damage responses develops and hopefully the experiments proposed in this section will further contribute to the understanding of this process. In addition, given the great conservation of the region throughout evolution, it will be interesting to examine its function in mammalian cells and its implications on checkpoint recovery and disease.

CHAPTER 6

MATERIALS AND METHODS

Tetrahymena reagents and media

Proteose peptone and yeast extract were purchased from Difco (DB). Dextrose was from Fisher. Reagents and chemicals purchased from Sigma include common lab chemicals, phenylmethylsulfonyl fluoride (PMSF), and sequestrine. The commonly used *Tetrahymena* media were prepared as described previously by Gorovsky et al, 1975. Super proteose peptone media contains 0.2% dextrose, 1% proteose peptone, 0.1% yeast extract and 0.003% sequestrine.

Tetrahymena strains and culture conditions

Tetrahymena wild-type strains CU427 and C428 (provided by P. J. Bruns, *Tetrahymena* Stock Center, Cornell University) were grown in 1% super proteose peptone (SPP) medium at 30°C. For conjugation, log-phase cultures of two different mating types were washed and starved while stationary in 10 mM Tris-HCl buffer (pH 7.5) for 16-24 hrs at 30°C. Conjugation was then induced by mixing equal numbers of starved cells of opposite mating types at a concentration of $2x10^5$ cells/ml and allowed to proceed at 30°C without shaking.

Tetrahymena transformation and gene replacement

XhoI and BamHI digested constructs of wild-type or mutated HTA.X genes were transformed into 15-17 hr conjugating HTA double knockout heterokaryons (for somatic transformation). Selection was performed by serial dilutions every 2-3 days into fresh medium containing increasing concentrations of paramomycin

sulfate (Sigma) starting with 60 μg/ml. The genotypes of all transformants were confirmed by sequencing PCR with gene specific primers.

Tetrahymena nuclear isolation and histone extraction

Cells were collected at the appropriate time point during conjugation and pelleted for 5 min at 3,000 rpm. All the procedures hereafter were performed at 4°C. The pellet was resuspended in cold medium B (0.5 M sucrose, 4% gum arabic, 0.002 M $MgCl_2$, 10 mM sodium butyrate, 1 mM phenylmethylsulfonyl fluoride and 0.1% octanol) to a final density of $2x10^3$ cells/ml followed with homogenization by blending for 30 sec at high speed Waring Blendor. Nuclei were collected by differential centrifugation steps at increasing speeds followed by rehomogenization of the supernatant. Appropriate nuclear fractions were pulled together, aliquoted and stored at -20°C. In some cases when better purity of isolated nuclei was required, total nuclei were further fractionated by sucrose sedimentation at unit gravity. Histones were extracted from nuclei with 0.4 N H_2SO_4 for 2-24 hrs at 4°C and precipitated with 20% trichloroacetic acid for 1hr at 4°C. For alkaline phosphatase treatment, histones were incubated with 10 U/μl of γ protein phosphatase for 5 hrs at 30°C.

Indirect immunofluorescence microscopy

6 ml of cells ($2x10^5$ cells/ml) were fixed for 5 min at room temperature after addition of 20 μl partial Schaudin's fixative (2 parts saturated $HgCl_2$ to 1 part 90% EtOH v/v). Cells were gently pelleted (250g for 2 min), resuspended in 6 ml MeOH, repelleted and resuspended in 2 ml MeOH. 20 μl of cells were spread onto a cover slip and allowed to air dry for 30 min. Staining was done for 1 hr at room temperature with anti-phospho H2A.X MAb (Upstate) at a 1:70 dilution, followed by an incubation with Cy3-conjugated second secondary antibody

(1:1,000; Jackson ImmunoResearch, 111-165-144) for 1 hr. DAPI was applied at 1μg/ml in H_2O to facilitate visualization of nuclei. Immunostaining was visualized on a Zeiss Axioskop 2 Plus microscope and images were captured using SPOT software.

AU-PAGE

Histones were separated on a long acid-urea polyacrylamide gels (15% acrylamide, 6M urea and 5% acetic acid) as described (Allis et al, 1980) followed by a wet transfer in 0.7% acetic acid for 15 min at 0.5 A onto Immobilon-P PVDF membrane (Millipore).

Immunoblotting

Nuclear extracts or acid-extracted histones were separated on a 15 % SDS-PAGE followed by a semi-dry transfer with Towbin buffer (192 mM glycine, 25 mM Tris-Cl, 0.1% SDS and 20% methanol, final pH 8.0) onto Immobilon-P PVDF membrane (Millipore). The membrane was blocked for 1 hr at room temperature (or 4°C overnight) with 5% non-fat dry milk in TBS (20 mM Tris-Cl, pH 7.6 and 137 mM NaCl) and subsequently incubated for 1 hr at room temperature with α-H2A (1:5,000), α-γ-H2A.X (1:1,000, Upstate) or α-Rad53 (1:500, sc-6749 Santa Cruz Biotechnology, Inc). All primary and secondary antibody dilutions were in 5% milk dissolved in TBS-T buffer (TBS with 0.1% Tween-20). The membrane was washed with TBS-T for 10 min three times, followed by incubation with appropriate HRP-conjugated secondary antibody (1:5,000, Amersham Pharmacia). Blots were washed with TBS-T again and developed using ECL Western blotting detection kit (Amersham Pharmacia) according to the manufacturer's instructions.

Yeast reagents and media

Yeast extract, peptone, Bacto-Agar, dextrose, and yeast nitrogen base were purchased from Fisher Scientific Co. Galactose was purchased from Acros Organic. Amino acid drop out mix and 5-FOA were purchased from Bio101 systems. Restriction enzymes *Dpn I* and *XhoI* were from New England Biolabs (NEB). SuperScript III First Strand Synthesis System for RT-PCR and Platinum SYBR Green qPCR SuperMix were purchased from Invitrogen. High copy cDNA library was a generous gift from Dr. Mitchell Smith at the University of Virginia. Reagents and chemicals purchased from Sigma include common lab chemicals, phenylmethylsulfonyl fluoride (PMSF), methylmethane sulfonyl methyl ester (MMS), hydroxyurea (HU). Complete EDTA-free protease inhibitor cocktail was purchased from Roche Diagnostincs GmbH. Phosphatase inhibitor cocktails were purchased from Calbiochem. Zymolyase 100T was purchased from USBiological. PfuTurbo DNA polymerase (for DNA mutagenesis) was purchased from Stratagene. Frozen-EZ Yeast Transformation II kit is a Zymo research product.

The commonly used yeast media were prepared as described previously (Sherman et al, 1979). Rich media YPD consists of 1% yeast extract, 2% peptone and 2% dextrose. The synthetic complete (SC) medium consist of 0.36% yeast nitrogen base without amino acids, 2% dextrose and amino acid drop out mix. YEP-lactate media consist of 1.2% NaOH adjusted to pH 5.5 with appropriate volume of 85% lactic acid, before addition of 1% yeast extract and 2% peptone.

Plasmids

Plasmid pJH64 (CEN TRP1 HTA1-HTB1) was used to generate histone mutant plasmids pEG2-60 by QuickChange site-directed mutagenesis. pJH64 contains

an HTA1-HTB1 genomic fragment incorporated in a pRS314 (Sikorski and Hieter) backbone.

Mutation of histone genes

QuickChange site-directed mutagenesis protocol by Stratagene was used to generate histone site-specific mutated versions of plasmid pJH64 (CEN TRP1 HTA1-HTB1). Histone mutations were introduced in pJH64 by PCR, using the wild-type histone plasmid as a template together with two complementary oligonucleotides containing and centered around the desired mutation site. The PCR reactions was carried out in a 50 μl total reaction volume with 10 ng of plasmid DNA, 250 μM dNTPs, 20 μM mutation specific oligonucleotides, 1 x *Pfu Turbo* DNA polymerase buffer and 1 unit of *Pfu Turbo* polymerase. The cycling parameters included 1 cycle at 95°C for 30 sec, followed by 16 three-step cycles (95°C for 30 sec, 55°C for 1 min and 68°C for 14 mins) and concluded with 1 cycle at 75°C for 10 min after which the PCR reaction was stored at 4°C. Following temperature cycling, the product was treated for 2 hrs at 37°C with 1 μl of *Dpn I* endonuclease to digest the parental (wild-type) plasmid template and select for the PCR plasmid product containing the desired mutation. 7 μl of the digestion reaction were then transformed into *E. coli* DH5α competent cells to amplify and purify the mutation-containing plasmid. Mutations were subsequently confirmed by DNA sequencing.

Yeast transformation

Yeast transformation was performed either by a commercially available Frozen-EZ Yeast Transformation Kit II (Zymo research) using manufacturer's instructions or using the lithium acetate method described by Gietz et al. 1992. Briefly, for the lithium acetate method, 10 ml cell cultures were grown in YPD at

30°C to late log phase and harvested by centrifugation at 2,000 g for 3 min. Cells were washed in 10 ml lithium acetate in TE buffer twice and resuspended in 50 μL residual supernatant after it was decanted. 10 μl of single stranded salmon sperm DNA carrier (previously boiled for 5 min and chilled on ice) was added to the yeast cell suspension, followed by addition of 1 μg transforming DNA and 500 μL of sterile 50% PEG 3350 solution (in 1 x LiOAc-TE). The suspension was mixed by vortexing gently and incubated at 30°C for 30 min with agitation, followed by a heat shock at 42°C water bath for 15 min. 10 ml of YPD was added and cells were allowed to rest for 10 min after which the cells were collected by centrifugation at 2,000g for 3 min and resuspended in residual supernatant. ~250 μL of cells were plated on the appropriate SC selection plates.

Yeast strains

Strains used in this study are listed in Table 4. All strains are derivatives of W303C (BY4741; Research Genetics) background. The histone shuffle strain Y131 which contains a resident wild-type histone plasmid, was used to generate cells with mutations in histones H2A and H2B. Briefly, plasmids with histone gene mutations were transformed into Y131 and selected for on SC-TPR plates. Individual transformants were then grown in SC-TRP medium at 30°C for 3 days, and plated on 5-FOA plates to select for cells that have lost the resident URA3 histone plasmid. Cells that retained the histone mutations were screened by plasmid rescue followed by DNA sequencing.

The strains used in the single strand annealing (SSA) assay and analysis of checkpoint kinetics are also listed in Table 4. All the strains were derivatives from the parental strain (DD1260), which contains the HO-endonuclease gene under a galactose inducible promoter. The parental strain also lacks HO sites within *MAT*, HMLa or HMRa on Chr III, but has a cut-site within a centromere-

proximal *LEU2* gene (leu2::cs) on Chr III. The HTA1 gene in this strain is disrupted by replacement with the G418 resistance-conferring gene, KAN-MX6. Site specific and HA epitope tagged mutations were introduced in the genomic copy of the HTA2 gene by recombination after transformation with an appropriate DNA containing a desired mutation. DNA was generated by overlapping PCR of two products, one generated by amplifying a HA-TRP1 cassette from pFA6-3HA-TRP1 and the other by amplifying the genomic fragment of HTA2 with mutation specific oligonucleotides. Correct integration of the epitope tagged HTA2 mutation and marker cassette was confirmed by DNA sequencing of PCR amplified regions from isolated genomic DNA from mutant strains.

Table 4. Genotypes of yeast strains

Strain	Genotype	Source
Y131	*MATa hta1-htb1::LEU2 hta2-htb2Δ leu2-3,-112 his3-11,-15 trp1-1 ura3-1 ade2-1 can1-100 ssd1 [2μ, URA3, HTA1-HTB1]*	M. A. Osley
EG2	*MATa hta1-htb1::LEU2 hta2-htb2Δ leu2-3,-112 his3-11,-15 trp1-1 ura3-1 ade2-1 can1-100 ssd1 pEG2[CEN, TRP1, hta1-Δ1-20-HTB1]*	This study
EG3	*MATa hta1-htb1::LEU2 hta2-htb2Δ leu2-3,-112 his3-11,-15 trp1-1 ura3-1 ade2-1 can1-100 ssd1 pEG3[CEN, TRP1, hta1-K4R K7R-HTB1]*	This study
EG4	*MATa hta1-htb1::LEU2 hta2-htb2Δ leu2-3,-112 his3-11,-15 trp1-1 ura3-1 ade2-1 can1-100 ssd1 pEG4[CEN, TRP1, hta1-S17A S19A-HTB1]*	This study
EG7	*MATa hta1-htb1::LEU2 hta2-htb2Δ leu2-3,-112 his3-11,-15 trp1-1 ura3-1 ade2-1 can1-100 ssd1 pEG7[CEN, TRP1, hta1-S129A-HTB1]*	This study
EG11	*MATa hta1-htb1::LEU2 hta2-htb2Δ leu2-3,-112 his3-11,-15 trp1-1 ura3-1 ade2-1 can1-100 ssd1 pEG11[CEN, TRP1, hta1-S17A-HTB1]*	This study
EG12	*MATa hta1-htb1::LEU2 hta2-htb2Δ leu2-3,-112 his3-11,-15 trp1-1 ura3-1 ade2-1 can1-100 ssd1 pEG12[CEN, TRP1, hta1-S19A-HTB1]*	This study
EG14	*MATa hta1-htb1::LEU2 hta2-htb2Δ leu2-3,-112 his3-11,-15 trp1-1 ura3-1 ade2-1 can1-100 ssd1 pEG14[CEN, TRP1, hta1-K13R-HTB1]*	This study
EG15	*MATa hta1-htb1::LEU2 hta2-htb2Δ leu2-3,-112 his3-11,-15 trp1-1 ura3-1 ade2-1 can1-100 ssd1 pEG15[CEN, TRP1, hta1-K4R K7R K13R-HTB1]*	This study
EG16	*MATa hta1-htb1::LEU2 hta2-htb2Δ leu2-3,-112 his3-11,-15 trp1-1 ura3-1 ade2-1 can1-100 ssd1 pEG16[CEN, TRP1, hta1-K4R-HTB1]*	This study
EG17	*MATa hta1-htb1::LEU2 hta2-htb2Δ leu2-3,-112 his3-11,-15 trp1-1 ura3-1 ade2-1 can1-100 ssd1 pEG17[CEN, TRP1, hta1-K7R-HTB1]*	This study
EG18	*MATa hta1-htb1::LEU2 hta2-htb2Δ leu2-3,-112 his3-11,-15 trp1-1 ura3-1 ade2-1 can1-100 ssd1 pEG18[CEN, TRP1, hta1-K4Q K7Q-HTB1]*	This study
EG19	*MATa hta1-htb1::LEU2 hta2-htb2Δ leu2-3,-112 his3-11,-15 trp1-1 ura3-1 ade2-1 can1-100 ssd1 pEG19[CEN, TRP1, hta1-K13Q-HTB1]*	This study
EG21	*MATa hta1-htb1::LEU2 hta2-htb2Δ leu2-3,-112 his3-11,-15 trp1-1 ura3-1 ade2-1 can1-100 ssd1 pEG21[CEN, TRP1, hta1-K4R K13R-HTB1]*	This study
EG22	*MATa hta1-htb1::LEU2 hta2-htb2Δ leu2-3,-112 his3-11,-15 trp1-1 ura3-1 ade2-1 can1-100 ssd1 pEG22[CEN, TRP1, hta1-K7R K13R-HTB1]*	This study

Strain	Genotype	Source
EG23	*MATa hta1-htb1::LEU2 hta2-htb2Δ leu2-3,-112 his3-11,-15 trp1-1 ura3-1 ade2-1 can1-100 ssd1 pEG23[CEN, TRP1, hta1-K4Q-HTB1]*	This study
EG24	*MATa hta1-htb1::LEU2 hta2-htb2Δ leu2-3,-112 his3-11,-15 trp1-1 ura3-1 ade2-1 can1-100 ssd1 pEG24[CEN, TRP1, hta1-K7Q-HTB1]*	This study
EG25	*MATa hta1-htb1::LEU2 hta2-htb2Δ leu2-3,-112 his3-11,-15 trp1-1 ura3-1 ade2-1 can1-100 ssd1 pEG25[CEN, TRP1, hta1-K4Q K13Q-HTB1]*	This study
EG26	*MATa hta1-htb1::LEU2 hta2-htb2Δ leu2-3,-112 his3-11,-15 trp1-1 ura3-1 ade2-1 can1-100 ssd1 pEG26[CEN, TRP1, hta1-K7Q K13Q-HTB1]*	This study
EG35	*MATa hta1-htb1::LEU2 hta2-htb2Δ leu2-3,-112 his3-11,-15 trp1-1 ura3-1 ade2-1 can1-100 ssd1 pEG35[CEN, TRP1, hta1-S1E-HTB1]*	This study
EG36	*MATa hta1-htb1::LEU2 hta2-htb2Δ leu2-3,-112 his3-11,-15 trp1-1 ura3-1 ade2-1 can1-100 ssd1 pEG36[CEN, TRP1, hta1-S10E-HTB1]*	This study
EG37	*MATa hta1-htb1::LEU2 hta2-htb2Δ leu2-3,-112 his3-11,-15 trp1-1 ura3-1 ade2-1 can1-100 ssd1 pEG37[CEN, TRP1, hta1-S19E-HTB1]*	This study
EG38	*MATa hta1-htb1::LEU2 hta2-htb2Δ leu2-3,-112 his3-11,-15 trp1-1 ura3-1 ade2-1 can1-100 ssd1 pEG38[CEN, TRP1, hta1-S15E-HTB1]*	This study
EG39	*MATa hta1-htb1::LEU2 hta2-htb2Δ leu2-3,-112 his3-11,-15 trp1-1 ura3-1 ade2-1 can1-100 ssd1 pEG39[CEN, TRP1, hta1-S17E-HTB1]*	This study
EG40	*MATa hta1-htb1::LEU2 hta2-htb2Δ leu2-3,-112 his3-11,-15 trp1-1 ura3-1 ade2-1 can1-100 ssd1 pEG40[CEN, TRP1, hta1-K4Q K7Q K13Q-HTB1]*	This study
EG41	*MATa hta1-htb1::LEU2 hta2-htb2Δ leu2-3,-112 his3-11,-15 trp1-1 ura3-1 ade2-1 can1-100 ssd1 pEG41[CEN, TRP1, hta1-R18A-HTB1]*	This study
EG42	*MATa hta1-htb1::LEU2 hta2-htb2Δ leu2-3,-112 his3-11,-15 trp1-1 ura3-1 ade2-1 can1-100 ssd1 pEG42[CEN, TRP1, hta1-Δ1-16-HTB1]*	This study
EG43	*MATa hta1-htb1::LEU2 hta2-htb2Δ leu2-3,-112 his3-11,-15 trp1-1 ura3-1 ade2-1 can1-100 ssd1 pEG43[CEN, TRP1, hta1-Δ17-19-HTB1]*	This study
EG44	*MATa hta1-htb1::LEU2 hta2-htb2Δ leu2-3,-112 his3-11,-15 trp1-1 ura3-1 ade2-1 can1-100 ssd1 pEG44[CEN, TRP1, hta1-R18K-HTB1]*	This study
EG45	*MATa hta1-htb1::LEU2 hta2-htb2Δ leu2-3,-112 his3-11,-15 trp1-1 ura3-1 ade2-1 can1-100 ssd1 pEG45[CEN, TRP1, hta1-S17E S19E-HTB1]*	This study

Strain	Genotype	Source
EG49	*MATa hta1-htb1::LEU2 hta2-htb2Δ leu2-3,-112 his3-11,-15 trp1-1 ura3-1 ade2-1 can1-100 ssd1 pJH64[CEN, TRP1, HTA1-HTB1]*	This study
EG60	*MATa hta1-htb1::LEU2 hta2-htb2Δ leu2-3,-112 his3-11,-15 trp1-1 ura3-1 ade2-1 can1-100 ssd1 pEG60[CEN, TRP1, HTA1-htb1-Δ1-32]*	This study
DD1260	*MATaΔ::hisG hoΔ hmlΔ::ADE1 hmrΔ::ADE1 ade1 lys5 his4::URA3-leu2 (Xho1-to Asp718)-pBR322-his4 ura3-52 trp1::hisG leu2::HOcs ade3::GAL::HO hta2Δ::KanMX*	D. Durocher
DD983	*MATaΔ::hisG hoΔ hmlΔ::ADE1 hmrΔ::ADE1 ade1 lys5 his4::ura3::TRP1-leu2 (Xho1-to Asp718)-pBR322-his4 ura3-52 trp1::hisG leu2::HOcs ade3::GAL::HO hta2Δ::KanMX hta1-S129A*	D. Durocher
EG81	*MATaΔ::hisG hoΔ hmlΔ::ADE1 hmrΔ::ADE1 ade1 lys5 his4::URA3-leu2 (Xho1-to Asp718)-pBR322-his4 ura3-52 trp1::hisG leu2::HOcs ade3::GAL::HO hta2Δ::KanMX hta1-S17A-HA::TRP1*	This study
EG82	*MATaΔ::hisG hoΔ hmlΔ::ADE1 hmrΔ::ADE1 ade1 lys5 his4::URA3-leu2 (Xho1-to Asp718)-pBR322-his4 ura3-52 trp1::hisG leu2::HOcs ade3::GAL::HO hta2Δ::KanMX hta1-S17E-HA::TRP1*	This study
EG83	*MATaΔ::hisG hoΔ hmlΔ::ADE1 hmrΔ::ADE1 ade1 lys5 his4::URA3-leu2 (Xho1-to Asp718)-pBR322-his4 ura3-52 trp1::hisG leu2::HOcs ade3::GAL::HO hta2Δ::KanMX hta1-S19A-HA::TRP1*	This study
EG84	*MATaΔ::hisG hoΔ hmlΔ::ADE1 hmrΔ::ADE1 ade1 lys5 his4::URA3-leu2 (Xho1-to Asp718)-pBR322-his4 ura3-52 trp1::hisG leu2::HOcs ade3::GAL::HO hta2Δ::KanMX hta1-S19E-HA::TRP1*	This study
EG85	*MATaΔ::hisG hoΔ hmlΔ::ADE1 hmrΔ::ADE1 ade1 lys5 his4::URA3-leu2 (Xho1-to Asp718)-pBR322-his4 ura3-52 trp1::hisG leu2::HOcs ade3::GAL::HO hta2Δ::KanMX hta1-R18A-HA::TRP1*	This study
EG86	*MATaΔ::hisG hoΔ hmlΔ::ADE1 hmrΔ::ADE1 ade1 lys5 his4::URA3-leu2 (Xho1-to Asp718)-pBR322-his4 ura3-52 trp1::hisG leu2::HOcs ade3::GAL::HO hta2Δ::KanMX hta1-R18K-HA::TRP1*	This study
EG87	*MATaΔ::hisG hoΔ hmlΔ::ADE1 hmrΔ::ADE1 ade1 lys5 his4::URA3-leu2 (Xho1-to Asp718)-pBR322-his4 ura3-52 trp1::hisG leu2::HOcs ade3::GAL::HO hta2Δ::KanMX hta1-S129A-HA::TRP1*	This study

Yeast nuclear isolation and histone extraction

1 L yeast cultures were grown overnight in YPD at 30°C to mid-log phase (cell density of 1.5-3 x 10^7 cells/ml, corresponding to OD_{600} of 0.8). Cells were harvested by centrifugation at room temperature for 5 min at 3,000 rpm (JA-10 rotor). Cell pellet was washed once with 100 mls ice-cold water and resuspended in 40 mls of cold SPheroplasting buffer (1 M Sorbitol, 50 mM potassium phosphate pH 6.5, and fresh 14 mM β-mercaptoethanol). Spheroplasting was initiated by addition of 0.4 mg/ml of zymolyase (USBiological) and allowed to proceed at 30°C with mild agitation (~120 rpm) for ~30 min or until 90% of the cells were spheroplasted. Efficiency of spheroplasting was monitored by OD_{600} readings of 5 μl of cells in 1 ml 1% SDS. When OD_{600} values dropped to ~0.05, spheroplasted cells were pelleted by centrifugation in a tabletop clinical centrifuge at 3,000g and washed once with equal volume of SPheroplasting buffer. All the procedures hereafter were carried out on ice or at 4°C. Pelleted spheroplasts were resuspended in 40 mls of lysis buffer (18% ficoll 400, 20 mM potassium phosphate pH 6.5, 1 mM $MgCl_2$, 0.5 M EDTA pH 8, plus protease and phosphatase inhibitors) and lysed by douncing with ~100 strokes using pestle B. Lysed cells were diluted with 40 mls of lysis buffer and nuclei were separated from debris and harvested by centrifugation in a clinical centrifuge for 20 min at 3,200 rpm. The nuclei-containing supernatant was transferred to an ultracentrifuge tube (14 x 95 mm, Beckman) and nuclei were pelleted by ultracentrifugation at 50,000g for 30 min (SW-40 rotor). Nuclei were either resuspended in ~5 ml of NP buffer (0.34 M sucrose, 20 mM Tris-Cl pH 7.4, 50 mM KCl, 5 mM $MgCl_2$, plus protease and phosphatase inhibitors), aliquoted and stored at -80°C or used to extract histones.

For histone extraction, nuclei from 1 ml NP buffer were washed once with 1 ml of buffer A (10 mM Tris-Cl pH 8, 0.5% NP-4, 75 mM NaCl and protease and

phosphatase inhibitors) and collected by spinning at microfuge for 5 min at maximum speed (14,000 rpm). The nuclear pellet was then resuspended in 100 μl of buffer B (10 mM Tris-Cl pH 8, 0.4 M NaCl, plus protease and phosphataase inhibitors) to which 10 μl of 4N H_2SO_4 was gradually added. The histones were extracted by gentle agitation at 4°C for ~30 min and precipitated by 20% TCA for 1 hr on ice followed by microfuge centrifugation for 10 min at maximum speed. Precipitated histones were washed with acetone containing 0.1% HCl followed by another wash with acetone and dissolved in appropriate amounts of H_2O.

DNA damage sensitivity assay

Strains grown overnight at 30°C in non-selective medium, were diluted to a density corresponding to an absorbance of 0.1 at 600 nm (OD_{600}) and grown for another 3 hrs at 30°C. Cultures were diluted to equivalent densities and five fold serial dilutions were spotted onto medium containing the indicated DNA damaging agent. The plates were incubated for 3 days at 30°C.

Yeast whole-cell extraction

Cultures were grown in YPD medium at 30°C to an OD_{600} of 0.6-0.8. 10-15 ml cell aliquots were harvested by centrifugation at 2,000g in a tabletop centrifuge for 3 min and washed once with 0.5 ml of 20% TCA. Cell pellets were then stored at -80°C for up to a week or processed immediately. All purification steps were carried out on ice or at 4°C. The pellets were resuspended in 200 μl of 20% TCA and transferred into an O-ring tube containing ~500 μl acid-washed glass beads (500 μm in diameter). Cells were disrupted by bead beating in a Mini-Beadbeater (Biospec Products) for 1 min at 4°C. The beads were then flushed with 1 ml of 5% TCA, and the liquid was collected into a separate eppendorf tube. Proteins were precipitated on ice for 10 min and collected by a 20 min

centrifugation at maximum speed. The supernatant was removed and the pellets were solubilized in ~100 μl of 80% 2X SDS-PAGE loading buffer (60 mM Tris pH 6.8, 2% SDS, 10% glycerol, 0.2% bromophenol blue) with 10% β-mercaptoethanol (BME) and 10% unbuffered 2M Tris base. Insoluble material was removed by centrifugation after 5 min boiling at 95°C and the soluble extract was analyzed by SDS-PAGE.

MMS time course

Yeast cultures were grown in YPD at 30°C to OD_{600} density of ~0.5. An aliquot of each culture was collected for analysis. 0.05% MMS (Sigma) was added to the remainder of the cultures and treatment was extended for 2 hrs at 30°C after which the cells were pelleted at 2,000g for 2 min and washed once with fresh YPD. After the wash, the cells were resuspended in YPD and allowed to recover from MMS treatment at 30°C for indicated lengths of time, at which point aliquots were collected for analysis by appropriate assays.

Flow cytometry

Aliquots corresponding to 1 ml of cell density equivalent to exponentially growing cells (~$1x10^7$cells/ml) were collected at appropriate time points before, during, and after MMS treatment or induction of HO endonuclease and pelleted at 2,000 rpm for 5 min. The supernatant was removed and cells were washed once with 1 ml H_2O followed by a 15 sec spin. Cells were then fixed with 1 ml 70% cold ethanol and stored at 4°C. For staining, 0.3 ml of fixed cells were spun once for 10 sec in a microcentrifuge to remove the ethanol and rehydrated by resuspending in 1 ml 50 mM Na citrate which was removed following another 10 sec spin. The pellet was then resuspended in 0.5 ml 50 mM Na citrate containing 0.1 mg/ml RNase A (Qiagen) and incubated at 37°C overnight (or at least 2 hrs).

The next day, 0.5 ml 50 mM Na citrate containing 4 μg/ml propidium iodide (PI) was added to the cells to bring the final concentration of PI to 2 μg/ml. The cells were then either stored in the dark at 4°C or processed immediately. Before processing, the cells were briefly sonicated (5 sec constant pulse on medium setting) to prevent clumping. Cells were analyzed for DNA content with the use of a BD FACSCalibur system.

NHEJ plasmid repair assay

H2A mutant and wild-type strains were grown at 30°C in YPD to OD_{600} density of 0.5. The cultures were harvested and subjected to Frozen-EZ Yeast Transformaton II (Zymo research) with either *XhoI* restriction-enzyme-digested pRS416 or its mock-digested counterpart. Transformations were plated onto selective SC-TRP medium and colonies were counted after 3 days at 30°C.

Galactose-HO sensitivity assay

Strains containing the galactose-inducible HO endonuclease were grown at 30°C in lactic acid media to mid-log phase. Galactose (2% final) was added to induce HO. 20 ml aliquots were removed at appropriate time points and genomic DNA as well as whole cell proteins were extracted.

DNA extraction and repair analysis

Genomic DNA was extracted from ~5 ml cultures collected at different time points before and after galactose induction of HO endonuclease. Cells were harvested by a 3 min centrifugation at 2,000 g and washed once with 0.5 ml of distilled H_2O. The cell pellet remaining after the H_2O wash was resuspended in 0.2 ml of DNA extraction buffer (2% Triton X-100, 1% SDS, 100 mM NaCl, 10 mM Tris-Cl pH 8, 1 mM EDTA) and transferred to a screw-cap O-ring tube containing

~200 μl of acid-washed glass beads (500 μm in diameter). 0.2 ml of phenol:chloroform:isoamyl alcohol (25:24:1) was added to the tube and cells were disrupted by vortexing at maximum speed for 5 min. Insoluble material and beads were removed by a 5 min centrifugation in a microfuge. The upper, aqueous DNA containing layer was then transferred to a fresh tube and DNA was precipitated with 2.5 volumes of 100% cold ethanol using 1/10 volumes of 3M sodium acetate pH 5.2 as a carrier. The DNA was pelleted by a 5 min centrifugation and the pellet was washed once with 70% cold ethanol, after which the pellet was solubilized in 200 μl of TE containing 2 μl of 10 mg/ml RNase A (Qiagen) followed by incubation at 37°C for 30 min to remove RNA contaminants. Pure DNA was then precipitated and washed with 70% ethanol as before, the pellet was air dried for 5 min and solubilized in 20 μl of H_2O. 100 ng of thus purified DNA was subsequently used as a template in a PCR reaction with DNA repair specific oligonucleotides. Oligonucleotide sequences used for the repair analysis are listed in Table 5. PCR products were analyzed on a 1.2% agarose gel.

Table 5. Oligonucleotides for single strand annealing (SSA) repair assay

Primer or pair	Location	Orient	Primer Sequence
SSA P1	Chr III	F	GCT GGG AAG CAT ATT TGA GAA GAT GCG
SSA P2	Chr III	R	TGG GTT GAA GGC TCT CAA GGG CAT C
SSA P3	Chr III	F	GGT GAC CAC GTT GGT CAA GAA ATC A
SSA P4	Chr III	R	GCA TTA GCC CAT TCT TCC ATC AG
SSA Control	Chr IV	CDC13 F CDC13 R	CGA CGG AAA TTC GAT CAG GC CCA AAT AGA CTA GGG ATA CCT TAC

High copy suppressor screen

10 ml cell culture of the S17E HTA1 histone plasmid strain (pEG39) were grown in YPD at 30°C. 0.75 μl of cDNA library was transformed using the lithium acetate method described above. Transformants were plated on SC-TRP-URA

plates containing 200 mM hydroxyurea and surviving colonies were counted after 6 days at 30°C.

Sample collection and RNA isolation

Cultures were grown in YPD medium at 30°C to OD_{600} density of ~0.5. 10-15 ml cell aliquots of each culture, before and after 2 hr treatment with 0.02% MMS (Sigma) at 30°C, were harvested for analysis by centrifugation at 2,000g in a tabletop centrifuge for 3 min. The cells pellets were resuspended in 400 μl of TES buffer (10 mM Tris-Cl pH 7.5, 10 mM EDTA and 0.5% SDS). 400 μl of acid phenol was added and the solution was mixed by vortexing. RNA was isolated by incubation at 65°C for 30 min with occasional vortexing, followed by a 5 min incubation of ice and 5 min maximum speed spin in a microfuge. The RNA-containing top aqueous layer was transferred to a clean eppendorf tube and re-extracted with 400 μl of acid phenol as above. RNA was precipitated from the final aqueous layer with 1 ml (2.5 volumes) 100% ethanol, using 40 μl (1/10 volume) NaOAc pH 5.2 as a carrier. The pellet was washed with 70% ethanol, air dried and resuspended in appropriate amount of H_2O. Purity and concentration of the RNA was determined by OD_{260} measurements.

RT-PCR

RT-PCR reaction was performed according using SuperScript III First-Strand Synthesis System (Invitrogen) according to the manufacturer's instructions. Briefly, up to 5 μg of RNA was mixed with 50 μM oligo$(dT)_{20}$, 10 mM dNTP mix, and DEPC-treated water to a total 10 μl reaction volume, and incubated at 65°C for 5 min and placed on ice for at least 1 min. 10 μl of cDNA synthesis mix (1X final concentration of RT buffer, 25 mM $MgCl_2$, 0.1 M DTT, 1 μl of RNaseOUT (40U/μl) and 1 μl of SuperScript III RT enzyme) was added to the RNA/primer

mixture and cDNA was extended by incubation at 50°C for 50 min. The reaction was terminated by heating to 70°C for 15 min and remaining RNA was removed by incubation for 20 min at 37°C after addition of 1 μl of RNase H (2U/μl). The cDNA was either stored at -20°C or immediately used in a real-time quantitative PCR using a Platinum SYBR Green qPCR SuperMix (Invitrogen) according to the manifacturer's protocol.

APPENDIX

S17E mutation exhibits alterations in cellular morphology in response to DNA damage

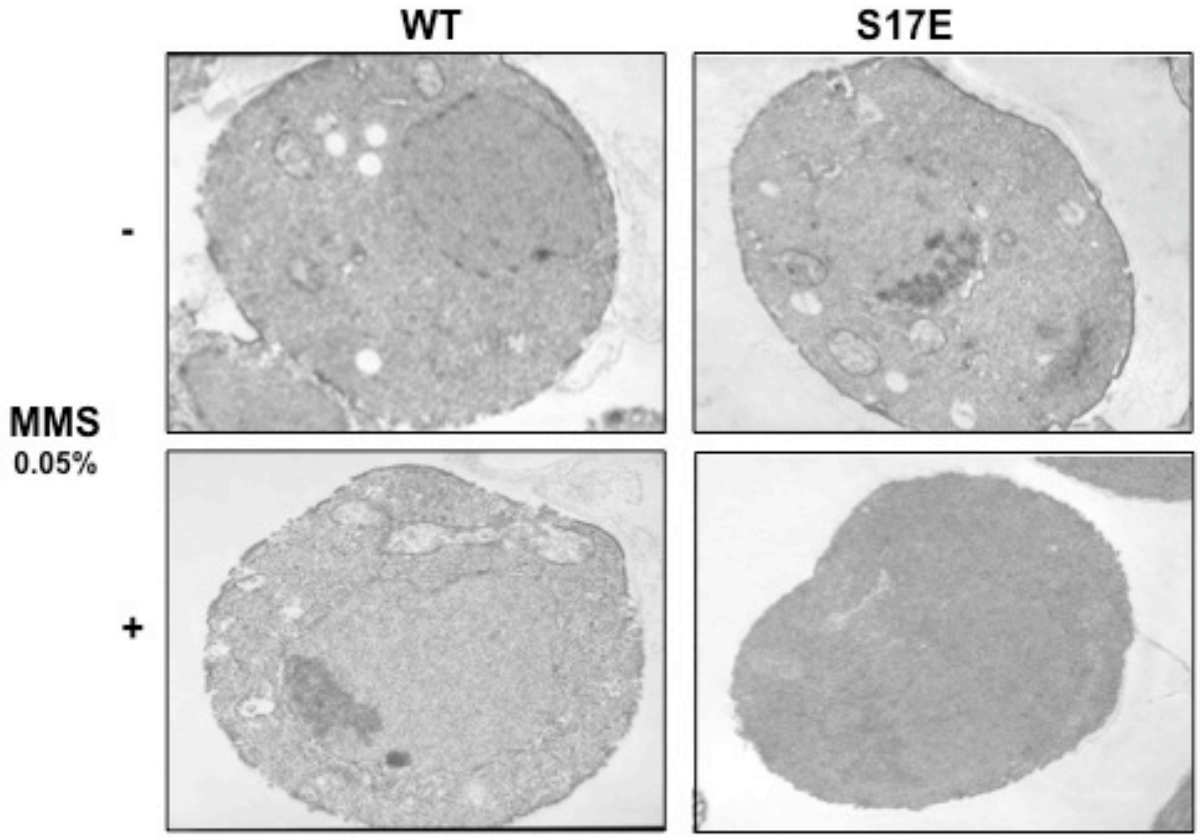

Electron micrographs of histone H2A wild type and S17E strains before and after treatment with 0.05% methyl methane sulfonate (MMS) for 2 hours.

REFERENCES

Ahmad, K., and Henikoff, S. (2002). The histone variant H3.3 marks active chromatin by replication-independent nucleosome assembly. Mol Cell *9*, 1191-1200.

Ahn, S.H., Cheung, W.L., Hsu, J.Y., Diaz, R.L., Smith, M.M., and Allis, C.D. (2005a). Sterile 20 kinase phosphorylates histone H2B at serine 10 during hydrogen peroxide-induced apoptosis in S. cerevisiae. Cell *120*, 25-36.

Ahn, S.H., Henderson, K.A., Keeney, S., and Allis, C.D. (2005b). H2B (Ser10) phosphorylation is induced during apoptosis and meiosis in S. cerevisiae. Cell Cycle *4*, 780-783.

Allard, S., Utley, R.T., Savard, J., Clarke, A., Grant, P., Brandl, C.J., Pillus, L., Workman, J.L., and Cote, J. (1999). NuA4, an essential transcription adaptor/histone H4 acetyltransferase complex containing Esa1p and the ATM-related cofactor Tra1p. EMBO J *18*, 5108-5119.

Allfrey, V.G., Faulkner, R., and Mirsky, A.E. (1964). Acetylation and Methylation of Histones and Their Possible Role in the Regulation of Rna Synthesis. Proc Natl Acad Sci U S A *51*, 786-794.

Allis, C.D., Glover, C.V., Bowen, J.K., and Gorovsky, M.A. (1980). Histone variants specific to the transcriptionally active, amitotically dividing macronucleus of the unicellular eucaryote, Tetrahymena thermophila. Cell *20*, 609-617.

Allis, C.D., Glover, C.V., and Gorovsky, M.A. (1979). Micronuclei of Tetrahymena contain two types of histone H3. Proc Natl Acad Sci U S A *76*, 4857-4861.

Allis, C.D., Ziegler, Y.S., Gorovsky, M.A., and Olmsted, J.B. (1982). A conserved histone variant enriched in nucleoli of mammalian cells. Cell *31*, 131-136.

Aragay, A.M., Diaz, P., and Daban, J.R. (1988). Association of nucleosome core particle DNA with different histone oligomers. Transfer of histones between DNA-(H2A,H2B) and DNA-(H3,H4) complexes. J Mol Biol *204*, 141-154.

Arents, G., Burlingame, R.W., Wang, B.C., Love, W.E., and Moudrianakis, E.N. (1991). The nucleosomal core histone octamer at 3.1 A resolution: a tripartite protein assembly and a left-handed superhelix. Proc Natl Acad Sci U S A *88*, 10148-10152.

Baarends, W.M., Wassenaar, E., van der Laan, R., Hoogerbrugge, J., Sleddens-Linkels, E., Hoeijmakers, J.H., de Boer, P., and Grootegoed, J.A. (2005). Silencing of unpaired chromatin and histone H2A ubiquitination in mammalian meiosis. Mol Cell Biol *25*, 1041-1053.

Bannon, G.A., Calzone, F.J., Bowen, J.K., Allis, C.D., and Gorovsky, M.A. (1983). Multiple, independently regulated, polyadenylated messages for histone H3 and H4 in Tetrahymena. Nucleic Acids Res *11*, 3903-3917.

Bassing, C.H., Chua, K.F., Sekiguchi, J., Suh, H., Whitlow, S.R., Fleming, J.C., Monroe, B.C., Ciccone, D.N., Yan, C., Vlasakova, K., *et al.* (2002). Increased ionizing radiation sensitivity and genomic instability in the absence of histone H2AX. Proc Natl Acad Sci U S A *99*, 8173-8178.

Bender, A., and Pringle, J.R. (1991). Use of a screen for synthetic lethal and multicopy suppressee mutants to identify two new genes involved in morphogenesis in Saccharomyces cerevisiae. Mol Cell Biol *11*, 1295-1305.

Bennett, C.B., Lewis, L.K., Karthikeyan, G., Lobachev, K.S., Jin, Y.H., Sterling, J.F., Snipe, J.R., and Resnick, M.A. (2001). Genes required for ionizing radiation resistance in yeast. Nat Genet *29*, 426-434.

Bergink, S., Salomons, F.A., Hoogstraten, D., Groothuis, T.A., de Waard, H., Wu, J., Yuan, L., Citterio, E., Houtsmuller, A.B., Neefjes, J., *et al.* (2006). DNA damage triggers nucleotide excision repair-dependent monoubiquitylation of histone H2A. Genes Dev *20*, 1343-1352.

Bird, A.W., Yu, D.Y., Pray-Grant, M.G., Qiu, Q., Harmon, K.E., Megee, P.C., Grant, P.A., Smith, M.M., and Christman, M.F. (2002). Acetylation of histone H4 by Esa1 is required for DNA double-strand break repair. Nature *419*, 411-415.

Birger, Y., Catez, F., Furusawa, T., Lim, J.H., Prymakowska-Bosak, M., West, K.L., Postnikov, Y.V., Haines, D.C., and Bustin, M. (2005). Increased tumorigenicity and sensitivity to ionizing radiation upon loss of chromosomal protein HMGN1. Cancer Res *65*, 6711-6718.

Black, B.E., and Bassett, E.A. (2008). The histone variant CENP-A and centromere specification. Curr Opin Cell Biol *20*, 91-100.

Boeke, J.D., LaCroute, F., and Fink, G.R. (1984). A positive selection for mutants lacking orotidine-5'-phosphate decarboxylase activity in yeast: 5-fluoro-orotic acid resistance. Mol Gen Genet *197*, 345-346.

Bostelman, L.J., Keller, A.M., Albrecht, A.M., Arat, A., and Thompson, J.S. (2007). Methylation of histone H3 lysine-79 by Dot1p plays multiple roles in the response to UV damage in Saccharomyces cerevisiae. DNA Repair (Amst) *6*, 383-395.

Botuyan, M.V., Lee, J., Ward, I.M., Kim, J.E., Thompson, J.R., Chen, J., and Mer, G. (2006). Structural basis for the methylation state-specific recognition of histone H4-K20 by 53BP1 and Crb2 in DNA repair. Cell *127*, 1361-1373.

Boulton, S.J., and Jackson, S.P. (1996). Saccharomyces cerevisiae Ku70 potentiates illegitimate DNA double-strand break repair and serves as a barrier to error-prone DNA repair pathways. EMBO J *15*, 5093-5103.

Briggs, S.D., Xiao, T., Sun, Z.W., Caldwell, J.A., Shabanowitz, J., Hunt, D.F., Allis, C.D., and Strahl, B.D. (2002). Gene silencing: trans-histone regulatory pathway in chromatin. Nature *418*, 498.

Brown, D.T. (2003). Histone H1 and the dynamic regulation of chromatin function. Biochem Cell Biol *81*, 221-227.

Brownell, J.E., and Allis, C.D. (1995). An activity gel assay detects a single, catalytically active histone acetyltransferase subunit in Tetrahymena macronuclei. Proc Natl Acad Sci U S A *92*, 6364-6368.

Brownell, J.E., Zhou, J., Ranalli, T., Kobayashi, R., Edmondson, D.G., Roth, S.Y., and Allis, C.D. (1996). Tetrahymena histone acetyltransferase A: a homolog to yeast Gcn5p linking histone acetylation to gene activation. Cell *84*, 843-851.

Burma, S., Chen, B.P., Murphy, M., Kurimasa, A., and Chen, D.J. (2001). ATM phosphorylates histone H2AX in response to DNA double-strand breaks. J Biol Chem *276*, 42462-42467.

Cao, L., Alani, E., and Kleckner, N. (1990). A pathway for generation and processing of double-strand breaks during meiotic recombination in S. cerevisiae. Cell *61*, 1089-1101.

Celeste, A., Fernandez-Capetillo, O., Kruhlak, M.J., Pilch, D.R., Staudt, D.W., Lee, A., Bonner, R.F., Bonner, W.M., and Nussenzweig, A. (2003). Histone H2AX phosphorylation is dispensable for the initial recognition of DNA breaks. Nat Cell Biol *5*, 675-679.

Celeste, A., Petersen, S., Romanienko, P.J., Fernandez-Capetillo, O., Chen, H.T., Sedelnikova, O.A., Reina-San-Martin, B., Coppola, V., Meffre, E., Difilippantonio, M.J., *et al.* (2002). Genomic instability in mice lacking histone H2AX. Science *296*, 922-927.

Celic, I., Masumoto, H., Griffith, W.P., Meluh, P., Cotter, R.J., Boeke, J.D., and Verreault, A. (2006). The sirtuins hst3 and Hst4p preserve genome integrity by controlling histone h3 lysine 56 deacetylation. Curr Biol *16*, 1280-1289.

Chadwick, B.P., and Willard, H.F. (2001). Histone H2A variants and the inactive X chromosome: identification of a second macroH2A variant. Hum Mol Genet *10*, 1101-1113.

Chadwick, B.P., and Willard, H.F. (2003). Chromatin of the Barr body: histone and non-histone proteins associated with or excluded from the inactive X chromosome. Hum Mol Genet *12*, 2167-2178.

Chai, B., Huang, J., Cairns, B.R., and Laurent, B.C. (2005). Distinct roles for the RSC and Swi/Snf ATP-dependent chromatin remodelers in DNA double-strand break repair. Genes Dev *19*, 1656-1661.

Chen, C.C., Carson, J.J., Feser, J., Tamburini, B., Zabaronick, S., Linger, J., and Tyler, J.K. (2008). Acetylated lysine 56 on histone H3 drives chromatin assembly after repair and signals for the completion of repair. Cell *134*, 231-243.

Chen, H.T., Bhandoola, A., Difilippantonio, M.J., Zhu, J., Brown, M.J., Tai, X., Rogakou, E.P., Brotz, T.M., Bonner, W.M., Ried, T., *et al.* (2000). Response to RAG-mediated VDJ cleavage by NBS1 and gamma-H2AX. Science *290*, 1962-1965.

Cheung, P., Allis, C.D., and Sassone-Corsi, P. (2000). Signaling to chromatin through histone modifications. Cell *103*, 263-271.

Cheung, W.L., Ajiro, K., Samejima, K., Kloc, M., Cheung, P., Mizzen, C.A., Beeser, A., Etkin, L.D., Chernoff, J., Earnshaw, W.C., *et al.* (2003). Apoptotic phosphorylation of histone H2B is mediated by mammalian sterile twenty kinase. Cell *113*, 507-517.

Cheung, W.L., Turner, F.B., Krishnamoorthy, T., Wolner, B., Ahn, S.H., Foley, M., Dorsey, J.A., Peterson, C.L., Berger, S.L., and Allis, C.D. (2005). Phosphorylation of histone H4 serine 1 during DNA damage requires casein kinase II in S. cerevisiae. Curr Biol *15*, 656-660.

Chowdhury, D., Keogh, M.C., Ishii, H., Peterson, C.L., Buratowski, S., and Lieberman, J. (2005). gamma-H2AX dephosphorylation by protein phosphatase 2A facilitates DNA double-strand break repair. Mol Cell *20*, 801-809.

Clarke, A.S., Lowell, J.E., Jacobson, S.J., and Pillus, L. (1999). Esa1p is an essential histone acetyltransferase required for cell cycle progression. Mol Cell Biol *19*, 2515-2526.

Cole, E.S., Cassidy-Hanley, D., Hemish, J., Tuan, J., and Bruns, P.J. (1997). A mutational analysis of conjugation in Tetrahymena thermophila. 1. Phenotypes affecting early development: meiosis to nuclear selection. Dev Biol *189*, 215-232.

Collins, K., Kobayashi, R., and Greider, C.W. (1995). Purification of Tetrahymena telomerase and cloning of genes encoding the two protein components of the enzyme. Cell *81*, 677-686.

Costanzi, C., and Pehrson, J.R. (1998). Histone macroH2A1 is concentrated in the inactive X chromosome of female mammals. Nature *393*, 599-601.

Cui, B., and Gorovsky, M.A. (2006). Centromeric histone H3 is essential for vegetative cell division and for DNA elimination during conjugation in Tetrahymena thermophila. Mol Cell Biol *26*, 4499-4510.

Dai, J., Hyland, E.M., Yuan, D.S., Huang, H., Bader, J.S., and Boeke, J.D. (2008). Probing nucleosome function: a highly versatile library of synthetic histone H3 and H4 mutants. Cell *134*, 1066-1078.

Davey, C.A., Sargent, D.F., Luger, K., Maeder, A.W., and Richmond, T.J. (2002). Solvent mediated interactions in the structure of the nucleosome core particle at 1.9 a resolution. J Mol Biol *319*, 1097-1113.

Davis, M.C., Ward, J.G., Herrick, G., and Allis, C.D. (1992). Programmed nuclear death: apoptotic-like degradation of specific nuclei in conjugating Tetrahymena. Dev Biol *154*, 419-432.

de Laat, W.L., Jaspers, N.G., and Hoeijmakers, J.H. (1999). Molecular mechanism of nucleotide excision repair. Genes Dev *13*, 768-785.

Dhalluin, C., Carlson, J.E., Zeng, L., He, C., Aggarwal, A.K., and Zhou, M.M. (1999). Structure and ligand of a histone acetyltransferase bromodomain. Nature *399*, 491-496.

Dougherty, M.K., and Morrison, D.K. (2004). Unlocking the code of 14-3-3. J Cell Sci *117*, 1875-1884.

Downs, J.A., Allard, S., Jobin-Robitaille, O., Javaheri, A., Auger, A., Bouchard, N., Kron, S.J., Jackson, S.P., and Cote, J. (2004). Binding of chromatin-modifying activities to phosphorylated histone H2A at DNA damage sites. Mol Cell *16*, 979-990.

Downs, J.A., and Cote, J. (2005). Dynamics of chromatin during the repair of DNA double-strand breaks. Cell Cycle *4*, 1373-1376.

Downs, J.A., Lowndes, N.F., and Jackson, S.P. (2000). A role for Saccharomyces cerevisiae histone H2A in DNA repair. Nature *408*, 1001-1004.

Downs, J.A., Nussenzweig, M.C., and Nussenzweig, A. (2007). Chromatin dynamics and the preservation of genetic information. Nature *447*, 951-958.

Driscoll, R., Hudson, A., and Jackson, S.P. (2007). Yeast Rtt109 promotes genome stability by acetylating histone H3 on lysine 56. Science *315*, 649-652.

Evans, E., Moggs, J.G., Hwang, J.R., Egly, J.M., and Wood, R.D. (1997). Mechanism of open complex and dual incision formation by human nucleotide excision repair factors. EMBO J *16*, 6559-6573.

Fernandez-Capetillo, O., Allis, C.D., and Nussenzweig, A. (2004a). Phosphorylation of histone H2B at DNA double-strand breaks. J Exp Med *199*, 1671-1677.

Fernandez-Capetillo, O., Chen, H.T., Celeste, A., Ward, I., Romanienko, P.J., Morales, J.C., Naka, K., Xia, Z., Camerini-Otero, R.D., Motoyama, N., *et al.* (2002). DNA damage-induced G2-M checkpoint activation by histone H2AX and 53BP1. Nat Cell Biol *4*, 993-997.

Fernandez-Capetillo, O., Lee, A., Nussenzweig, M., and Nussenzweig, A. (2004b). H2AX: the histone guardian of the genome. DNA Repair (Amst) *3*, 959-967.

Fernandez-Capetillo, O., Mahadevaiah, S.K., Celeste, A., Romanienko, P.J., Camerini-Otero, R.D., Bonner, W.M., Manova, K., Burgoyne, P., and Nussenzweig, A. (2003). H2AX is required for chromatin remodeling and inactivation of sex chromosomes in male mouse meiosis. Dev Cell *4*, 497-508.

Fishman-Lobell, J., Rudin, N., and Haber, J.E. (1992). Two alternative pathways of double-strand break repair that are kinetically separable and independently modulated. Mol Cell Biol *12*, 1292-1303.

Gasch, A.P., Huang, M., Metzner, S., Botstein, D., Elledge, S.J., and Brown, P.O. (2001). Genomic expression responses to DNA-damaging agents and the regulatory role of the yeast ATR homolog Mec1p. Mol Biol Cell *12*, 2987-3003.

Giannattasio, M., Lazzaro, F., Plevani, P., and Muzi-Falconi, M. (2005). The DNA damage checkpoint response requires histone H2B ubiquitination by Rad6-Bre1 and H3 methylation by Dot1. J Biol Chem *280*, 9879-9886.

Gibbons, I.R., and Rowe, A.J. (1965). Dynein: A Protein with Adenosine Triphosphatase Activity from Cilia. Science *149*, 424-426.

Gillet, L.C., and Scharer, O.D. (2006). Molecular mechanisms of mammalian global genome nucleotide excision repair. Chem Rev *106*, 253-276.

Gong, F., Fahy, D., and Smerdon, M.J. (2006). Rad4-Rad23 interaction with SWI/SNF links ATP-dependent chromatin remodeling with nucleotide excision repair. Nat Struct Mol Biol *13*, 902-907.

Gordon, F., Luger, K., and Hansen, J.C. (2005). The core histone N-terminal tail domains function independently and additively during salt-dependent oligomerization of nucleosomal arrays. J Biol Chem *280*, 33701-33706.

Greider, C.W., and Blackburn, E.H. (1985). Identification of a specific telomere terminal transferase activity in Tetrahymena extracts. Cell *43*, 405-413.

Greider, C.W., and Blackburn, E.H. (1989). A telomeric sequence in the RNA of Tetrahymena telomerase required for telomere repeat synthesis. Nature *337*, 331-337.

Hakem, R. (2008). DNA-damage repair; the good, the bad, and the ugly. EMBO J *27*, 589-605.

Hara, R., and Sancar, A. (2002). The SWI/SNF chromatin-remodeling factor stimulates repair by human excision nuclease in the mononucleosome core particle. Mol Cell Biol *22*, 6779-6787.

Harrison, J.C., and Haber, J.E. (2006). Surviving the breakup: the DNA damage checkpoint. Annu Rev Genet *40*, 209-235.

Harvey, A.C., Jackson, S.P., and Downs, J.A. (2005). Saccharomyces cerevisiae histone H2A Ser122 facilitates DNA repair. Genetics *170*, 543-553.

Hirschhorn, J.N., Bortvin, A.L., Ricupero-Hovasse, S.L., and Winston, F. (1995). A new class of histone H2A mutations in Saccharomyces cerevisiae causes specific transcriptional defects in vivo. Mol Cell Biol *15*, 1999-2009.

Hochwagen, A., and Amon, A. (2006). Checking your breaks: surveillance mechanisms of meiotic recombination. Curr Biol *16*, R217-228.

Howman, E.V., Fowler, K.J., Newson, A.J., Redward, S., MacDonald, A.C., Kalitsis, P., and Choo, K.H. (2000). Early disruption of centromeric chromatin organization in centromere protein A (Cenpa) null mice. Proc Natl Acad Sci U S A *97*, 1148-1153.

Huang, H., Maertens, A.M., Hyland, E.M., Dai, J., Norris, A., Boeke, J.D., and Bader, J.S. (2009). HistoneHits: a database for histone mutations and their phenotypes. Genome Res *19*, 674-681.

Huyen, Y., Zgheib, O., Ditullio, R.A., Jr., Gorgoulis, V.G., Zacharatos, P., Petty, T.J., Sheston, E.A., Mellert, H.S., Stavridi, E.S., and Halazonetis, T.D. (2004). Methylated lysine 79 of histone H3 targets 53BP1 to DNA double-strand breaks. Nature *432*, 406-411.

Jazayeri, A., McAinsh, A.D., and Jackson, S.P. (2004). Saccharomyces cerevisiae Sin3p facilitates DNA double-strand break repair. Proc Natl Acad Sci U S A *101*, 1644-1649.

Kamakaka, R.T., and Biggins, S. (2005). Histone variants: deviants? Genes Dev *19*, 295-310.

Keeney, S., Giroux, C.N., and Kleckner, N. (1997). Meiosis-specific DNA double-strand breaks are catalyzed by Spo11, a member of a widely conserved protein family. Cell *88*, 375-384.

Keogh, M.C., Kim, J.A., Downey, M., Fillingham, J., Chowdhury, D., Harrison, J.C., Onishi, M., Datta, N., Galicia, S., Emili, A., *et al.* (2006). A phosphatase complex that dephosphorylates gammaH2AX regulates DNA damage checkpoint recovery. Nature *439*, 497-501.

Khorasanizadeh, S. (2004). The nucleosome: from genomic organization to genomic regulation. Cell *116*, 259-272.

Kim, J.A., and Haber, J.E. (2009). Chromatin assembly factors Asf1 and CAF-1 have overlapping roles in deactivating the DNA damage checkpoint when DNA repair is complete. Proc Natl Acad Sci U S A *106*, 1151-1156.

Kimura, H. (2005). Histone dynamics in living cells revealed by photobleaching. DNA Repair (Amst) *4*, 939-950.

Kimura, H., and Cook, P.R. (2001). Kinetics of core histones in living human cells: little exchange of H3 and H4 and some rapid exchange of H2B. J Cell Biol *153*, 1341-1353.

Kireeva, M.L., Walter, W., Tchernajenko, V., Bondarenko, V., Kashlev, M., and Studitsky, V.M. (2002). Nucleosome remodeling induced by RNA polymerase II: loss of the H2A/H2B dimer during transcription. Mol Cell *9*, 541-552.

Kobayashi, J., Tauchi, H., Sakamoto, S., Nakamura, A., Morishima, K., Matsuura, S., Kobayashi, T., Tamai, K., Tanimoto, K., and Komatsu, K. (2002). NBS1 localizes to gamma-H2AX foci through interaction with the FHA/BRCT domain. Curr Biol *12*, 1846-1851.

Kouzarides, T. (2007). Chromatin modifications and their function. Cell *128*, 693-705.

Krogan, N.J., Keogh, M.C., Datta, N., Sawa, C., Ryan, O.W., Ding, H., Haw, R.A., Pootoolal, J., Tong, A., Canadien, V., *et al.* (2003). A Snf2 family ATPase complex required for recruitment of the histone H2A variant Htz1. Mol Cell *12*, 1565-1576.

Kruger, K., Grabowski, P.J., Zaug, A.J., Sands, J., Gottschling, D.E., and Cech, T.R. (1982). Self-splicing RNA: autoexcision and autocyclization of the ribosomal RNA intervening sequence of Tetrahymena. Cell *31*, 147-157.

Kruhlak, M.J., Celeste, A., Dellaire, G., Fernandez-Capetillo, O., Muller, W.G., McNally, J.G., Bazett-Jones, D.P., and Nussenzweig, A. (2006a). Changes in chromatin structure and mobility in living cells at sites of DNA double-strand breaks. J Cell Biol *172*, 823-834.

Kruhlak, M.J., Celeste, A., and Nussenzweig, A. (2006b). Spatio-temporal dynamics of chromatin containing DNA breaks. Cell Cycle *5*, 1910-1912.

Kusch, T., Florens, L., Macdonald, W.H., Swanson, S.K., Glaser, R.L., Yates, J.R., 3rd, Abmayr, S.M., Washburn, M.P., and Workman, J.L. (2004). Acetylation by Tip60 is required for selective histone variant exchange at DNA lesions. Science *306*, 2084-2087.

Lachner, M., O'Sullivan, R.J., and Jenuwein, T. (2003). An epigenetic road map for histone lysine methylation. J Cell Sci *116*, 2117-2124.

Lan, F., Nottke, A.C., and Shi, Y. (2008). Mechanisms involved in the regulation of histone lysine demethylases. Curr Opin Cell Biol *20*, 316-325.

Lee, M.S., Edwards, R.A., Thede, G.L., and Glover, J.N. (2005). Structure of the BRCT repeat domain of MDC1 and its specificity for the free COOH-terminal end of the gamma-H2AX histone tail. J Biol Chem *280*, 32053-32056.

Lee, Y.H., and Stallcup, M.R. (2009). Minireview: protein arginine methylation of nonhistone proteins in transcriptional regulation. Mol Endocrinol *23*, 425-433.

Lenfant, F., Mann, R.K., Thomsen, B., Ling, X., and Grunstein, M. (1996). All four core histone N-termini contain sequences required for the repression of basal transcription in yeast. EMBO J *15*, 3974-3985.

Liu, X., Li, B., and GorovskyMa (1996). Essential and nonessential histone H2A variants in Tetrahymena thermophila. Mol Cell Biol *16*, 4305-4311.

Loidl, J. (1990). The initiation of meiotic chromosome pairing: the cytological view. Genome *33*, 759-778.

Loidl, J., and Scherthan, H. (2004). Organization and pairing of meiotic chromosomes in the ciliate Tetrahymena thermophila. J Cell Sci *117*, 5791-5801.

Lu, C., Zhu, F., Cho, Y.Y., Tang, F., Zykova, T., Ma, W.Y., Bode, A.M., and Dong, Z. (2006). Cell apoptosis: requirement of H2AX in DNA ladder formation, but not for the activation of caspase-3. Mol Cell *23*, 121-132.

Luger, K., Mader, A.W., Richmond, R.K., Sargent, D.F., and Richmond, T.J. (1997). Crystal structure of the nucleosome core particle at 2.8 A resolution. Nature *389*, 251-260.

Luger, K., Rechsteiner, T.J., and Richmond, T.J. (1999). Preparation of nucleosome core particle from recombinant histones. Methods Enzymol *304*, 3-19.

Luger, K., and Richmond, T.J. (1998). The histone tails of the nucleosome. Curr Opin Genet Dev *8*, 140-146.

Lukas, C., Melander, F., Stucki, M., Falck, J., Bekker-Jensen, S., Goldberg, M., Lerenthal, Y., Jackson, S.P., Bartek, J., and Lukas, J. (2004). Mdc1 couples DNA

double-strand break recognition by Nbs1 with its H2AX-dependent chromatin retention. EMBO J *23*, 2674-2683.

Maas, N.L., Miller, K.M., DeFazio, L.G., and Toczyski, D.P. (2006). Cell cycle and checkpoint regulation of histone H3 K56 acetylation by Hst3 and Hst4. Mol Cell *23*, 109-119.

Macdonald, N., Welburn, J.P., Noble, M.E., Nguyen, A., Yaffe, M.B., Clynes, D., Moggs, J.G., Orphanides, G., Thomson, S., Edmunds, J.W., *et al.* (2005). Molecular basis for the recognition of phosphorylated and phosphoacetylated histone h3 by 14-3-3. Mol Cell *20*, 199-211.

Mahadevaiah, S.K., Turner, J.M., Baudat, F., Rogakou, E.P., de Boer, P., Blanco-Rodriguez, J., Jasin, M., Keeney, S., Bonner, W.M., and Burgoyne, P.S. (2001). Recombinational DNA double-strand breaks in mice precede synapsis. Nat Genet *27*, 271-276.

Malik, H.S., and Henikoff, S. (2003). Phylogenomics of the nucleosome. Nat Struct Biol *10*, 882-891.

Malkova, A., Ross, L., Dawson, D., Hoekstra, M.F., and Haber, J.E. (1996). Meiotic recombination initiated by a double-strand break in rad50 delta yeast cells otherwise unable to initiate meiotic recombination. Genetics *143*, 741-754.

Mannironi, C., Bonner, W.M., and Hatch, C.L. (1989). H2A.X. a histone isoprotein with a conserved C-terminal sequence, is encoded by a novel mRNA with both DNA replication type and polyA 3' processing signals. Nucleic Acids Res *17*, 9113-9126.

Martindale, D.W., Allis, C.D., and Bruns, P.J. (1982). Conjugation in Tetrahymena thermophila. A temporal analysis of cytological stages. Exp Cell Res *140*, 227-236.

Martindale, D.W., Allis, C.D., and Bruns, P.J. (1985). RNA and protein synthesis during meiotic prophase in Tetrahymena thermophila. J Protozool *32*, 644-649.

Martindale, D.W., and Bruns, P.J. (1983). Cloning of abundant mRNA species present during conjugation of Tetrahymena thermophila: identification of mRNA species present exclusively during meiosis. Mol Cell Biol *3*, 1857-1865.

Masumoto, H., Hawke, D., Kobayashi, R., and Verreault, A. (2005). A role for cell-cycle-regulated histone H3 lysine 56 acetylation in the DNA damage response. Nature *436*, 294-298.

Maurer-Stroh, S., Dickens, N.J., Hughes-Davies, L., Kouzarides, T., Eisenhaber, F., and Ponting, C.P. (2003). The Tudor domain 'Royal Family': Tudor, plant Agenet, Chromo, PWWP and MBT domains. Trends Biochem Sci *28*, 69-74.

Megee, P.C., Morgan, B.A., Mittman, B.A., and Smith, M.M. (1990). Genetic analysis of histone H4: essential role of lysines subject to reversible acetylation. Science *247*, 841-845.

Mizuguchi, G., Shen, X., Landry, J., Wu, W.H., Sen, S., and Wu, C. (2004). ATP-driven exchange of histone H2AZ variant catalyzed by SWR1 chromatin remodeling complex. Science *303*, 343-348.

Mochizuki, K., Fine, N.A., Fujisawa, T., and Gorovsky, M.A. (2002). Analysis of a piwi-related gene implicates small RNAs in genome rearrangement in tetrahymena. Cell *110*, 689-699.

Mochizuki, K., and Gorovsky, M.A. (2005). A Dicer-like protein in Tetrahymena has distinct functions in genome rearrangement, chromosome segregation, and meiotic prophase. Genes Dev *19*, 77-89.

Mochizuki, K., Novatchkova, M., and Loidl, J. (2008). DNA double-strand breaks, but not crossovers, are required for the reorganization of meiotic nuclei in Tetrahymena. J Cell Sci *121*, 2148-2158.

Moore, J.D., Yazgan, O., Ataian, Y., and Krebs, J.E. (2007). Diverse roles for histone H2A modifications in DNA damage response pathways in yeast. Genetics *176*, 15-25.

Morrison, A.J., Highland, J., Krogan, N.J., Arbel-Eden, A., Greenblatt, J.F., Haber, J.E., and Shen, X. (2004). INO80 and gamma-H2AX interaction links ATP-dependent chromatin remodeling to DNA damage repair. Cell *119*, 767-775.

Moser, J., Kool, H., Giakzidis, I., Caldecott, K., Mullenders, L.H., and Fousteri, M.I. (2007). Sealing of chromosomal DNA nicks during nucleotide excision repair requires XRCC1 and DNA ligase III alpha in a cell-cycle-specific manner. Mol Cell *27*, 311-323.

Nakamura, T.M., Du, L.L., Redon, C., and Russell, P. (2004). Histone H2A phosphorylation controls Crb2 recruitment at DNA breaks, maintains checkpoint arrest, and influences DNA repair in fission yeast. Mol Cell Biol *24*, 6215-6230.

Nimmo, E.R., Pidoux, A.L., Perry, P.E., and Allshire, R.C. (1998). Defective meiosis in telomere-silencing mutants of Schizosaccharomyces pombe. Nature *392*, 825-828.

O'Neill, L.P., and Turner, B.M. (1995). Histone H4 acetylation distinguishes coding regions of the human genome from heterochromatin in a differentiation-dependent but transcription-independent manner. EMBO J *14*, 3946-3957.

Ohba, R., Steger, D.J., Brownell, J.E., Mizzen, C.A., Cook, R.G., Cote, J., Workman, J.L., and Allis, C.D. (1999). A novel H2A/H4 nucleosomal histone acetyltransferase in Tetrahymena thermophila. Mol Cell Biol *19*, 2061-2068.

Oohara, I., and Wada, A. (1987). Spectroscopic studies on histone-DNA interactions. I. The interaction of histone (H2A, H2B) dimer with DNA: DNA sequence dependence. J Mol Biol *196*, 389-397.

Orias, E. (1998). Mapping the germ-line and somatic genomes of a ciliated protozoan, Tetrahymena thermophila. Genome Res *8*, 91-99.

Ozdemir, A., Spicuglia, S., Lasonder, E., Vermeulen, M., Campsteijn, C., Stunnenberg, H.G., and Logie, C. (2005). Characterization of lysine 56 of histone H3 as an acetylation site in Saccharomyces cerevisiae. J Biol Chem *280*, 25949-25952.

Palmer, D.K., O'Day, K., Wener, M.H., Andrews, B.S., and Margolis, R.L. (1987). A 17-kD centromere protein (CENP-A) copurifies with nucleosome core particles and with histones. J Cell Biol *104*, 805-815.

Panyim, S., and Chalkley, R. (1969). High resolution acrylamide gel electrophoresis of histones. Arch Biochem Biophys *130*, 337-346.

Papamichos-Chronakis, M., Krebs, J.E., and Peterson, C.L. (2006). Interplay between Ino80 and Swr1 chromatin remodeling enzymes regulates cell cycle checkpoint adaptation in response to DNA damage. Genes Dev *20*, 2437-2449.

Pardo, B., Gomez-Gonzalez, B., and Aguilera, A. (2009). DNA repair in mammalian cells: DNA double-strand break repair: how to fix a broken relationship. Cell Mol Life Sci *66*, 1039-1056.

Parra, M.A., and Wyrick, J.J. (2007). Regulation of gene transcription by the histone H2A N-terminal domain. Mol Cell Biol *27*, 7641-7648.

Parseghian, M.H., and Hamkalo, B.A. (2001). A compendium of the histone H1 family of somatic subtypes: an elusive cast of characters and their characteristics. Biochem Cell Biol *79*, 289-304.

Pena, P.V., Davrazou, F., Shi, X., Walter, K.L., Verkhusha, V.V., Gozani, O., Zhao, R., and Kutateladze, T.G. (2006). Molecular mechanism of histone H3K4me3 recognition by plant homeodomain of ING2. Nature *442*, 100-103.

Pena, P.V., Hom, R.A., Hung, T., Lin, H., Kuo, A.J., Wong, R.P., Subach, O.M., Champagne, K.S., Zhao, R., Verkhusha, V.V., *et al.* (2008). Histone H3K4me3 binding is required for the DNA repair and apoptotic activities of ING1 tumor suppressor. J Mol Biol *380*, 303-312.

Peng, A., and Chen, P.L. (2003). NFBD1, like 53BP1, is an early and redundant transducer mediating Chk2 phosphorylation in response to DNA damage. J Biol Chem *278*, 8873-8876.

Peterson, C.L., and Cote, J. (2004). Cellular machineries for chromosomal DNA repair. Genes Dev *18*, 602-616.

Poccia, D.L., and Green, G.R. (1992). Packaging and unpackaging the sea urchin sperm genome. Trends Biochem Sci *17*, 223-227.

Prado, F., Cortes-Ledesma, F., Huertas, P., and Aguilera, A. (2003). Mitotic recombination in Saccharomyces cerevisiae. Curr Genet *42*, 185-198.

Qian, C., and Zhou, M.M. (2006). SET domain protein lysine methyltransferases: Structure, specificity and catalysis. Cell Mol Life Sci *63*, 2755-2763.

Qin, S., and Parthun, M.R. (2002). Histone H3 and the histone acetyltransferase Hat1p contribute to DNA double-strand break repair. Mol Cell Biol *22*, 8353-8365.

Ramanathan, B., and Smerdon, M.J. (1986). Changes in nuclear protein acetylation in u.v.-damaged human cells. Carcinogenesis *7*, 1087-1094.

Ramanathan, B., and Smerdon, M.J. (1989). Enhanced DNA repair synthesis in hyperacetylated nucleosomes. J Biol Chem *264*, 11026-11034.

Rappold, I., Iwabuchi, K., Date, T., and Chen, J. (2001). Tumor suppressor p53 binding protein 1 (53BP1) is involved in DNA damage-signaling pathways. J Cell Biol *153*, 613-620.

Recht, J., Dunn, B., Raff, A., and Osley, M.A. (1996). Functional analysis of histones H2A and H2B in transcriptional repression in Saccharomyces cerevisiae. Mol Cell Biol *16*, 2545-2553.

Recht, J., Tsubota, T., Tanny, J.C., Diaz, R.L., Berger, J.M., Zhang, X., Garcia, B.A., Shabanowitz, J., Burlingame, A.L., Hunt, D.F., *et al.* (2006). Histone chaperone Asf1 is required for histone H3 lysine 56 acetylation, a modification associated with S phase in mitosis and meiosis. Proc Natl Acad Sci U S A *103*, 6988-6993.

Reddy, K.C., and Villeneuve, A.M. (2004). C. elegans HIM-17 links chromatin modification and competence for initiation of meiotic recombination. Cell *118*, 439-452.

Redon, C., Pilch, D., Rogakou, E., Sedelnikova, O., Newrock, K., and Bonner, W. (2002). Histone H2A variants H2AX and H2AZ. Curr Opin Genet Dev *12*, 162-169.

Redon, C., Pilch, D.R., Rogakou, E.P., Orr, A.H., Lowndes, N.F., and Bonner, W.M. (2003). Yeast histone 2A serine 129 is essential for the efficient repair of checkpoint-blind DNA damage. EMBO Rep *4*, 678-684.

Ren, Q., and Gorovsky, M.A. (2003). The nonessential H2A N-terminal tail can function as an essential charge patch on the H2A.Z variant N-terminal tail. Mol Cell Biol *23*, 2778-2789.

Richmond, T.J., and Davey, C.A. (2003). The structure of DNA in the nucleosome core. Nature *423*, 145-150.

Robzyk, K., Recht, J., and Osley, M.A. (2000). Rad6-dependent ubiquitination of histone H2B in yeast. Science *287*, 501-504.

Roeder, G.S. (1997). Meiotic chromosomes: it takes two to tango. Genes Dev *11*, 2600-2621.

Rogakou, E.P., Boon, C., Redon, C., and Bonner, W.M. (1999). Megabase chromatin domains involved in DNA double-strand breaks in vivo. J Cell Biol *146*, 905-916.

Rogakou, E.P., Nieves-Neira, W., Boon, C., Pommier, Y., and Bonner, W.M. (2000). Initiation of DNA fragmentation during apoptosis induces phosphorylation of H2AX histone at serine 139. J Biol Chem *275*, 9390-9395.

Rogakou, E.P., Pilch, D.R., Orr, A.H., Ivanova, V.S., and Bonner, W.M. (1998). DNA double-stranded breaks induce histone H2AX phosphorylation on serine 139. J Biol Chem *273*, 5858-5868.

Roth, S.Y., Denu, J.M., and Allis, C.D. (2001). Histone acetyltransferases. Annu Rev Biochem *70*, 81-120.

Sanders, S.L., Portoso, M., Mata, J., Bahler, J., Allshire, R.C., and Kouzarides, T. (2004). Methylation of histone H4 lysine 20 controls recruitment of Crb2 to sites of DNA damage. Cell *119*, 603-614.

Sarma, K., and Reinberg, D. (2005). Histone variants meet their match. Nat Rev Mol Cell Biol *6*, 139-149.

Schalch, T., Duda, S., Sargent, D.F., and Richmond, T.J. (2005). X-ray structure of a tetranucleosome and its implications for the chromatin fibre. Nature *436*, 138-141.

Scherthan, H. (2001). A bouquet makes ends meet. Nat Rev Mol Cell Biol *2*, 621-627.

Schotta, G., Sengupta, R., Kubicek, S., Malin, S., Kauer, M., Callen, E., Celeste, A., Pagani, M., Opravil, S., De La Rosa-Velazquez, I.A., *et al.* (2008). A chromatin-wide transition to H4K20 monomethylation impairs genome integrity and programmed DNA rearrangements in the mouse. Genes Dev *22*, 2048-2061.

Sciurano, R., Rahn, M., Rey-Valzacchi, G., and Solari, A.J. (2007). The asynaptic chromatin in spermatocytes of translocation carriers contains the histone variant gamma-H2AX and associates with the XY body. Hum Reprod *22*, 142-150.

Seet, B.T., Dikic, I., Zhou, M.M., and Pawson, T. (2006). Reading protein modifications with interaction domains. Nat Rev Mol Cell Biol *7*, 473-483.

Shechter, D., Dormann, H.L., Allis, C.D., and Hake, S.B. (2007). Extraction, purification and analysis of histones. Nat Protoc *2*, 1445-1457.

Shen, X., Mizuguchi, G., Hamiche, A., and Wu, C. (2000). A chromatin remodelling complex involved in transcription and DNA processing. Nature *406*, 541-544.

Shi, X., Hong, T., Walter, K.L., Ewalt, M., Michishita, E., Hung, T., Carney, D., Pena, P., Lan, F., Kaadige, M.R., *et al.* (2006). ING2 PHD domain links histone H3 lysine 4 methylation to active gene repression. Nature *442*, 96-99.

Shi, Y., Lan, F., Matson, C., Mulligan, P., Whetstine, J.R., Cole, P.A., and Casero, R.A. (2004). Histone demethylation mediated by the nuclear amine oxidase homolog LSD1. Cell *119*, 941-953.

Shim, E.Y., Ma, J.L., Oum, J.H., Yanez, Y., and Lee, S.E. (2005). The yeast chromatin remodeler RSC complex facilitates end joining repair of DNA double-strand breaks. Mol Cell Biol *25*, 3934-3944.

Shroff, R., Arbel-Eden, A., Pilch, D., Ira, G., Bonner, W.M., Petrini, J.H., Haber, J.E., and Lichten, M. (2004). Distribution and dynamics of chromatin modification induced by a defined DNA double-strand break. Curr Biol *14*, 1703-1711.

Smerdon, M.J. (1991). DNA repair and the role of chromatin structure. Curr Opin Cell Biol *3*, 422-428.

Solari, A.J. (1974). The behavior of the XY pair in mammals. Int Rev Cytol *38*, 273-317.

Song, X., Gjoneska, E., Ren, Q., Taverna, S.D., Allis, C.D., and Gorovsky, M.A. (2007). Phosphorylation of the SQ H2A.X motif is required for proper meiosis and mitosis in Tetrahymena thermophila. Mol Cell Biol *27*, 2648-2660.

Stargell, L.A., Bowen, J., Dadd, C.A., Dedon, P.C., Davis, M., Cook, R.G., Allis, C.D., and Gorovsky, M.A. (1993). Temporal and spatial association of histone H2A variant hv1 with transcriptionally competent chromatin during nuclear development in Tetrahymena thermophila. Genes Dev *7*, 2641-2651.

Stiff, T., O'Driscoll, M., Rief, N., Iwabuchi, K., Lobrich, M., and Jeggo, P.A. (2004). ATM and DNA-PK function redundantly to phosphorylate H2AX after exposure to ionizing radiation. Cancer Res *64*, 2390-2396.

Strahl, B.D., and Allis, C.D. (2000). The language of covalent histone modifications. Nature *403*, 41-45.

Strom, L., Lindroos, H.B., Shirahige, K., and Sjogren, C. (2004). Postreplicative recruitment of cohesin to double-strand breaks is required for DNA repair. Mol Cell *16*, 1003-1015.

Stucki, M., Clapperton, J.A., Mohammad, D., Yaffe, M.B., Smerdon, S.J., and Jackson, S.P. (2005). MDC1 directly binds phosphorylated histone H2AX to regulate cellular responses to DNA double-strand breaks. Cell *123*, 1213-1226.

Stucki, M., and Jackson, S.P. (2004). MDC1/NFBD1: a key regulator of the DNA damage response in higher eukaryotes. DNA Repair (Amst) *3*, 953-957.

Sugai, T., and Hiwatashi, K. (1974). Cytologic and autoradiographic studies of the micronucleus at meiotic prophase in Tetrahymena pyriformis. J Protozool *21*, 542-548.

Suka, N., Suka, Y., Carmen, A.A., Wu, J., and Grunstein, M. (2001). Highly specific antibodies determine histone acetylation site usage in yeast heterochromatin and euchromatin. Mol Cell *8*, 473-479.

Sun, H., Treco, D., Schultes, N.P., and Szostak, J.W. (1989). Double-strand breaks at an initiation site for meiotic gene conversion. Nature *338*, 87-90.

Sun, Z.W., and Allis, C.D. (2002). Ubiquitination of histone H2B regulates H3 methylation and gene silencing in yeast. Nature *418*, 104-108.

Suto, R.K., Clarkson, M.J., Tremethick, D.J., and Luger, K. (2000). Crystal structure of a nucleosome core particle containing the variant histone H2A.Z. Nat Struct Biol *7*, 1121-1124.

Tamburini, B.A., and Tyler, J.K. (2005). Localized histone acetylation and deacetylation triggered by the homologous recombination pathway of double-strand DNA repair. Mol Cell Biol *25*, 4903-4913.

Taunton, J., Hassig, C.A., and Schreiber, S.L. (1996). A mammalian histone deacetylase related to the yeast transcriptional regulator Rpd3p. Science *272*, 408-411.

Taverna, S.D., Coyne, R.S., and Allis, C.D. (2002). Methylation of histone h3 at lysine 9 targets programmed DNA elimination in tetrahymena. Cell *110*, 701-711.

Taverna, S.D., Li, H., Ruthenburg, A.J., Allis, C.D., and Patel, D.J. (2007). How chromatin-binding modules interpret histone modifications: lessons from professional pocket pickers. Nat Struct Mol Biol *14*, 1025-1040.

Thomas, J.O. (1999). Histone H1: location and role. Curr Opin Cell Biol *11*, 312-317.

Tsukada, Y., Fang, J., Erdjument-Bromage, H., Warren, M.E., Borchers, C.H., Tempst, P., and Zhang, Y. (2006). Histone demethylation by a family of JmjC domain-containing proteins. Nature *439*, 811-816.

Tsukuda, T., Fleming, A.B., Nickoloff, J.A., and Osley, M.A. (2005). Chromatin remodelling at a DNA double-strand break site in Saccharomyces cerevisiae. Nature *438*, 379-383.

Turner, J.M., Mahadevaiah, S.K., Ellis, P.J., Mitchell, M.J., and Burgoyne, P.S. (2006). Pachytene asynapsis drives meiotic sex chromosome inactivation and leads to substantial postmeiotic repression in spermatids. Dev Cell *10*, 521-529.

Turner, J.M., Mahadevaiah, S.K., Fernandez-Capetillo, O., Nussenzweig, A., Xu, X., Deng, C.X., and Burgoyne, P.S. (2005). Silencing of unsynapsed meiotic chromosomes in the mouse. Nat Genet *37*, 41-47.

Utley, R.T., Lacoste, N., Jobin-Robitaille, O., Allard, S., and Cote, J. (2005). Regulation of NuA4 histone acetyltransferase activity in transcription and DNA repair by phosphorylation of histone H4. Mol Cell Biol *25*, 8179-8190.

van Attikum, H., Fritsch, O., Hohn, B., and Gasser, S.M. (2004). Recruitment of the INO80 complex by H2A phosphorylation links ATP-dependent chromatin remodeling with DNA double-strand break repair. Cell *119*, 777-788.

van Attikum, H., and Gasser, S.M. (2005). The histone code at DNA breaks: a guide to repair? Nat Rev Mol Cell Biol *6*, 757-765.

van Vugt, M.A., and Medema, R.H. (2004). Checkpoint adaptation and recovery: back with Polo after the break. Cell Cycle *3*, 1383-1386.

Vicent, G.P., Nacht, A.S., Smith, C.L., Peterson, C.L., Dimitrov, S., and Beato, M. (2004). DNA instructed displacement of histones H2A and H2B at an inducible promoter. Mol Cell *16*, 439-452.

Volpe, T.A., Kidner, C., Hall, I.M., Teng, G., Grewal, S.I., and Martienssen, R.A. (2002). Regulation of heterochromatic silencing and histone H3 lysine-9 methylation by RNAi. Science *297*, 1833-1837.

Wang, H., Zhai, L., Xu, J., Joo, H.Y., Jackson, S., Erdjument-Bromage, H., Tempst, P., Xiong, Y., and Zhang, Y. (2006). Histone H3 and H4 ubiquitylation by the CUL4-DDB-ROC1 ubiquitin ligase facilitates cellular response to DNA damage. Mol Cell *22*, 383-394.

Ward, I.M., and Chen, J. (2001). Histone H2AX is phosphorylated in an ATR-dependent manner in response to replicational stress. J Biol Chem *276*, 47759-47762.

Ward, I.M., Minn, K., Jorda, K.G., and Chen, J. (2003). Accumulation of checkpoint protein 53BP1 at DNA breaks involves its binding to phosphorylated histone H2AX. J Biol Chem *278*, 19579-19582.

Wei, Y., Yu, L., Bowen, J., Gorovsky, M.A., and Allis, C.D. (1999). Phosphorylation of histone H3 is required for proper chromosome condensation and segregation. Cell *97*, 99-109.

West, M.H., and Bonner, W.M. (1980). Histone 2A, a heteromorphous family of eight protein species. Biochemistry *19*, 3238-3245.

White, C.L., Suto, R.K., and Luger, K. (2001). Structure of the yeast nucleosome core particle reveals fundamental changes in internucleosome interactions. EMBO J *20*, 5207-5218.

Wolfe, J., Hunter, B., and Adair, W.S. (1976). A cytological study of micronuclear elongation during conjugation in Tetrahymena. Chromosoma *55*, 289-308.

Wyatt, H.R., Liaw, H., Green, G.R., and Lustig, A.J. (2003). Multiple roles for Saccharomyces cerevisiae histone H2A in telomere position effect, Spt phenotypes and double-strand-break repair. Genetics *164*, 47-64.

Wysocka, J., Swigut, T., Milne, T.A., Dou, Y., Zhang, X., Burlingame, A.L., Roeder, R.G., Brivanlou, A.H., and Allis, C.D. (2005). WDR5 associates with histone H3 methylated at K4 and is essential for H3 K4 methylation and vertebrate development. Cell *121*, 859-872.

Wysocka, J., Swigut, T., Xiao, H., Milne, T.A., Kwon, S.Y., Landry, J., Kauer, M., Tackett, A.J., Chait, B.T., Badenhorst, P., *et al.* (2006). A PHD finger of NURF couples histone H3 lysine 4 trimethylation with chromatin remodelling. Nature *442*, 86-90.

Wysocki, R., Javaheri, A., Allard, S., Sha, F., Cote, J., and Kron, S.J. (2005). Role of Dot1-dependent histone H3 methylation in G1 and S phase DNA damage checkpoint functions of Rad9. Mol Cell Biol *25*, 8430-8443.

Xie, S., Xie, B., Lee, M.Y., and Dai, W. (2005). Regulation of cell cycle checkpoints by polo-like kinases. Oncogene *24*, 277-286.

Yamamoto, A., and Hiraoka, Y. (2001). How do meiotic chromosomes meet their homologous partners?: lessons from fission yeast. Bioessays *23*, 526-533.

Yang, Z., Zheng, C., and Hayes, J.J. (2007). The core histone tail domains contribute to sequence-dependent nucleosome positioning. J Biol Chem *282*, 7930-7938.

Yao, M.C., and Chao, J.L. (2005). RNA-guided DNA deletion in Tetrahymena: an RNAi-based mechanism for programmed genome rearrangements. Annu Rev Genet *39*, 537-559.

Yu, G.L., Hasson, M., and Blackburn, E.H. (1988). Circular ribosomal DNA plasmids transform Tetrahymena thermophila by homologous recombination with endogenous macronuclear ribosomal DNA. Proc Natl Acad Sci U S A *85*, 5151-5155.

Zenvirth, D., Arbel, T., Sherman, A., Goldway, M., Klein, S., and Simchen, G. (1992). Multiple sites for double-strand breaks in whole meiotic chromosomes of Saccharomyces cerevisiae. EMBO J *11*, 3441-3447.

Zheng, C., and Hayes, J.J. (2003). Intra- and inter-nucleosomal protein-DNA interactions of the core histone tail domains in a model system. J Biol Chem *278*, 24217-24224.